Wissenschaftszentrum Weihenstephan für Ernährung, Landnutzung und Umwelt

Lehrstuhl für Experimentelle Genetik

Paternal overweight controls transgenerational metabolic health via Polycomb

Raffaele Gerlini

Vollständiger Abdruck der von der Fakultät Wissenschaftszentrum Weihenstephan für Ernährung, Landnutzung und Umwelt der Technischen Universität München zur Erlangung des akademischen Grades eines

Doktors der Naturwissenschaften

Vorsitzender:	Prof. Angelika Schnieke, Ph.D.
Prüfer der Dissertation:	1. Prof. Dr. Martin Hrabě de Angelis
	2. Prof. Dr. Eckhard Wolf

Die Dissertation wurde am 25.09.2019 bei der Technischen Universität München eingereicht und durch die Fakultät Wissenschaftszentrum Weihenstephan für Ernährung, Landnutzung und Umwelt am 15.05.2020 angenommen.

TABLE OF CONTENTS

I. TABLES AND FIGURES

II. SUMMARY/ZUSAMMENFASSUNG

The incredible rise of obesity and related diseases suggests a role for additional contributing factors beyond the genetic predisposition, such as gene/environment interaction and epigenetic mechanisms. Obesity is spreading in parallel with diabetes and because of its complications, is known for being among the first causes of death in developed countries. Genomic studies have been useful to identify genetic variants associated with diabetes and obesity, however, their relevance to disease etiology has been limited as they cannot fully explain heritability as do not account for the contribution of environmental factors.

Epigenetic inheritance describes the non-genetic transmission of acquired complex phenotypes from parents to offspring and it is supported by epidemiological and mostly animal studies, in which the environmental conditions are more easily controllable. As a matter of fact, lifestyle choices and living habits influence not only the health of directly exposed individuals but also that of their descendant inter- or transgenerationally. The germline is key to this transfer and, despite the presence of physiological barriers, it can sense environmental stressors acting on somatic cells and influence developmental and adult phenotypic trajectories. In this regard, parental obesity, preconceptional or gestational, are major risk factors for offspring obesity. While the direct influence of the mother on the fetuses is well established, less is known from the paternal side. Recent studies have shown that also the father contributes to the embryonic development and potentially influences the health of the offspring.

The present study attempts to shed light on mechanisms of paternal epigenetic inheritance triggered by an environmental exposure such as a high-fat diet. My findings show that paternal overweight affects descendant metabolic health in human and mouse. Intriguingly, a paternal preconceptional acute high-fat diet challenge induces a sex specific transgenerational inheritance of glucose intolerance and reduced insulin sensitivity across two unexposed generations.
Mechanistically, the acute high fat diet in mice impinges on Polycomb Repressive Complex 2 (PRC2) activity during spermatogenesis and affects transcriptional program of germ cell and embryo. PRC2 is a histone methyltransferase complex that promotes epigenetic gene silencing through the tri-methylation of histone H3 at lysine 27.

Taken together the data indicate that paternal weight in humans and mice influence offspring metabolic health and associates to a reduction of Polycomb activity during spermatogenesis. The reduced histone modification observed in sperm of overweight donors reveals that the heterochromatin alteration may be a common feature of paternal inheritance of obesity and diabetes in mammals. This study is the first to reveal a function of Polycomb in mediating control of offspring metabolic health in mammals and has potential to explain the rapid increase in obesity and diabetes epidemic worldwide.

Der enorme Anstieg der Prävalenz von Adipositas und verwandten Krankheiten wie unter anderem Diabetes in den letzten Jahren deutet auf Faktoren hin, die neben der genetischen Veranlagung die Krankheitsausprägung zusätzlich beeinflussen wie z.B. Gen-Umwelt Interaktionen und epigenetische Mechanismen. Adipositas ist aufgrund der damit einhergehenden Komplikationen eine der häufigsten Todesursachen in entwickelten Ländern. In genomischen Studien wurden genetische Varianten identifiziert, die mit Diabetes und Adipositas assoziiert sind. Die Relevanz dieser Studien für die Krankheitsätiologie ist jedoch begrenzt, da dadurch weder die Erblichkeit vollständig erklärt werden kann noch der Einfluss von Umweltfaktoren berücksichtigt wurde.
Die epigenetische Vererbung beschreibt die nicht-genetische Übertragung von erworbenen komplexen Phänotypen von Eltern auf die Nachkommen. Dies wird durch epidemiologische Studien und vor allem durch Studien an Tieren untersucht, da in diesem Fall die Umweltbedingungen leichter kontrollierbar sind. Tatsächlich beeinflussen Gewohnheiten und die Lebensweise nicht nur die Gesundheit von direkt ausgesetzten Individuen, sondern auch die der Nachkommen auf inter- oder transgenerationale Weise. Die Keimbahn ist dabei der Schlüssel für diese Vererbung. Trotz bestehender physiologischer Barrieren können Umweltstressoren direkt auf die somatischen Zellen wirken und die Entwicklung sowie adulte phänotypische Ausprägungen beeinflussen. In diesem Zusammenhang ist parentale Adipositas, sowohl präkonzeptionell als auch während der Gestation, ein wichtiger Risikofaktor für Adipositas bei den Nachkommen. Während der direkte Einfluss der Mutter auf den Fötus gut untersucht ist, ist von dem Einfluss der väterlichen Seite weniger bekannt. Neuere Studien haben gezeigt, dass auch Einflüsse desVaters aktiv zur Embryonalentwicklung beitragen und sich möglicherweise auf die Gesundheit der Nachkommen auswirken.

Diese Studie strebt an, Aufschluss über die Mechanismen der väterlichen epigenetischen Vererbung zu geben, die durch Umwelteinflüsse, wie z.B. fettreiche Ernährung, ausgelöst werden. Meine Ergebnisse zeigen, dass paternales Übergewicht die metabolische Gesundheit der Nachkommen beim Menschen wie auch bei Mäusen beeinflusst. Faszinierenderweise führt eine akute paternale fettreiche Ernährung vor der Konzeption in Mäusen zur transgenerationalen Vererbung von geschlechtsspezifischer Glukoseintoleranz und verminderter Insulinsensitivität über zwei Generationen.

Mechanistisch betrachtet beeinflusst die akute fettreiche Ernährung die Aktivität des Polycomb Repressive Complex 2 (PRC2) während der Spermatogenese und verändert das Transkriptom von Keimzellen und Embryos. PRC2 ist ein Histon-Methyltransferase-Komplex, der durch dreifache Methylierung des Histons H3 am Lysin 27 zu epigenetisch unterdrückter Genexpression führt.

Zusammengefasst deuten die Daten darauf hin, dass väterliches Übergewicht die metabolische Gesundheit von Menschen und Mäusen beeinflusst und zu einer Reduktion der Polycomb-Aktivität während der Spermatogenese führt. Diese verringerte Histon-Modifikation, die im Sperma von übergewichtigen humanen Donoren beobachtet wurde, deutet darauf hin, dass die Veränderung des Heterochromatins ein gemeinsames Merkmal der paternalen Vererbung von Adipositas und Diabetes in Säugetieren ist. Dies ist die erste Studie, die zeigt, dass Polycomb funktionell die Gesundheit von Säugetier-Nachkommen beeinflusst. Dies trägt potentiell zur Erklärung des rapiden Anstiegs der weltweiten Adipositas- und Diabetes-Epidemie bei.

1. INTRODUCTION

1.1 Obesity, diabetes and metabolic disease pandemic

When the ingestion of energy-rich food far outweighs the energy necessary for life processes and everyday physical challenges, the caloric intake and the expended calories are unbalanced, thus resulting in fat accumulation and overweight that tends to obesity when prolonged over time. High-calorie diets characterize modern times. The unhealthy food is accessible to the majority of the world population and, by being tasteful and affordable, is causing serious health problems. Obesity is described by an increase in body fat amount, waist circumference (WC) and high body mass index (BMI). The World Health Organization (WHO) defines obesity as the condition in which BMI is higher than 30 Kg/m^2 and identifies 3 classes of intensity depending on its value (Class I: 30-34.99 Kg/m^2, Class II: 35-39.99 Kg/m^2 and Class III: $\geq$ 40 Kg/m^2). An elevated BMI is a well-established contributor of cardiovascular disease and associates with premature death and disability of several kinds [1, 2]. Recent studies have identified abdominal obesity as the major risk factor for cardiovascular disease. Having an abdominal circumference of more than 102 cm in men and 88 cm in women, indeed, denotes high risk of disease development despite BMI categories [3]. Therefore, abdominal adiposity, more than BMI, should be taken into account as predictor of health risk, from the moment that the effects of abdominal fat occur not only in those who have a high BMI but also in non-obese individuals showing reduced insulin sensitivity [4].

Today, childhood obesity touches over 340 million children and adolescents aged 5-19. They experience breathing difficulties, musculoskeletal problems, insulin resistance and early signs of cardiovascular disease [5-7]. Multiple pediatric studies have shown association between adolescent obesity and obesity during adulthood [8, 9], however intervention in reducing body weight lowers the risk of comorbidities later in life [10]. The duration of obesity is directly associated with an increased risk of type 2 diabetes. Indeed, if obesity persists until adolescence, the risk of cardiovascular disease increases significantly [11]. Briefly, being overweight during adolescence already undermines health [12]; overweight prepubescents and adolescents have 5 times higher risk of developing adult obesity than lean ones [13, 14] with 7 and 13 as the ages with the strongest influence on future obesity [15, 16].

Figure 1.1 - Diabetes spread worldwide
Numbers of adults (20-79 years) living with diabetes according to areas of the world. In 2017, 425 million people were found affected and it is predicted that the number will increase of about 50% by the next 25 years (IDF Diabetes Atlas 2017).

1.2 Obesity in children

BMI during childhood heavily influences the one during the adulthood. In this regard, prevention strategies should address primarily the children. Nowadays, several parameteres are used to define obesity in children. However, to compensate for child development and ethnicity, waist measurement in percentile is preferred to absolute values. Therefore, children with a waist circumference higher than the 90th percentile are more prone to develop cardiovascular disease than those with lower WC [17].

Political strategies but also social and economic inequality, strongly influence health of populations worldwide. In emerging countries, for instance, the rapid change in diet and eating habits, subsequent to a rapid economic growth and working hours, has also helped to fuel the obesity epidemic. Inadequate prenatal and early childhood nutrition characterizes developing but also well-developed countries where parental education, parents age, open areas for recreation and social status impact on life quality and expectation. A variety of environmental factors influence the development of the unhealthy nutrition. Among those, a high density of cheap and of poor-quality restaurants for instance is associated with increased risk of obesity within a living area [18]. Having

socioeconomic disadvantages such as unemployed parents or with low income and low education level also impacts on children metabolic health, independently from the type of diet assumed during life, lifestyle or unhealthy behaviors [19, 20]. As a matter of fact, these pieces of evidence suggest that the environment exerts a strong influence on the human health by working on different levels.

It is well established that parental overweight influences children BMI [21, 22], even though a distinction must be drawn with regards to parental obesity, sex and offspring health. Having a father but not the mother overweight, means for a child to have a risk of 318% to develop obesity later in life [23], while infants born to obese mothers have higher chances of being fat and have increased waist circumference at birth [24], thus, predisposing to later adverse metabolic outcomes.

Obesity is a complex disease in which gene/environment interaction contributes to its pathogenesis. Indeed, beside their genetic variability, parental lifestyle and behaviors influence offspring predisposition to metabolic derangement, a risk that is further potentiated in case of direct experience of obesogenic environment throughout life [25].

1.3 Diabetes mellitus

The increase in obesity proceeds in parallel with the increase in diabetes, a chronic condition that occurs when the blood glucose levels exceed the normal values as a result of inability to produce insulin, or reduced sensitivity to it.

Glucose is the preferred fuel of the body; it is transported from the bloodstream into the tissues and converted to energy. High levels of postprandial glucose in the blood stimulate insulin release from pancreas, which mediates glucose uptake into the major insulin-sensitive tissues such as the skeletal muscle, the adipose tissue and the liver. In the Figure 1.2 is represented the crosstalk between tissues in the regulation of glucose metabolism. Food ingestion raises plasma glucose levels. The postprandial hyperglycemia stimulates pancreatic beta cells to release insulin while inhibits the secretion of glucagon from alpha cells, together, these cause glucose uptake in various tissues [26]. When the body does not respond correctly to insulin and its long-term effects, or when occur irregular gluconeogenesis and glycogenolysis, blood glucose levels rise and remain constant. The persistent high glucose concentration in the blood refers to chronic hyperglycemia, the hallmark of diabetes, leading to serious complications. Indeed, hyperglycemia for long

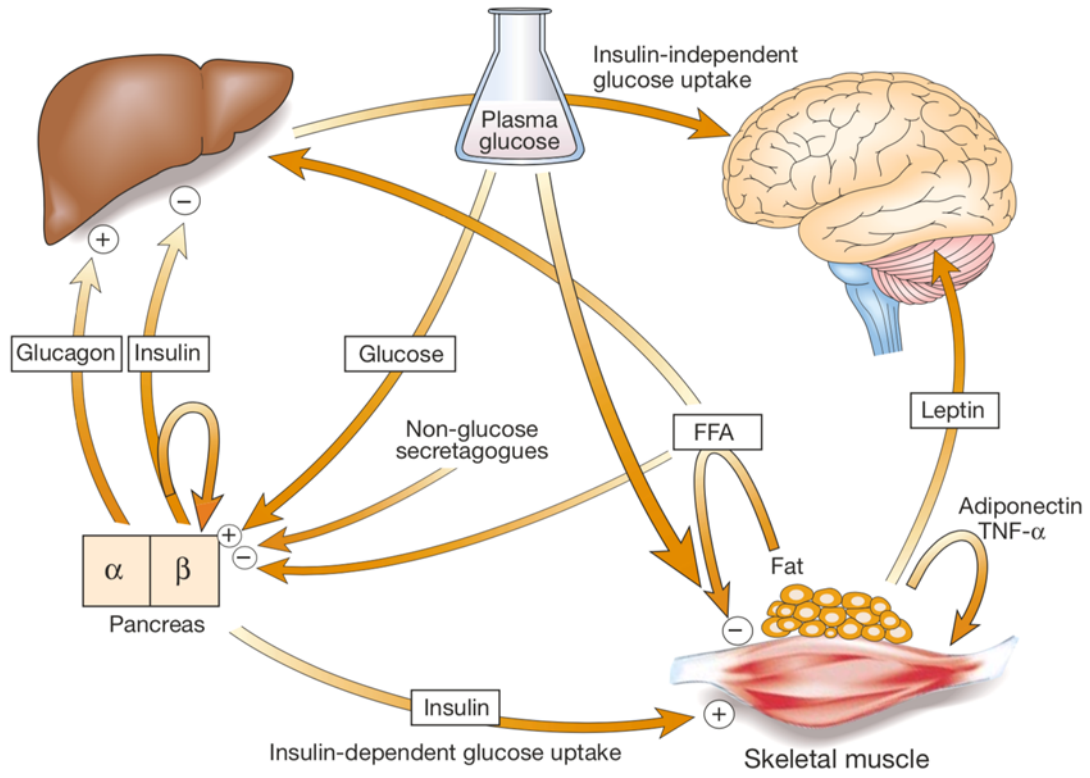

Figure 1.2 - Crosstalk in the regulation of glucose metabolism
Insulin is secreted from the pancreatic beta-cells in response to elevated plasma glucose, it inhibits the glucose production from the liver and stimulates glucose uptake in fat and muscle. Fat tissue, through the FFAs, reduces glucose uptake in muscle and insulin secretion from the pancreas while stimulates glucose production from the liver. Adipokines, leptin and adiponectin such as TNF are other products of the adipose tissue that can regulate the energy expenditure and insulin sensitivity. Modified from [28].

periods endangers various organs and conducts with time to several pathologies such as cardiovascular disease, neuropathy, nephropathy and retinopathy. These complications place diabetes among the leading causes of death [27]. Reduced insulin secretion, increased glucose production (through gluconeogenesis or glycogenolysis) or decreased glucose utilization are the main contributing factors to chronic hyperglycaemia. Of note, elevated glucose levels in diabetic patients generate advanced glycation end products (AGEs) via non-enzymatic intra- and extracellular glycation of protein. AGEs are formed by the interaction of glucose with the amino groups of proteins and their production correlates with glycemia. AGEs accumulate in the circulation when the kidney filtration starts to fail. They interact and cross-link endothelial proteins promoting atherosclerosis and alteration of extracellular matrix composition and structure [28-30]. Early detection of the disease is therefore important for its proper management, which aims at delaying

its onset and, if possible, at preventing further complications. Diagnosis of diabetes is made according to criteria shown in Table 1.1 [31].

1.	**Fasting plasma glucose ≥126 mg/dl (7.0 mmol/l).** Fasting is defined as no caloric intake for at least 8 h.*
	Or
2.	**Hyperglycemia and casual plasma glucose ≥200 mg/dl (11.1 mmol/l).** Casual is defined as any time of day without regard to time since last meal. The classic symptoms of hyperglycemia include polyuria, polydipsia, and unexplained weight loss.
	Or
3.	**2-h plasma glucose ≥200 mg/dl (11.1 mmol/l) during an oral glucose tolerance test (OGTT**). The test should be performed as described by the World Health Organization, using a glucose load containing the equivalent of 75 g anhydrous glucose dissolved in water.*

* In the absence of unequivocal hyperglycemia, these criteria should be confirmed by repeat testing on a different day.

Table 1.1 - Criteria for diagnosis of diabetes
The table describes the conventional parameters utilized for the diagnosis of diabetes in humans. Modified from [33].

1.4 Insulin biosynthesis, secretion and action

Insulin is a hormone synthesized as an 86 amino acid single-chain polypeptide. Subsequent proteolytic removal of the N-terminal part of the molecule, transforms the pre-proinsulin polypeptide precursor in proinsulin. The proinsulin binds weakly to the insulin receptor; hence, a further cut of an internal fragment of 31 residues generates the C peptide together with the final form of insulin. The mature hormone is formed of chain A (21 amino acids) and B (30 amino acids) connected by disulfide bonds between the cysteine residues. This bridge gives the molecule the tertiary structure required for receptor binding. The active configuration of insulin is packaged together with the C peptide into small granules within the Golgi complex of the beta cells. Here, insulin molecules form hexamers with zinc ions that separate rapidly following secretion.

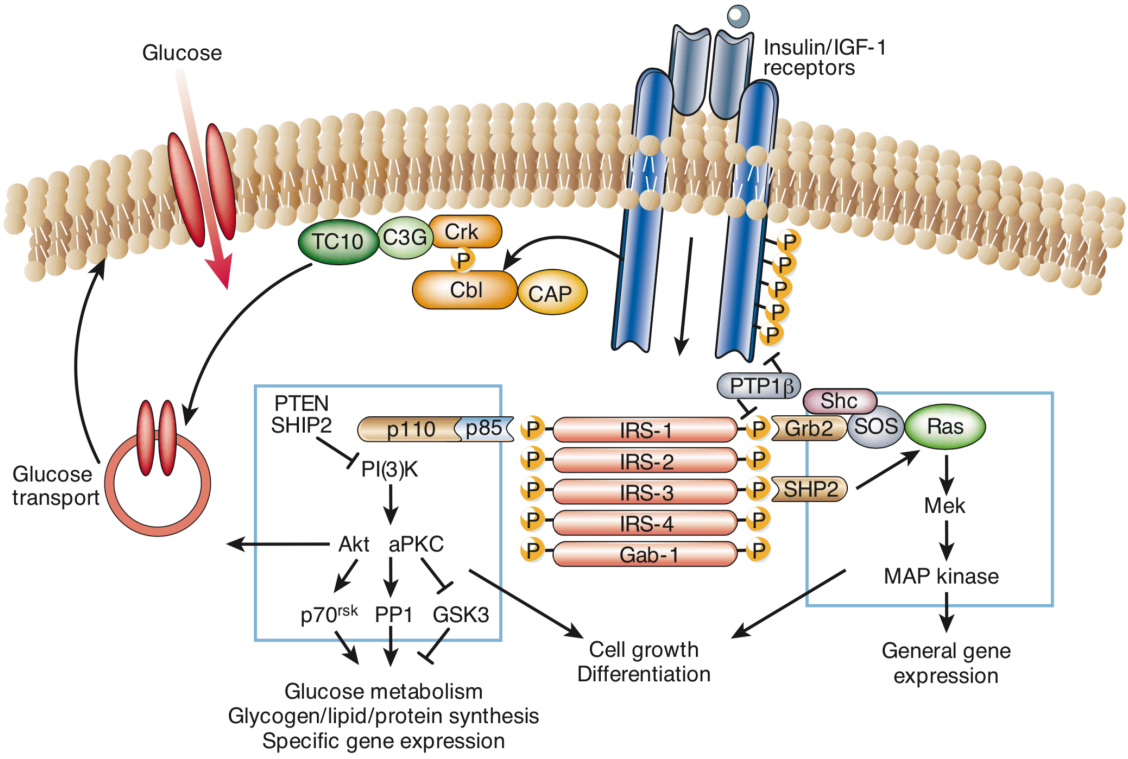

Figure 1.3 - Insulin signaling upon binding to the receptor
Insulin receptor is a tyrosine kinase that, after its binding with insulin, undergoes to autophosphorylation and catalyzes the phosphorylation of other intracellular proteins such as IRS. This results in activation of diverse signaling pathways involved in glucose metabolism, glycogen, lipid and protein synthesis, cell growth and differentiation through the regulation of gene expression. Modified from [28].

Glucose is the key regulator of insulin production and release, however, amino acids, ketones and gastrointestinal peptides, neurotransmitters and other nutrients can also

influence its secretion. When plasma glucose levels rise, glucose enters the beta cell through the glucose transporter GLUT2. The limiting step of the insulin release from beta cells is operated by the glucokinase, an enzyme that phosphorylates glucose at the hydroxy group on carbon 6 (G6P) that is subsequently metabolized through glycolysis. The production of ATP and the increase in ATP/ADP ratio induce the closure of ATP-dependent potassium channels causing depolarization of the beta cell membrane with activation of calcium sensitive channels. As a consequence, the influx of calcium in the cells provokes fusion of the insulin granules with the membrane and release in the blood by exocytosis of insulin, C peptide and other molecules. Insulin secretion shows a rhythmic pattern of hormone release occurring every 10 minutes; meals and other major stimuli increase its secretion of four- to five-fold and these elevated levels usually last for 2-3 hours before returning to a relatively constant basal rate. Disruption of the normal secretory patterns is a clear symptom of beta cell dysfunction occurring in diabetes [32].
Once insulin is secreted into the portal venous system, it enters the circulation and reaches the target sites. Figure 1.3 defines dynamic processes activated by the insulin binding to the receptor. Importantly, the activation of the insulin receptor grants the glucose uptake through the translocation of glucose transporters to the cell membrane. Insulin receptor signaling has been largely studied and reviewed in terms of cellular mechanisms on metabolism; in this respect, a detailed overview can be already found in literature and will not be further discussed here [33].
When the insulin is released from the pancreas, about 50% is already cleared by the liver while passing through the portal system. The remaining amount has anyway a short half-life in the circulation of around 5 minutes. This system assures a tight regulation of metabolism by allowing quick responses and changes. Additionally, the kidney influences blood insulin levels as well, as it is directly involved in insulin clearance. Importantly, the C peptide is more stable than insulin and more resistant to degradation in liver, for this reason it is considered as a good marker suitable for evaluation of endogenous insulin production (as produced in equimolar amounts) and informative in case of systemic insulin resistance (or altered glucose homeostasis) [34].
When glucose in the blood is insufficient, the liver generates glucose through glycogenolysis and gluconeogenesis. The balance between hepatic glucose production, peripheral glucose uptake and utilization refers to glucose homeostasis. Insulin and glucagon are the major hormones regulating this equilibrium [35]. While insulin is produced by the beta cells of the pancreas, glucagon is produced and secreted by the alpha cells, the latter antagonize the insulin action [36]. Briefly, low insulin levels promote

glucose production from the liver, inhibit glycogen synthesis and reduce glucose uptake in the insulin-sensitive tissues. In the opposite situation, high levels of glucose in the blood lead to insulin production and release, increase in glucose uptake and glycogen synthesis and reduction in glucagon-mediated hepatic glucose production.

1.5 Forms of Diabetes

After many decades of studies, it is well accepted that there are three types of diabetes: type 1 diabetes (T1D), type 2 (T2D) and gestational diabetes (GDM). Of note, there are other, less common, types of diabetes including monogenic forms or secondary diabetes (Table 1.2). Conditions like maturity onset diabetes of the young (MODY) or neonatal diabetes mellitus represent the genetic forms [37]. Contrary to other types, monogenic diabetes is the result of a single genetic mutation in a dominant gene, however only 1-5% of all diabetes forms are due to a single gene alteration. Among the less common, others can emerge from different diseases that correlate with hormone production (e.g. Cushing's disease), pancreatitis or are the consequences of drug treatments such as corticosteroids therapy (Table 1.2).

1.5.1 Type 1 Diabetes

T1D is the result of autoimmune beta cell destruction. In the pancreas, beta cells are insulin producing cell, thus relative or absolute insulin deficiency characterizes this condition. Genetic susceptibility is undoubtedly the major trigger although a combination of factors such as environmental elements like nutrition, toxins and viral infections can be also implicated [38]. Since it occurs most frequently in children and adolescents, this type of diabetes it is known as the early onset diabetes, nevertheless it can develop at any age. In the majority of the cases, immunological markers appear before diabetes becomes clinically overt. Indeed, besides the progressive decline in beta cells and insulin secretion, normal glucose tolerance is maintained until the majority of beta cells are destroyed; only at this stage the symptoms start to become evident. Since T1D is not subject of this work, it will not be deepened, however, comprehensive reviews on the pathogenesis [39, 40] and the genetics of the T1D [41] are largely available in the literature.

Type 1 Diabetes	**a. Immune mediated** **b. Idiopathic**	
Type 2 Diabetes	**a. Insulin resistance** **b. Insulin deficiency**	
Gestational diabetes mellitus (GDM)	**a. Hyperglycemia in pregnancy**	
Other Types	**A. Genetic defects of β-cell function** 1. Chromosome 12, HNF-1α (MODY3) 2. Chromosome 7, glucokinase (MODY2) 3. Chromosome 20, HNF-4α (MODY1) 4. Chromosome 13, (IPF-1; MODY4) 5. Chromosome 17, HNF-1β (MODY5) 6. Chromosome 2, *NeuroD1* (MODY6) 7. Mitochondrial DNA 8. Others	**E. Drug or chemical-induced** 1. Vacor 2. Pentamidine 3. Nicotinic acid 4. Glucocorticoids 5. Thyroid hormone 6. Diazoxide 7. β-adrenergic agonists 8. Thiazides 9. Dilantin 10. α-Interferon 11. Others
	B. Genetic defects in insulin action 1. Type A insulin resistance 2. Leprechaunism 3. Rabson-Mendenhall syndrome 4. Lipoatrophic diabetes 5. Others	**F. Infections** 1. Congenital rubella 2. Cytomegalovirus 3. Others
	C. Diseases of the exocrine pancreas 12. Pancreatitis 13. Trauma/pancreatectomy 14. Neoplasia 15. Cystic fibrosis 16. Hemochromatosis 17. Fibrocalculous pancreatopathy 18. Others	**G. Uncommon forms of immune-mediated diabetes** 1. "Stiff-man" syndrome 2. Anti–insulin receptor antibodies 3. Others
	D. Endocrinopathies 1. Acromegaly 2. Cushing's syndrome 3. Glucagonoma 4. Pheochromocytoma 5. Hyperthyroidism 6. Somatostatinoma 7. Aldosteronoma 8. Others	**H. Other genetic syndromes associated with diabetes** 1. Down's syndrome 2. Klinefelter's syndrome 3. Turner's syndrome 4. Wolfram's syndrome 5. Friedreich's ataxia 6. Huntington's chorea 7. Laurence-Moon-Biedl syndrome 8. Myotonic dystrophy 9. Porphyria 10. Prader-Willi syndrome 11. Others

Table 1.2 - Classification of diabetes mellitus
Modified from [33]

1.5.2 Type 2 Diabetes

T2D, is the most common type of diabetes accounting for the majority of all diagnosed cases of the disease (WHO, 2018). It refers to a heterogeneous group of disorders characterized by different levels of severity in which insulin resistance and impaired insulin secretion contribute to sustained hyperglycaemia.

When the insulin response is inadequate for the glucose uptake, glucose levels in the blood rapidly increase. In the condition of chronic hyperglycemia, islets are constantly overstimulated to produce insulin in order to lower the blood glucose levels. The stimulation of the islets overtime induces a progressive decline of functional beta cell mass, called hyperplasia and described as dedifferentiation and failure of the cells [42].

Reduced affinity of insulin to its receptor refers to insulin resistance and, when combines with beta cell dedifferentiation, further complicates the situation [43]. Of note, insulin resistance is an early feature of T2D and it is frequently accompanied by defects in the PI3K signaling that normally induces the translocation of the glucose receptor to the membrane for glucose uptake [44]. In both skeletal muscle and fat, insulin resistance reduces glucose uptake, but while in the muscle it impairs the utilization of glucose by inducing non-oxidative pathways, in the adipose tissue it increases free fatty acid (FFA) production and export [45]. In liver instead, insulin resistance impairs the negative feedback of insulin on the gluconeogenesis and on glycogen breakdown, thus, fueling the hyperglycemia [46]. In case of insulin resistance, the pancreas increases the insulin production and release in order to maintain a normal glucose tolerance; however, the overstimulation of beta cells causes a reduction of insulin secretion with time, eventually resulting in inadequate amount of insulin.

The onset of chronic hyperglycemia, characteristic of diabetes, is associated with long term damage and dysfunction. The impaired glucose homeostasis observed in T2D reflects impaired fasting glucose (IFG) or impaired glucose tolerance (IGT). The first condition refers to an increased level of fasting blood glucose while the second reflects an inadequate insulin action. In both cases the body struggles to maintain glycemia within the normal ranges.

T2D and T1D share similar symptoms including in particular sudden weight loss, thirst and frequent urination, tiredness and slow-healing wounds. Compared to the T1D, T2D does not show an acute metabolic phase and, therefore, its onset cannot be easily determined.

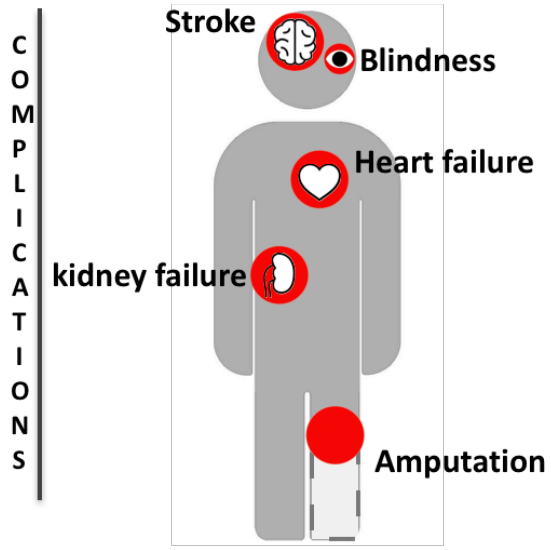

Figure 1.4 - Diabetes complications
Stroke, blindness, heart failure, kidney failure and amputation are common complications of a long-term persistent hyperglycemia.

A large percentage of affected individuals do not show the symptoms for years and importantly, asymptomatic patients are identified through secondary complications only later in time (Figure 1.4).

Obesity is the strongest risk factor for type 2 diabetes [47]. The visceral adipose tissue is a very important organ for metabolism, as adipocytes secrete factors (leptin, TNF-alpha, fatty acids, resistin, and adiponectin) able to influence body weight and composition, modulate insulin secretion and insulin action and contribute to the insulin resistance [48-50]. Although debated, there is evidence of the existence of a healthy obesity, in which affected individuals appear as metabolically healthy. Indeed, glucose tolerant and insulin sensitive obese individuals show reduced risk of associated comorbidities. Importantly, we recently demonstrated that the impaired glucose tolerance, rather than insulin resistance, is a major determinant of adipocyte transcriptional reprogramming in human obesity and identified new potential targets (NEMF and ENC1) for the management of metabolic health in obesity [51]. While the link between obesity and T2D is well-established, the association of obesity with T1D is a relatively new problem gaining more attention in the last decades [52].

T2D is most commonly seen in older adults, however the change in lifestyle and nutrition increased its incidence and prevalence among children and teenagers. Epidemiologists highlight a time-related prevalence of obesity in T1D patients as well [53, 54], where

diagnosed children show a race-dependent significant increase in BMI when detected between 2 to 18 years of age [55, 56].

1.5.3 Gestational Diabetes

The increased glucose level in blood observed during pregnancy is identified as gestational diabetes or hyperglycaemia in pregnancy according to the grade of severity. The diagnosis can occur anytime during gestation but, usually, GDM appears between the second and the third trimesters. Symptoms are very frequently masked by the pregnancy itself. The condition arises when the insulin sensitivity is impaired by placental adipokines [57]. GDM is, in most cases, a transient disorder and it resolves after delivery. However, women with GDM are at higher risk of developing it again in future pregnancies and transmitting the risk to the newborns to develop T2D later in life [58]. Besides having consequences on the newborns, increased blood glucose during pregnancy can have also implication on delivery difficulty and blood pressure that may undermine the health of the future mothers.

1.5.4 Disease management and treatment

Patients with T2D should receive education about nutrition, exercise and care of the disease during illness. Disease management translates in teaching patients to be responsible about their care, this is firstly done with proper medication, but also adjusting nutrition to lower the plasma glucose. Glycemic control requires measurements of glucose levels in the blood. A short-term picture of the glycemic status can be obtained with the self-monitoring of blood glucose or with the measurement of glycated hemoglobin A1C, which instead provides an average of glycemia over the previous 2-3 months. Glycemic control must be combined with a therapy that includes treatment of associated conditions such as obesity, hypertension, dyslipidemia and cardiovascular disease. Exercise regimen may help to increase insulin sensitivity and promote weight loss [59].

Diabetic patients need insulin treatment, the hormone is produced by recombinant DNA technology and it is necessary for their survival. T2D develops when insulin secretion no longer compensates for the metabolic derangement, thus most of the patients will also require insulin therapy with time. Several studies and clinical trials have highlighted the positive effects of insulin therapy on micro- and macrovascular protection when started early.

Different strategies can be used for the treatment; however, physicians should select the most effective and the better tolerated by the patients to tailor a treatment specific for every background. Besides new discoveries, to date Metformin remains the first choice of treatment for most of patients. It reduces glycemia by reducing glucose production and increasing insulin sensitivity [60, 61].

1.6 Genetics and epigenetics factors in diabetes

1.6.1 Molecular basis of obesity and diabetes

Diabetes is a multifactorial disease in which multiple genes, with low penetrance, are involved in a non-Mendelian pattern of inheritance. Indeed, the discrepancy of genetics in T1D identical twins suggested that other factors may be involved in the development of the disease. It was with the advent of genome-wide association studies (GWAS), aimed at dissecting causal genetic variants for many complex diseases, that in 2005 the prospective improved. GWAS have revealed that genetic components play an important role in the pathogenesis of T2D. Monozygotic twin concordance, together with adoption studies have confirmed this evidence [62-64]. Indeed, despite being separated from the parents, adopted children show a BMI that correlates more with the one of their biological parents highlighting a strong genetic component behind metabolic disorders [65-70]. T2D prevalence according to ethnic groups and families within the world populations further support the genetic influence on the disease risk [71-74].

Genetically, the heritability in the population can be explained by common single nucleotide polymorphisms (SNPs) [75]. More than 300 SNPs have been found associated with common forms of T2D and traits such as fasting glucose, BMI and gain in adiposity [76-79].

Polymorphism in Peroxisome Proliferator Activated Receptor Gamma (PPARG) and Potassium Voltage-Gated Channel Subfamily J Member 11 (KCNJ11) were the first robustly associated with T2D [80]. Later, large scale studies with a “hypothesis free” approach allowed to identify also Transcription Factor 7 Like 2 (TCF7L2) among T2D susceptibility genes. TCF7L2 encodes for a transcription factor of the Wnt signaling pathway, not previously known to be a candidate for type 2 diabetes [81, 82]. This gene modulates the function of pancreatic islet and its alteration affects insulin secretion and proglucagon gene expression [83]. In this respect, SNPs in the gene associate with a 40% increased risk for T2D (when considered alone) [84]. Importantly, GWAS have increased

the number of validated T2D susceptibility genes. Solute Carrier Family 30 Member 8 (SLC30A8), Haematopoietically Expressed Homeobox (HHEX/IDE), CDK5 Regulatory Subunit Associated Protein 1 Like 1 (CDKAL1), Insulin Like Growth Factor 2 MRNA Binding Protein 2 (IGF2BP2) and Cyclin Dependent Kinase Inhibitor 2A and 2B (CDKN2A/B) [85-87] have been the next identified genes of the European population studies, followed by other six new loci detected by the diabetes and Genetics Replication and Meta-Analysis (DIAGRAM) consortium: JAZF Zinc Finger 1 (JAZF1), intergenic region between Cell Division Cycle 123 and Calcium/Calmodulin Dependent Protein Kinase ID (CDC123-CAMK1D), the locus between Tetraspanin 8 and Leucine Rich Repeat Containing G Protein-Coupled Receptor 5 (TSPAN8-LGR5), THADA Armadillo Repeat Containing (THADA), ADAM Metallopeptidase With Thrombospondin Type 1 Motif 9 (ADAMTS9) and Notch Receptor 3 (NOTCH2) [85, 88-90]. Subsequently, the Meta-Analyses of Glucose and Insulin related traits Consortium (MAGIC) identified genetic association with glycemic phenotypes in non-diabetic individuals where other nine novel loci were found associated for fasting glucose such as MAP Kinase Activating Death Domain (MADD), Adrenoceptor Alpha 2 (ADRA2), Adenylate Cyclase 5 (ADCY5), Cryptochrome Circadian Regulator 2 (CRY2), Fatty Acid Desaturase 1 (FADS1), C2 Calcium Dependent Domain Containing 4B (C2CD4B), Prospero Homeobox 1 (PROX1), GLIS Family Zinc Finger 3 (GLIS3) and Solute Carrier Family 2 Member 2 (SLC2A2) [91], together with a polymorphism near the IGF1 locus influencing fasting insulin and the insulin resistance index HOMA-IR (Homeostatic Model Assessment for Insulin Resistance). The same consortium found novel association of three loci Glucokinase (GCK), Glucokinase regulator (GCKR) and Diacylglycerol Kinase Beta (DGKB-TMEM195) and replicated the known signals at TCF7L2 and SLC30A8 loci [83, 92].

Studies conducted in different populations have allowed to uncover additional T2D loci. Indeed, novel association loci reaching genome-wide significance at Protein Tyrosine Phosphatase Receptor Type D (PTPRD), Serine Racemase (SRR), Ubiquitin Conjugating Enzyme E2 E2 (UBE2E2) and F box protein (CDC4A-CDC4B) have been also observed in an Asian ancestry study, highlighting ethnic differences [93].

Finally, heritability observed in families supports the hypothesis that diabetes is primarily a genetic disease, despite that, individuals of the same family or community frequently share same environment besides genetics, thus revealing the importance of considering external factors for the disease risk development together with the genetics [94-97] .

1.6.2 Monogenic obesity

Studies on monogenic obesity have also been precious. A genetic approach allowed the discovery, among others, of the Leptin-Melanocortin key pathway of energy intake [98] and evidenced Fat Mass and Obesity Associated Protein (FTO) and TCF7L2 among the variants with clinical relevance and with the strongest association with the disease [99]. Noteworthy, a homozygous mutation in the leptin (LEP) gene resulted in a truncated form of the protein that causes early onset of severe obesity [100]. The same phenotypes arise from mutations in the LEP receptor leading to reduced leptin sensitivity [101]. Proopiomelanocortin (POMC) deficiency can also cause obesity when combined with hypocortisolism, skin hypopigmentation, and neonatal hypoglycemia [102] and lastly can influence the appetite [103]. FTO variants have been found in different ancestries correlating with childhood obesity, suggesting contribution to the adult onset of obesity and T2D [99]. The association of FTO variants with BMI has been repeatedly confirmed but other loci such as Neuronal Growth Regulator 1 (NEGR1), Transmembrane Protein 18 (TMEM18), Potassium Channel Tetramerization Domain Containing 15 (KCTD15), SH2B Adapter Protein (SH2B), ETS Variant 5 (ETV5) and Brain Derived Neurotrophic Factor (BDNF1) have been additionally identified [104, 105]. Obesity-related genes are reported in Figure 1.5.

A large scale GWAS analysis that focused more on fat distribution, than on total fat amount, allowed the identification of additional 49 associated loci. The outcomes highlighted that the fat distribution is locally regulated [106].

Most of the GWAS have been conducted in adults, however the increase in obesity in children requires more attention. Studies on childhood BMI and common obesity identified many similar loci in common with the adults, whereas no correlation between birth weight and early onset extreme obesity could be found [77].

Finally, despite the number of genetic variants identified, GWAS studies could only explain less than 10% of the observed inheritance of obesity and T2D susceptibility [95, 107]. Indeed, the identified SNPs have the potential to explain only a small fraction of the heritability [108, 109] and importantly, they can easily lead to false association from the moment that rare variants often occur at common sites of a specific allele [110-112]. These pieces of evidence strongly suggest that genetics alone cannot fully explain disease heritability and risk, for this reason, caution must be taken when interpreting these results as unaccounted shared conditions may significantly influence the outcomes [113].

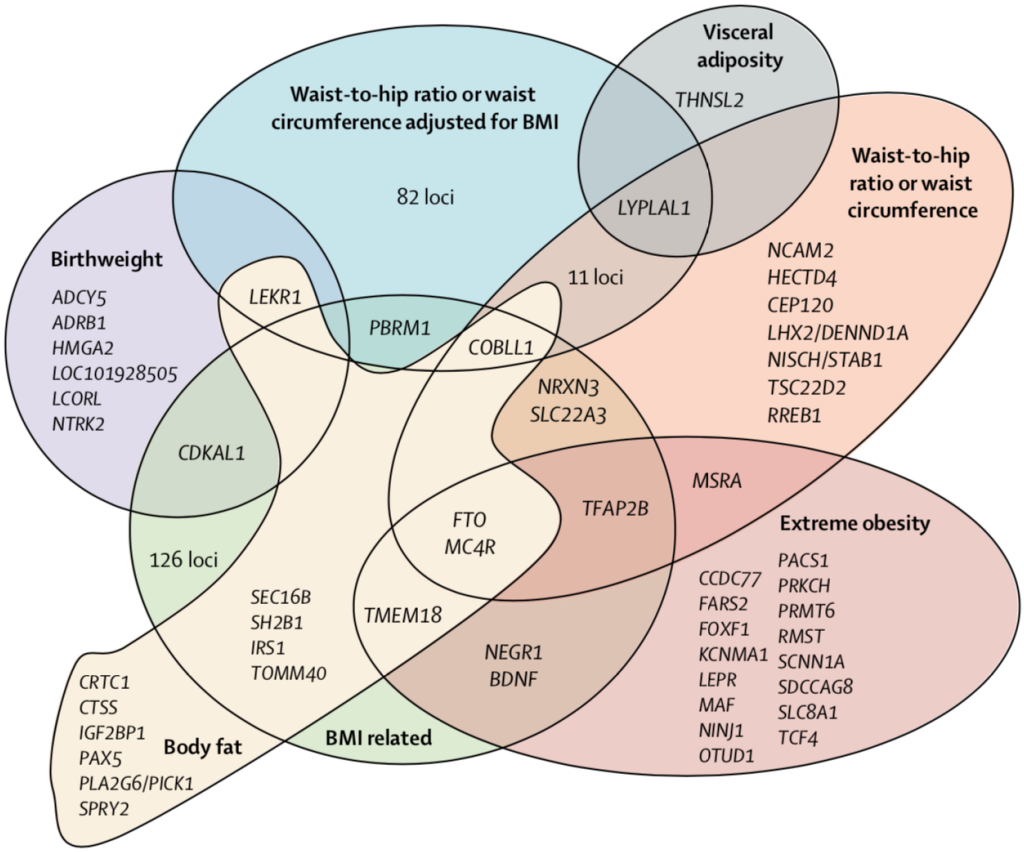

Figure 1.5 - Major GWAS discoveries related to adiposity traits
Conditions are grouped in 7 categories: birth weight, waist-to-hip ratio adjusted for BMI, visceral adiposity, waist-to-hip ration, extreme obesity, BMI and body fat. Modified from [77].

1.7 Epigenetic and acquired inheritance

Life-time acquired characteristics can be passed down from parents to offspring and influence their phenotypic manifestations [114]. Jean-Baptiste Lamarck proposed the theory that exposure to environmental factors can induce reactions and adaptation across generations and that the memory of exposure is the driver of the evolution. Depending on the genetic background, the environment can exert different effects. The same environmental exposure can lead to disparate phenotypes in genetically different individuals [115], alternatively, same genotypes may result in variable phenotypes because of a different environment [116]. To this regard, monozygotic twins who have grown up in different environments, showed different phenotypes and different phenotypic penetrance despite an identical genetic risk [117].

Understanding gene/environment interaction and their influence on phenotypic developments is therefore important to predict individual's susceptibility to complex

diseases within, and across, generations and to develop more efficient intervention strategies.

External influences have the power to induce adaptive evolutionary responses, revealing a mechanism of inheritance that does not emerge from the DNA sequence but, instead, requires epigenetic mechanisms. Conrad Waddington introduced the concept of Epigenetics in the 1940s defining it as "the branch of biology that studies the causal interactions between genes and their products which bring the phenotype into being". It can be described as the sum of mechanisms necessary to unfold the genetic program into development [118].

Epigenetics differs from genetics in the way that the variation observed in gene expression is independent from changes in DNA sequence. Its plastic mechanisms explain the fact that, beside a single genetic blueprint, there is a number of highly specialized and differentiated cell types. Epigenetic mechanisms involve chromatin modifying enzymes, DNA methyltransferase, demethylase and non-coding RNAs which collaborate to constitute the cell-type specific epigenomes (Figure 1.6). Alterations in these mechanisms lead to altered gene expression with phenotypic consequences [119].

1.7.1 Epigenetic mechanisms

1.7.1.1 DNA methylation

Methylation of the DNA is one of the major and best characterized epigenetic mechanisms in mammals. It consists of the insertion of a small methyl group on the cytosine base when directly precedes guanine, forming a 5-methylcytosine (5mC). It has been recognized as an epigenetic mechanism of silencing [120] and thought to be irreversible [121] until a decade ago, when the function of the Ten-Eleven Translocation (TET) family of dioxygenases in demethylating DNA was reported [122, 123]. DNA methylation is more dynamic than previously thought. Methyltransferases such as DNMT1, DNMT3A and DNMT3B attach methyl groups to DNA during replication and following embryo implantation. S-adenosyl-L-methionine (SAM) is the methyl donor. Demethylation can happen passively as a consequence of a reduction of the cellular SAM pool, or actively by the activity of TET enzymes which oxidize the 5mC to 5-hydroxy-methylcytosine (5hmC) [124]. This mark is usually associated with active transcription

and constitutes the first step towards the removal of locus-specific DNA methylation during cellular replication.

As well-regulated mechanism, DNA methylation is essential during development, genomic imprinting and X chromosome inactivation for gene silencing and suppression of retrotransposons [125-129]. It preferentially occurs at CpG islands, which are on average 1000 base pairs long and show elevated C+G dinucleotides composition [130]. DNA methylation of CpGs influences gene expression by directly inhibiting the interaction between DNA and transcription factors and by recruiting mediators of chromatin remodeling and histone deacetylases. These events together induce, and potentiate, the repression of gene transcription [120, 131].

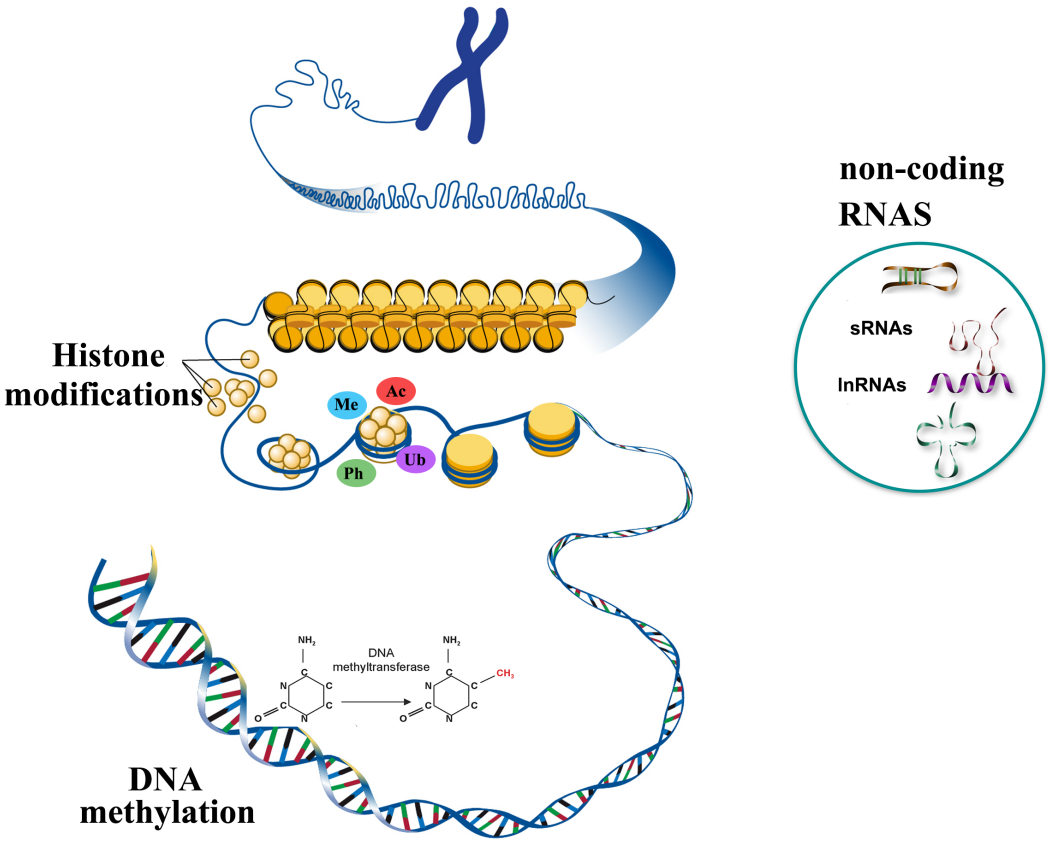

Figure 1.6 - Epigenetic Mechanisms
DNA methylation is one of the epigenetic mechanisms controlling gene transcription. It consists in the methylation of the cytosines but also adenine bases. Histone post translational modifications (histone acetylation, methylation, phosphorylation and ubiquitylation) and non-coding RNAs have important role in gene regulation and chromatin conformation. Non-coding RNAs can be divided in two major groups: small-RNAs (e.g. miRNAs, piRNAs, tRNAs) or long-RNAs.

1.7.1.2 Histone post-translational modifications

Eukaryotic cells store their genetic information in in a more than 1-meter long DNA molecule. To well pack this sequence in the nucleus, the DNA interacts with histone proteins in a complex called chromatin. The first level of chromatin organization is represented by the nucleosome consisting of two copies of each histones H3, H4, H2A and H2B. This octameric core constitutes the building blocks of the nucleosomes around which 146-147 bp of DNA are wrapped [132, 133]. Nucleosome cores are regularly spaced by the internucleosomal histone H1 known as the linker histone. Packaged nucleosomes form the so-called 30 nm fiber, which represents the next level of chromatin organization [134]. Histone proteins can be reversibly post-translationally modified (PTMs) by phosphorylation, glycosylation, ubiquitination, nitrosylation, methylation, acetylation and lipidation [135]. The outcomes of PTMs are different according to specific amino acid residue involved. Indeed, different histone modifications have been seen implicated in transcriptional activation, silencing, chromatin assembly and DNA replication [136-138]. Methylation of the lysines 9 and 27 of the histone H3, for instance, associates with chromatin compaction and transcriptional repression (heterochromatin), while methylation of lysine 4 of the histone H3 has the opposite outcome since enriched at the promoters of transcribed genes (euchromatin) [139, 140].

Polycomb and Trithorax are chromatin modifying complexes of enzymes that catalyze methylation of K27 and K4 respectively and known to antagonize each other [141, 142]. Histone acetylation also affects chromatin states and consists of transferring acetyl groups to histone tails with a consequential increase in the negative charge on chromatin, thus resulting in the opening of the chromatin structure to the transcriptional machinery. The balance between acetylation and deacetylation, operated by the histone modifying complexes, determines chromatin compaction and transcriptional activity.

Importantly, the activity of the modifying enzymes depends on the cellular availability of co-factors, products of cellular metabolism. Those factors, which are required for methylation and acetylation, highlight a strong connection between the nutritional state and epigenetics, hence metabolism and gene expression [143-146]. Lastly, alteration of cellular metabolism, secondary to either genetic or environmental insults, impact on methylation, chromatin structure and cellular transcriptional activity with direct consequences on the physiology [147, 148].

1.7.1.3 Non-coding RNAs

RNAs that are non-coding for proteins are a relatively newly discovered members of the epigenetic machinery. This family is composed of RNAs able to regulate gene expression in-trans according to specific sequences [149]. Contrary to the past, the majority of transcripts in the cell are now known to remain untranslated and some have been involved in vital functions [150, 151]. Two major families of non-coding RNAs can be distinguished, both the small (sRNAs) and the long RNA (lnRNAs) classes are involved in the epigenetic control of gene expression [152].

The family of sRNAs (< 200 nucleotides) includes five subclasses: microRNA (miRNA), endogenous small interfering RNA (endo-siRNA), ribosomal RNAs (rRNAs), transfer RNAs (tRNAs) and Piwi-interacting RNAs (piRNAs).

MicroRNAs are the most conserved and extensively studied. With their 21 nt long sequence, are able to suppress the translation of target mRNAs by binding the complementary sequence of the 3′untranslated Region (3'UTR) and inducing their cleavage. They are generated in the nucleus as 70 nt long precursors and then exported in the cytoplasm where processed and matured [153].

Endo-siRNA are similar to miRNAs and act in the same way but, while the first recognize a perfectly complementary target sequence on the mRNA, miRNAs bind a partially complementary one in the 3'UTR region [154]. Piwi interacting RNAs are instead small single stranded sequences made of 21 to 32 nucleotides identified in the fly testis as novel class of long siRNAs [155]. They are almost exclusively expressed in the germline and important for gonad development and fertility [156, 157].

PiRNAs are generated from longer precursors of various length transcribed from genomic regions called piRNA clusters, mostly located in the intergenic regions of the genome. PiRNAs associate with Piwi proteins that, with their RNase activity, are able to cut RNA targets. Nuclear Piwi proteins are guided by piRNAs to nascent transposon transcripts and silence transcription through DNA or histone methylation [158, 159].

In order to prevent excessive mutations in the germline, piRNAs repress transposable elements transcriptionally and post-transcriptionally [160]. Beyond the repression of transposition, very little is known about piRNAs function in regulating gene expression outside the germline [160]. Interestingly, in the mammalian testis many piRNAs have been identified featuring unique sequences not associated with transposition [161]. Recently, they have been seen playing roles in somatic cells and found involved also in chromatin modifications [160, 162-164]. The three Piwi proteins PIWIL1, PIWIL2, and PIWIL4 (also known as MIWI, MILI, and MIWI2) are highly expressed together with

piRNAs in the gonocyte stage and in the pachytene spermatocyte to round spermatid stage of mouse spermatogenesis [165]. More precisely, PIWIL2 and PIWIL4 bind to gonocyte piRNAs [166, 167] while PIWIL1 and PIWIL2 bind to pachytene piRNAs in the testis [168, 169]. Ectopic expression of artificial pachytene piRNAs leads to the degradation of the complementary reporter RNA in pachytene spermatocytes and round spermatids [170] suggesting an important role for pachytene piRNAs in the degradation of target RNAs during this period of spermatogenesis (e.g. LINE-1) [171].

Transfer-RNAs are the most abundant class of small noncoding RNAs constituting 4-10% of all cellular RNA. Their main role is to mediate the translation of mRNA sequence in polypeptide chain by delivering amino acids to the ribosome [172]. In the last years, high resolution data from the translating ribosome have shed light on tRNAs plasticity and have revealed new roles and functions beyond their being simple adapter molecules. Originally discovered in biological fluids and considered as just disease biomarkers [173, 174], tRNAs are now known as products of stress response [175, 176] and development, holding the potential to influence the epigenome transgenerationally [177, 178]. Synthesized as precursor, tRNAs are processed in the nucleus where they become mature and are transported via nuclear receptor [179].

LncRNAs, instead, are usually longer than 200 nucleotides and less conserved across species than the small ones. They are stable and tissue specific, mis-regulated in several diseases therefore holding biological relevance [180-182] with role into etiopathogenesis [183-185]. LncRNAs interact with DNA or other RNAs, including mRNAs and miRNAs, and regulate their expression through specific target sites. The long non-coding RNAs associate with ribonucleoproteins and protein-RNA complexes, and their ability to bind histone modification complexes as well suggests a role as chromatin modifiers [184, 186-188].

RNAs as DNA are susceptible to epigenetic modulation, importantly, they are capable of modulating epigenetic regulators such as methyltransferases (DNMTs) and histone deacetylases (HDACs), at the same time, they can also be methylated and influence gene expression [189]. The most frequent modifications involve the adenosine and cytosine bases. The adenosine methylation guides post-translational regulation in 3' UTR and within internal long exons [190, 191], the cytosine methylation instead occurs mostly in the tRNAs and affects the translation of target mRNAs [192].

Recently miRNAs, mRNAs and lncRNAs have been identified in biological fluids in protein [193, 194], lipid complexes [195, 196] and in extracellular vesicles [197]. Their presence in blood [198], breast milk [199], saliva [200] or seminal fluid suggests a role

in communication among cells and tissues, together with trans-acting translational regulation.

1.7.1.4 Chromatin modifying complexes

1.7.1.4.1 Polycomb repressive complex 1 and 2

Polycomb Repressive Complex 1 (PRC1) and 2 (PRC2) represent the two major and best characterized chromatin modifying complexes for establishing and maintaining gene silencing. They are organized around core components with different subunits (Figure 1.7) [201]. PRC2 catalyzes mono-, di- and tri-methylation of histone 3 lysine 27 (H3K27) via its enzymatic subunits Ezh1 and Ezh2 [202, 203]. PRC1 recognizes the PRC2-deposited H3K27me3 mark and promotes further silencing through the ubiquitination of the Lysin 119 of the Histone H2A. This modification, operated by the ubiquitin ligase Ring1a or Ring1b of the complex 1, although non-essential [204, 205], induces further compaction of the chromatin [206]. Discovered in *D. Melanogaster* as regulators of embryonic development and body patterning [207], PRC1 and PRC2 are both required to maintain gene repression.

H3K27me3 is a stable mark resulting from mono-methylation of H3K27me2 [208]. This mark helps to stabilize cell identity by blocking alternate lineage programs and prevents the expression of embryonic genes in other phases of life [209]. A growing body of evidence suggests that PRC2 activity is important for spermatogenesis [210-212] and sperm architecture [213-216] and it is known to mediate epigenetic inheritance from plants to *Drosophila Melanogaster* [217, 218]. Other recent studies have seen PRC2 implied in the control of metabolic homeostasis including diabetes and obesity, elucidating the impact of chromatin regulation on metabolic signaling [156, 219-221]. The mammalian core of PRC2 is composed of histone methylases (EZH2 or EZH1), Embryonic Ectoderm Development (EED), Suppressor of Zeste (SUZ12) and the CAF1 histone binding proteins RBBP4 and RBB7. This structure is very well conserved among plants, animals, fungi and some yeasts [209, 222, 223]. Although highly conserved, Polycomb complexes differ significantly between species. The association of different subunits with the core enzymatic site of PRC2 specializes the complex for particular cell types. In this respect, different subunits form alternative PRC2 complexes [224, 225] (Figure 1.7A lower panel).

De novo recruitment of Polycomb Group Proteins (PcG) is highly debated. Evidence suggest that it does not rely on histone modifications [226], however, it can be guided by

multiple factors such as gene-specific transcriptional factors (repressing target genes), chromatin landscape or by the transcriptional state, long non-coding RNAs and also unmethylated CpG islands [206, 227-229].

Studies in *Drosophila* have also revealed the existence of binding sites or PcG proteins with sequence specific DNA binding activity, located in chromatin regions mostly devoid of nucleosomes [230]. Those sequences go under the name of Polycomb Responsive Elements (PREs) and represent assembly platform for the different PcG complexes through DNA-protein and protein-protein interactions.

Once PcG-mediated repression is established, it is maintained for indefinite number of cell cycles until reversed, in order to allow activation of cell specific gene programs [231].

Several models for the *de novo* recruitment of PcG have been proposed, some have reversed the hierarchical paradigm and suggest that PRC1 binding is independent from PRC2 and that the latter is instead guided by the monoubiquitylated H2A [226].

Many factors may contribute to stabilizing the chromatin and mediating the recruitment of PcG complexes which operate in turn with reciprocal feedback [232]. More research is necessary to dissect the complex mechanism of this tight regulation.

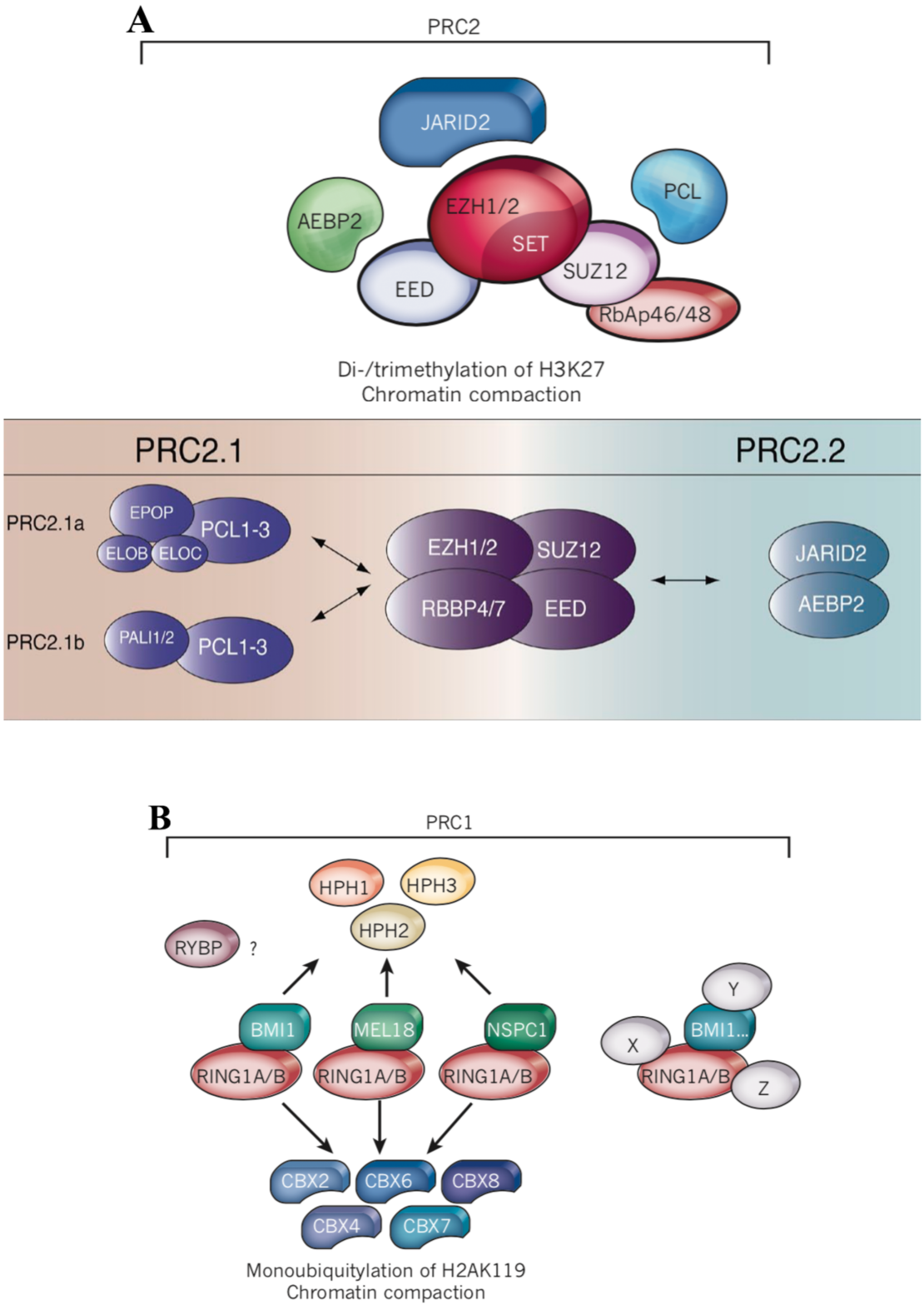

Figure 1.7 - Mammalian PRC2 and PRC1 complexes
A (upper panel). Classical polycomb repressive complex 2 components. **A (lower panel).** Association with PCL proteins defines a PRC2.1 subtype that can associate with either EPOP or PALI1/2 (PRC2.1a/b). Conversely, association with AEBP2 and JARID2 defines a PRC2.2 subtype. Modified from [202] **B.** Diagram showing classical component of PRC1. Modified from [204].

1.7.1.4.2 Thrithorax complex

Thrithorax group (TrxG) proteins form a heterogeneous complex involved in the gene expression of key genes in differentiation. TrxG plays a role in widespread activation of transcription during development and it is essential for the memory of active state over many cell generations [233]. However, TrxG is well known for being Polycomb antagonist in the establishment of epigenetic memory.

Two groups of TrxG have been identified, one regulates chromatin structure of a large number of genes involved in cell cycle and proliferation while the other is associated with histone modifying capacity through acetylation and methylation of the lysine 4 on histone H3 at bivalent promoters [234, 235], therefore counteracting the PRC2 activity on histone H3 [209].

Promoters simultaneously marked with H3K27me3 (repression) and H3K4me3 (activation) are called bivalent (poised). As a result, they are transcribed at very low levels and can be either activated or repressed depending on the cell state during the progression of embryogenesis. Indeed, H3K27me3 and H3K4me3 are found to be enriched at developmental genes in the mouse germ cells [236, 237], embryonic stem cells [238] and pre-implantation embryos [239] as well as several adult tissues such as testis, brain and blood cells [240-243]. They are characterized by low DNA methylation levels and are Pol2 (DNA Polymerase catalytic subunit) and RNA-seq negative [244] thus transcriptionally silent. Poised chromatin is necessary for the maintenance of undifferentiated state in embryonic stem cells, this bivalent system allows at the same time the relieve of silencing of pluripotency genes by TrxG and the blocking of alternative cell-fate genes by Polycomb proteins [245].

1.7.1.5 Transgenerational Epigenetic inheritance in mammals

Obesity and metabolic disease spread worldwide in a way that cannot be explained only with genetic. Population and familial aggregation observed in complex diseases may also reflect similar environmental inputs and therefore epigenetic influences. Accordingly, it is assumed that environmental factors impact on epigenetic processes in somatic and germ cells. Indeed, pre- and periconceptional environmental exposure can influence the embryonic development through alteration of gene expression leading to different phenotypes [246-248]. The idea of acquired inheritance have been introduced by Lamarck in the 19th century and discredited by most Mendelian geneticists. The principle is that physical changes during the lifetime can be transmitted to the offspring. Today,

this inheritance refers to transmission of environmentally induced phenotypes to the following generations, most likely through epigenetic mechanisms.

The terms “intergenerational” and “transgenerational" describe different phenomena of inheritance which depend on the number of generations affected. With the exposure occurring before conception, the term transgenerational refers to effect of environmental exposure at least up to the unexposed F2 generation (Figure 1.8). When the exposure occurs during pregnancy, instead, primordial germ cells in the fetus (F1) are also exposed, resulting in intergenerational transmission to the F2 generation. In this case, to have a transgenerational effect, the alteration must be observed at least until the unexposed F3 (Figure 1.8) [249, 250].

Epidemiological studies have provided some evidence of intergenerational inheritance in humans whose underlying mechanisms remain largely unclear. They aim at exploring how the lifestyle, education and environmental stress, which vary between communities and families, can affect outcomes and achievements from birth through lifetime and from one generation to the next.

In mammals, germ and somatic cells are separated by a genetic barrier, which allows the transfer of genetic and epigenetic information only from the germline to the nascent embryo. However, the Lamarckian theory of acquired characteristics and the capacity to reprogram somatic cells to a pluripotent stem cell (iPSC) opened the road to the idea that environmental cues could also flow from soma to germline thus making the epigenetic inheritance possible also for mammals [251]. The rapid changes in socio-economic status and nutritional habits, as well as the physical inactivity and unhealthy behaviors correlate with the rapid increase of complex metabolic disease and diabetes proposing the acquired inheritance as a potential explanation for the influence on offspring metabolic health [252, 253].

Ruling out external contributions in humans is unlikely to be possible, therefore most of our knowledge on epigenetic inheritance comes from studies in rodents and lower organisms. Exposure to toxicants or chemicals, nutrition and exercise influence the metabolic health of the directly exposed in several ways but, most importantly, also the health of unexposed progeny [254].

While maternal under or overnutrition have been reported to affect offspring development and adult traits [255-262], paternal influence instead is less known but it is nowadays attracting equal attention. Indeed, emerging evidence indicate that the developing embryo is not only controlled by the maternal influence. In this respect, the most indicative epidemiological study is perhaps the one concerning the Överkalix population in Sweden. This study revealed that paternal overnutrition during prepubescence correlated with increased risk of metabolic and cardiovascular defects in grandsons, thus indicating that a paternal environmental influence can have transgenerational effects and that the slow growth phase (prepubescence) is a sensitive period [263]. Experiments in mice confirmed

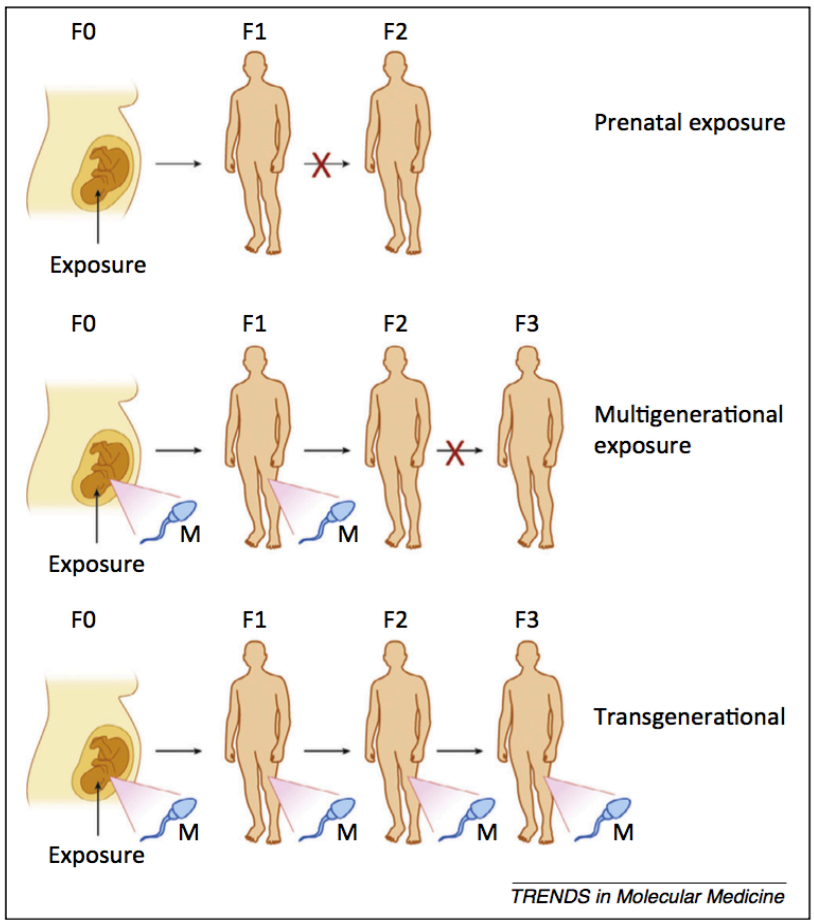

Figure 1.8 - Inheritance across generations
Different modalities of multiple generational transmission of parental experience. **Top**: prenatal exposure. The F0 mother is exposed during pregnancy together with the F1. F1 is programmed in somatic tissues but not germline and does not transmit the phenotype to the F2. **Middle**: multigenerational exposures. The F1 generation is exposed and the developing germ cells are modified so that the sperm of F1 will affect F2 development and phenotype. However, reprogramming of this modification during primordial germ cell differentiation of F2 will prevent transmission of the phenotype to F3. **Bottom**: transgenerational inheritance. The F1 gametes are modified during gestation and exposure of the F0 mother. The modified F1 sperm affect F2 development. If gamete modification is not erased during primordial germ cell differentiation the sperm of F2 are modified as well and will transmit the phenotype to F3. Modified from [116].

these findings and revealed the important role of the father in the offspring metabolic reprogramming, in particular, they highlight how the sperm epigenome is very sensitive to the external stressors [264-267].

1.7.1.6 Epigenetic inheritance of metabolic traits

In mammals, a functional gamete is a haploid cell that fuses with another haploid cell to generate a zygote. Gametogenesis is therefore a process in which a diploid germ cell undergoes reduction divisions, known as meiosis. Oogenesis and spermatogenesis are quite different in terms of achievement and time of occurrence during development. In females, the gametes are produced in a defined number and in a process that starts already before birth. Oocytes are used periodically over a phase of life and cannot be regenerated. In males instead, spermatogenesis starts only during puberty with the aim to generate millions of sperm cells in a continue process throughout life [268].

Spermatogenesis can be divided in three phases, a mitotic amplification phase, a meiotic and a post-meiotic phase called spermiogenesis (Figure 1.9). The mature sperm expelled from the organ (spermiation) induces the start of a new generation of germ cells originated from spermatogenic stem cells. In this respect, spermatogenesis and spermiation must be coordinated in order to maintain continuous sperm production. The time required for the maturation of germ cells is 64 days in human [269] and around 40 in mice [270]. The spermatogonium cell (SSC) is the stem cell from which the mature sperm cell is generated. Its self-renewal is important to maintain the population in the testis and to generate sperm progenitors such as spermatogonia, spermatocytes and spermatids in a process of mitotic expansion, reduction and morphological transformation, to finally end up with the mature form of the sperm cell. Sperm cells develop in the seminiferous tubules, get released into the lumen and reach the epididymis where they further mature (Figure 1.9). Spermatogenesis is determined by interaction of germ cells and somatic cells of the testis together with growth factors, so that any alteration of this complex interplay may lead to male infertility.

The first round of spermatogenesis in mice refers to the first germ cells that results in spermatozoa. It originates from an undifferentiated pool of “A prospermatogonia” that undergoes to an irreversible transition to differentiating “A1 spermatogonia” already at 2 days post-partum in the mouse and signifies the commitment to meiosis ending in spermiation 35 days later. Of note, a group of prospermatogonia remains undifferentiated and represents the pool of stem cells necessary for new generations.

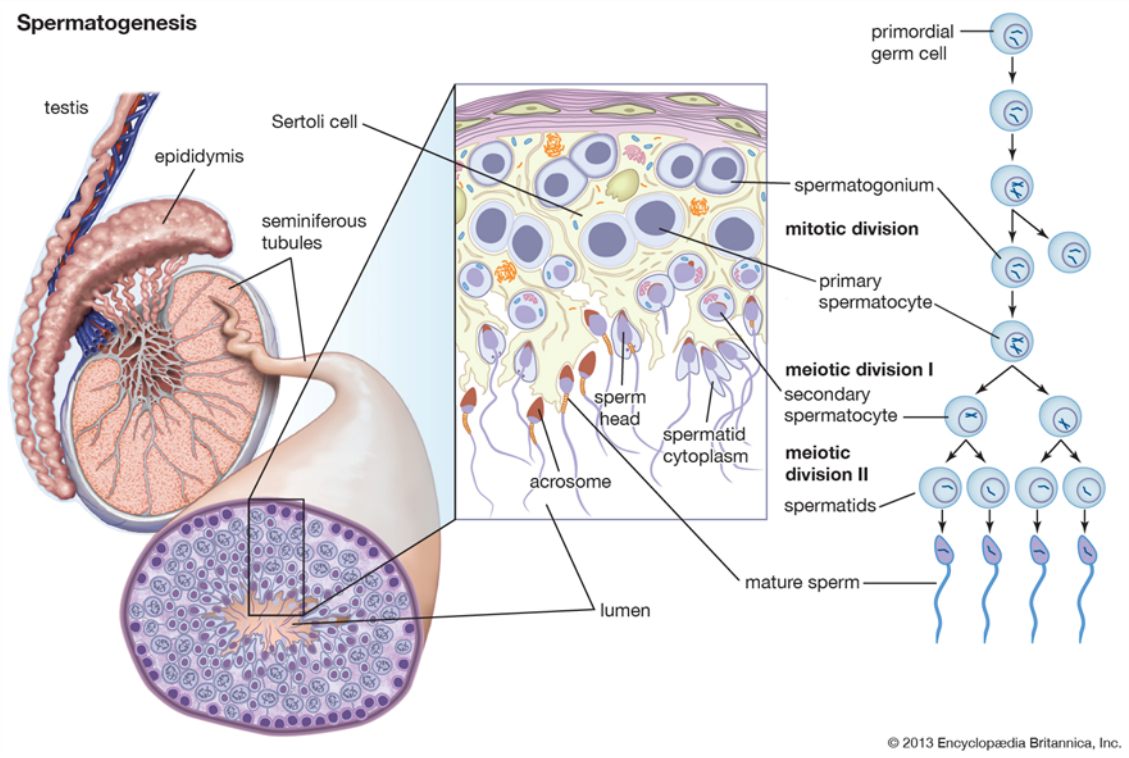

Figure 1.9 - Spermatogenesis in mammals
The mature sperm originates from one mitotic and two subsequent meiotic divisions. Primordial germ cells give rise to spermatogonium, the stem cell able of self-renewal, which undergoes through mitotic division to form the primary spermatocyte. The first meiotic division generates the secondary spermatocyte while the second forms the haploid spermatids. The latter develop to mature sperm that will be released in the lumen. (Encyclopedia Britannica, Inc., 2013).

The transition from A to A1 spermatogonia is followed by several divisions from A2 to A4 to reach the "B spermatogonia" stage, finally resulting in preleptotene spermatocyte through the final mitosis [271].

More precisely, the entire spermiation process in mouse from the A to A1 spermatogonia transition takes 35 days. The initiation of this process, however, occurs more frequently. Indeed, every 8.6 days new germ cells enter spermatogenesis, allowing their presence at any point along the seminiferous tubule [268]. This organization goes under the name of asynchronous spermatogenesis, it refers to asynchronous commitment to meiosis and it is highly conserved among species.

In order to generate germ cells with a hydrodynamic shape, chromatin undergoes through compaction by replacement of histones with protamines [272]. However, about 1-10% of the sperm genome retain histones (together with their posttranslational modifications), at loci important for embryonic development, suggesting potential mechanism of action of

epigenetic inheritance acting through it [273]. The retained histones have been observed mostly located at non-methylated CpG islands and modified on lysine 4 and 27 of the histone H3 [215, 274]. Apart from protamines and histones, the sperm epigenome is composed of methylated DNA and snRNAs [215, 216, 275, 276]. The paternal epigenetic information is almost completely erased at fertilization and established only later in development [277], at the same time, protamines are released from the genome and replaced by maternal histones [272]. Mainly, these steps are necessary for the generation of a totipotent zygote, as well as for the removal of paternal epigenetic signature and allow the development starting from one cell to complex multicellular organism [130, 278].

Some classes of snRNA (e.g. piRNAs), either derived from the spermatogenesis or acquired during the epididymal transit (e.g. tRNAs), are transferred to the zygote and contribute to embryonic development and adult health [177, 279-282]. Those RNAs are important for the preimplantation phase of development but are also subjected to the influence of external factors, which can alter RNA composition in the mature sperm and seminal fluid and promote metabolic disorders in the progeny [177, 178, 283]. Independent studies suggested that tRNAs are involved in the intergenerational effects of paternal dietary challenge. For instance, diet manipulation such as low-protein diet affects tRNA methylation [177, 284] and cause offspring metabolic disorders through the effect of Glycine tRNA fragments transferred during fertilization [178].

Apart from snRNAs, sperm DNA methylation is another mechanism involved in the epigenetic inheritance of phenotypic traits. Indeed, in utero undernutrition [285], pre-conceptional cold exposure [286] and prediabetes [246] impact on the DNA methylome and have effects on the next generations. Although these studies present great correlation between DNA methylation reprogramming and phenotypic traits, a direct connection is still lacking.

Histone post-translational modifications as well can mediate epigenetic inheritance. Indeed, levels of H3K27 and H3K4 methylation in the oocytes influence the embryonic chromatin and development [287-289]. In line with the evidence that some genomic regions in mature sperm escape the epigenetic reprogramming, genetic manipulation of chromatin structure during spermatogenesis has effects on wild-type progeny [290, 291]. Indeed, genetically induced demethylation of H3K4 causes chromatin remodeling in embryonic and metabolic loci of mature sperm with consequent alterations in embryonic development across three generations of wild-type descendants [290]. On the same line, a germline specific genetic disruption of Polycomb repressive complex 2 (PRC2)

determines reduction in male fertility and increased expression of transposable elements in the germ cells with alteration of the early embryonic development [291].

The embryo is massively reprogrammed after fertilization [292]. Despite that, paternal chromatin influences the embryonic heterochromatin in both humans and mice with different mechanisms. While in mice the paternal chromatin is recognized by the maternal PRC1 complex [293], in humans, paternal heterochromatin is propagated over the embryonic development by the maternal H3K9/HP1 pathway, highlighting the importance of the sperm chromatin on embryonic chromatin architecture and health in mammals [294].

1.8 Aim of the study

The investigation of genetic variability within individuals revealed that genetic alone cannot explain the rapid increase of obesity and metabolic disease and suggested that other factors are involved in the pathogenesis. Lately, evidence of an inheritance different than the classical genetics is attracting scientists' attention who aim at understanding how the historical background and environmental cues can directly, or indirectly, influence gene expression and give rise to unhealthy phenotypes. Genetic loci found associated with the metabolic phenotypes do not account alone for classical family aggregation observed in T2D, indicating that shared environment strongly impacts on the disorder through epigenetic mechanisms. Indeed, epigenetics appears as the gap filler of the missing heritability problem holding the potential to explain, at least in part, the susceptibility to diseases.

Epidemiological studies and experiments conducted in mice suggested that the lifestyle of the parents not only influence their health but also the one of their offspring. Besides the epigenetic reprogramming occurring during embryonic development and then in the gametes, some epigenetic marks resist the reset, holding potential to be transferred to the newborns. In spite of the many discoveries, mechanisms controlling the inter- or transgenerational epigenetic inheritance are still missing. The scientific community is currently working on answering these questions:

- *How does environmental information acquired by the somatic cells reach the germ cells for inheritance?*
- *How do the epigenetic marks acquired, as consequence of environmental exposure, escape the reprogramming?*
- *How could epigenetic therapy be used for disease prevention and treatment?*

While it is very well established that the maternal environment before and during pregnancy directly affect the health of the progeny, it became evident in the last years that also the father contributes significantly to the children health by affecting embryonic development.

In this context, the aim of this thesis is to shed light on the paternal contribution on offspring metabolic health and to dissect epigenetic mechanisms behind obesity and metabolic derangement. To this purpose, I have investigated the metabolic risk of children from overweight and obese individuals and recreated the condition in male mice to potentially dissect the molecular mechanism behind.

With the goal of finding inheritance of metabolic traits in children born to overweight or obese fathers, the current study utilizes the Leipzig LIFE human cohort (composed of thousands of trios of parents and children) and, based on the evidence found, will proceed with:

- Generation of a mouse model by challenging animals with an acute high fat diet exposure to reproduce the paternal overweight condition
- Examine unexposed offspring, derived from challenged fathers mated with unexposed females, to potentially observe inheritance of metabolic traits
- Investigation of molecular mechanisms by combining knowledge of physiology with molecular biology expertise
- Identification of common mechanisms in human

2. MATERIALS AND METHODS

2.1 Materials

2.1.1 Solutions and consumables

Buffers and Solutions	Recipes
Blocking Buffer	Tween 1x PBS 1x
Cold Lysis Buffer (ATAC)	10 mM Tris HCl, pH 7.4 10 mM NaCl2 3 mM MgCl2 0.1% Igepal (Np-40) 0.1% Tween-20
Digestion Solution 1	DMEM 4mg/ml Collagenase IV 20µg/ml DNase I
Digestion Solution 2	DMEM 4 mg/mL Collagenase IV 20 µg/mL DNase I 0.66 mg/mL Hyaluronidase
DNA Extraction (from ear clips)	10 mM NaOH 2.5 mM EDTA dH2O
MACS Buffer	1% PBS 0.5% bovine serum albumin (BSA) 2 mM EDTA
PBS Tween	1% PBS 1% Tween-20
Sperm Motility Medium	135 mM NaCl 5 mM KCl 1 mM MgSO4 2 mM CaCl2 30mM Hepes pH7.4 10 mM Lactate Acid 1 mM Sodium Pyruvate 20 mg/mL BSA 25 mM NaHCO3
Transposase Mixture	2X TD Buffer 16.5 µl 1X TDE1l 0.1% Tween-20 0.05% Digitonin dH2O

2.1.2 Chemicals and reagents

Chemical	Company	Catalogue No.
100 Bp DNA Ladder	Invitrogen - Thermo Fisher	15628019
Acid Tyrode Solution	Sigma Aldrich	T1788
Agarose	Sigma Aldrich	A9539
Agencourt ®Am Pure ® Xp	Beckman Coulter	A63882
Antigen Retrieval	Santa Cruz	6132-04-3
Bolt LDS	Life Technologies	BT00061
Bolt™ Sample Reducing Agent	Life Technologies	B0004
Bolt™ Transfer Buffer (20x)	Invitrogen - Thermo Fischer	Bt00061
Bradford Reagent	Sigma Aldrich	B6916
BSA	Sigma Aldrich - Life Science	A4503
Calcium Chloride	Sigma Aldrich	449709
Collagenase	Sigma Aldrich	C5138
Cryoprotect II	Nidacon International	-
Digitonin	Promega	G9441
DNA Gel Loading Dye (6x)	Thermo Fisher	R0611
DNase I	Sigma Aldrich	DN25
Donkey Serum	Sigma Aldrich - Life Science	D9663
EDTA	PanReac Applichem	A3145
Eosin	Sigma Aldrich	1024390500
Ethanol	Merck	100983
Fast Sybr™ Green Master Mix	Thermo Fisher Scientific	4385612
Formaldehyde Solution	Sigma Aldrich	F-8775
Gelred® Nucleic Acid Gel Stain	Biotium	41003
Glucose	Sigma Aldrich	G8644
Glycogen	Thermo Fischer Scientific	R0561
Haematoxylin	Sigma Aldrich	1051750500
HCG - OVOGEST	MSD	340100
Hepes	Fluka	54469
HTF - Human Tubal Fluid	Irvine Scientific	9922
Hyaluronidase IV	Sigma Aldrich	H4272
Hydrogen Peroxide	Supelco	1060971000
Igepal (NP-40 Substitute)	Sigma Aldrich	I8896

Ketamine	Heinrich Fromme	-
Magicmark™ XP Western Protein Standard	Invitrogen - Thermo Fisher	LC5602
Magnesium Chloride Solution	Sigma Aldrich	M1028
Magnesium Sulfate	Fluka	63138
Methanol	Merck	113351
NaCl 0.9%	B Braun	L4263
NebNext Master Mix	NEB	M0541S
Paraformaldehyde	Thermo Fischer Scientific	P/0840/53
PBS	Gibco - Thermo Fisher	10010023
PCRMaster Mix	Thermo Fisher Scientific	K0171
Pmsg - SERGON 500 IU/ml	BIOVETA	665624A
Potassium Chloride	Sigma Aldrich	P9333
Proteinase K	Invitrogen - Thermo Fisher	EO0492
Purelink™ Rnase A	Invitrogen - Thermo Fisher	12091021
PureSperm	Nidacon International	-
Pursept® A Xpress	Schülke	-
Rnase AWAY®	Thermo Fisher Scientific	83931
Rotiphorese ® (50x) TAE Buffer SL	Carl Roth	CL86.2
Seeblue™ Pre-Stained Protein Standard	Invitrogen - Thermo Fisher	LC5925
Sodium Bicarbonate	Sigma Aldrich	S5761
Sodium Chloride	Sigma Aldrich	31434
Sodium DL-Lactate Solution	Sigma Aldrich	L4263
Sodium Hydroxide (NaOH)	Sigma Aldrich	655104
Sodium Pyruvate	Sigma Aldrich	P2256
Sucrose	SAFC	RE509285-A102X
Sybr™ Green I	Invitrogen Thermo Fischer	S7563
Tris-HCl ph 7.4	Sigma Aldrich	T2319
Triton	Sigma Aldrich	X-100
Trizol	Invitrogen Thermo Fisher	15596026
Tween-20	Panreac Applichem	A4974
Vectashield	Vector Laboratories	H-1200
Cre Recombinase, TAT-Cre	Excellgen	RP-7

2.1.3 Kits and consumable

Product	Company	Catalogue No.
EpiQuik Global Acetyl Histone H3K27 Quantification Kit (Colorimetric)	Epigentek	P-4059
EpiQuik Global Tri-Methyl Histone H3K27 Quantification Kit (Fluorometric)	Epigentek	P-3043
Epiquik Total Histone Extraction Kit	Epigentek	OP-0006-100
EpiQuik Total Histone H3 Quantification Kit (Colorimetric)	Epigentek	P-3062
High Sensitivity DNA Kit	Agilent	5067-4626
i7 Index Plate for QuantSeq/SENSE for Illumina	Lexogen	044
LS Columns	Miltenyi Biotec	130-042-401
M tubes	Miltenyi Biotec	130-093-236
MethylFlash Global DNA methylation (colorimetric)	Epigentek	P-1030
MinElute Reaction Cleanup Kit (50)	Qiagen	28204
Mouse/Rat Insulin Kit	Meso Scale Diagnostics (MSD)	K152BZC
Nextera DNA Flex Library Prep Kit	Illumina	20018704
Pierce™ ECL Western Blotting Substrate	Thermo Fisher Scientific	32106
PureLink™ Genomic DNA Mini Kit	Invitrogen	K182001
QuantSeq 3’ mRNA-Seq Library Prep Kits for Illumina	Lexogen	015
Qubit™ dsDNA HS Assay Kit	Thermo Fisher Scientific	Q32854
RNA 6000 Pico	Agilent	5067-1513
V-PLEX Plus Proinflammatory Panel1 Mouse Kit	Meso Scale Diagnostics (MSD)	K15048G

2.1.4 Antibodies

Antibody	Company	Catalog No.
Anti H3K27me3	Millipore	07-449
Anti H3K27ac	Diagenode	C15410196
Anti Tra98	Abcam	Ab8252
Anti-rabbit IgG	Cell Signaling	70704
CD326 (EpCAM) MicroBeads	Miltenyi Biotec	130-105-958

2.2 Methods

2.2.1 Human study

2.2.1.1 Life Child population

LIFE Child Study is a prospective regional population-based longitudinal observational study aimed at characterizing contributing factors for civilization disease with comprehensive phenotyping including data on parental BMI and BMI of the offspring conducted in the city of Leipzig, Germany [295, 296]. For the assessment of association of parental weight and the clinical phenotype of the offspring children, data from the LIFE Child Study have been analyzed. With recruitment age ranging between the 24th week of gestation and 16 years of child age and annual follow-ups, the study combines a cross-sectional with a longitudinal design and covers a broad age range (NCT02550236). A LIFE Child substudy specifically focused on the origin and sequelae of childhood obesity in the frame of Leipzig Childhood Obesity Cohort. After exclusion of children with present or past severe disease (e.g. type 1 diabetes, syndromal obesity, cancer) and present or past interfering medical treatment (eg. insulin, immunosuppressive, growth hormone), children with both parental BMIs available into the analysis ($n = 3432$) have been included. In case of multiple visits, anthropometric data of the most recent visit of the child have been used. Parental data refers to the closest to the birth of the child.

2.2.1.2 Human sperm isolation and count

For human sperm analysis, semen samples were collected after at least 48 hours of sexual abstinence in the andrology laboratory of the University of Turku (Finland). Standard semen analysis, including semen volume, pH, sperm concentration, total sperm counts, percentage of motile sperm, and percentage of sperm with normal morphology was performed according to the World Health Organization Laboratory criteria. Spermatozoa were purified by centrifuging through a 50% gradient of Puresperm (Nidacon International AB). After washing with PBS, the purity was evaluated microscopically, spermatozoa were counted, resuspended in Sperm CryoProtec II (Nidacon International AB) and shipped to the research laboratory in Germany. Spermatozoa were further purified from somatic cell contamination by washing with somatic cell lysis buffer [297]. The purity of samples was validated microscopically. Spermatozoa were further counted and $20x10^6$ cells used for histone isolation.

2.2.2 Mouse study

2.2.2.1 Animal housing, diet composition and breeding strategies

Wild-type animals used in the study were purchased from Charles River Laboratories of Germany and co-housed at constant temperature (22 ± 1 °C) and controlled humidity in ventilated cages in the German Mouse Clinic at the Helmholtz Zentrum München (Germany) on a 12h light/dark cycle and fed ad libitum, according to the European Union directive and approved by the government of Upper Bavaria. For the 2 weeks diet challenge, 6 weeks old C57Bl/6J male mice were fed with high HFD (Rodent Diet with 60% Kcal from fat – Research Diet D12492i) or control LFD (Rodent Diet with 10% Kcal from fat – Research Diet D12450B). At the end of the 2weeks, each male was mated singularly with an unexposed female of the same strain, genetic background and age. During the mating, males and females had access to the chow food without restriction. To avoid isolation and social dysfunction, the female was kept with the male during the entire pregnancy. After the delivery, the mothers were maintained individually for nursing and lactation and the litter size, whenever higher, was adjusted to 8-9 pups to avoid undernourishment and to rule out potential litter effects. Offspring from LFD or HFD-fed mice where named first generation (F1). The F1 animals were weaned at 3 weeks of age, according to the standard procedures, and kept on ad libitum chow diet for their entire life. Six males descending from LFD and HFD fed fathers were mated with as many unexposed wild-type females for each generation. In the F1 generation HFDt and HFDi mice, coming from HFD challenged fathers, have been identified because showing glucose tolerance (HFDt) or intolerance (HFDi). F2 refers to the second generation raised from F1 males and unexposed wild-type females, at the age of 20 weeks. HFDt and HFDi subpopulations were followed up to the F2 generation. As for the F1, F2 animals had access to the chow diet starting from the weaning age for the rest of their life.

Eed heterozygous (Eed-het) mice have been generated via *in vitro* fertilization with Eed floxed (B6;129S1-Eedtm1Sho/J - JAX strain #022727 / RRID:IMSR_JAX022727) sperm and wild-type oocytes. Zygotes have then been treated with soluble Cre enzyme (Excellgen #RP-7 – 0.3) for 30 minutes to generate heterozygote embryos for transfer to, previously prepared, foster mothers. Eed line has been kept on chow diet for the entire life. Genotypic quality control has been carried out by PCR on blastocysts (to check Cre-mediated deletion in embryos) and ear clip-derived genomic DNA as described later on this section. Mice were backcrossed to the C57B/6J background for six generations for

Eed. Offspring animals have been used as F0 for the generation of the phenotyped wild-type progeny.

All animal experiments have been performed according to European Union directive 2010/63/EU and were approved by the responsible authorities of the government of Upper Bavaria (Germany). All efforts have been made to minimize suffering by considerate housing and husbandry. All phenotyping procedures were examined for potential refinements. Animal welfare was assessed routinely for all mice involved.

2.2.2.2 Genotyping

DNA is extracted from ear clip samples obtained at weaning time through 15 minutes incubation at 95 °C in 300 ul of 10mM NaOH and 2.5 mM EDTA dissolved in dH2O2. To determine the genotype of the Eed cohort, specific oligonucleotides were used to amplify defined fragments of the genome by polymerase chain reaction (PCR) as previously described [298]. For one PCR reaction three-primer PCR method was used to amplify wild-type, floxed, and deleted allele using reverse and forward oligonucleotide sequences:

Forward	CTACGGGCAGGAGGAAGAG
Reverse #1	GGGGGAGAGGGAGTTGTC
Reverse #2	CCACATAGGCTCATAGAATTG

Polymerase chain reaction was conducted in the thermal cycler following standard protocol. DNA fragments were separated on a 2% agarose gel according to their sizes in an electric field, with the smallest moving faster through the pores of the agarose gel matrix. For visualization of the DNA in UV light GelRed (Biotium) was diluted in the gel.

2.2.2.3 Body weight and composition

Regarding F0 LFD/HFD fed mice, body weight, together with lean and fat mass were analyzed before and after the challenge. In particular, body composition was determined by *in vivo* nuclear magnetic resonance (NMR) spectroscopy with a Minispec mq NMR analyzer (Brucker Optics, USA). The measurement was performed also for the F1 and F2 generations deriving from the challenged F0 mice, as well as for the wild-type/Eed-het

cohort. To avoid repeated stress, the procedure was executed every 4 weeks, starting from the 6th week of age until the 14th.

2.2.3 Metabolic phenotyping

2.2.3.1 Glucose tolerance test

Glucose tolerance was measured after an intraperitoneal injection of glucose subsequent an overnight fasting period of 16h. The intraperitoneal glucose tolerance test (ipGTT) entails injection of 2 g of glucose per kg of fasting body weight. Blood glucose levels were determined, from a drop of blood from the tail vein, before and after injection at 15, 30, 60 and 120 minutes using the Accu-chek Aviva blood glucose meter (Roche). At the same time, plasma samples were separated from the whole blood through EDTA-coated microvettes (Microvette® 100 K3E - Sarstedt) at time 0, 30, 60 (minutes) and snap-frozen in liquid nitrogen for further insulin analysis.

2.2.3.2 Insulin secretion and pro-inflammatory cytokine measurement

Insulin secretion was measured in plasma obtained from ipGTT test using Mouse/Rat insulin Kit of the Meso Scale Diagnostics (K152BZC). The 96-well plates were measured in the QuickPlex SQ 120 machinery, through electrochemiluminescence detection of insulin. Experiments were conducted according to the manufacturer's instructions. Plasma cytokine levels (Interferon γ (IFN-γ), IL-1β, IL-2, IL-4, IL-5, IL-6, KC/GRO, IL-10, IL-12p70) and TNF-α of the F0 LFD/HFD challenged mice blood samples were analyzed using the V-PLEX Proinflammatory Panel 1 Mouse Kit (Meso Scale Discovery) in the QuickPlex machine according the manufacturer's instructions.

2.2.3.3 Insulin tolerance test

To verify the glucose response after insulin injection, mice were tested with the insulin tolerance test (iTT). Mice were fasted at 8 am for 6 hours; at the time of the experiment, mice were injected with 0.5 U insulin/kg of fasting body weight. Blood glucose levels were analyzed from blood drop of the tail vein before and after the intraperitoneal injection at 15, 30, 60 and 120 minutes.

2.2.4 Biochemistry

2.2.4.1 Histone isolation

Total histone isolation from mature and developing germ cells was performed using the Epiquik Total Histone Extraction Kit (Epigentek) according to the manufacturer's instructions. The protein concentration was quantified with the plate reader Varioskan Lux (Thermo Scientific) with BSA used as a standard.

2.2.4.2 Western blot and ELISA assays

Western blot were performed using 5 µg of crude histone mixture extracted from testicular germ cells as previously described [299]. Histones for ELISA have been isolated with the Total Histone Extraction Kit (Epigentek) and subsequently 200 ng of total extract have been analyzed using Epigentek kits for H3K27me3 modification [EpiQuik Global Tri-Methyl Histone H3K27 Quantification Kit (Fluorometric)], for H3K27ac [EpiQuik Global Acetyl Histone H3K27 Quantification Kit (Colorimetric)] and for total H3 [EpiQuik Total Histone H3 Quantification Kit (Colorimetric)] according to the manufacturer's instructions. To quantify global DNA Methylation (5-methylcytosine), genomic DNA has been extracted from developing germ cells or mature sperm cells according to PureLink Genomic DNA kit (Invitrogen) instructions. DNA has been quantified with nanodrop spectrophotometer and 100 ng used for ELISA MethylFlash Global DNA methylation (colorimetric) (Epigentek) according to manufacturer's instructions.

2.2.5 Immunohistochemistry

2.2.5.1 Staining and histology

Sections were fixed for 48h in 10% formalin, dehydrated through ethanol series, cleared in xylene and embedded in paraffin. After rehydration, 4 mm sections were stained with hematoxylin and eosin, according to the manufacturer's instructions. For immunohistochemical analysis, 1.5 mm sections were dewaxed by standard techniques. Heat treatment was performed for antigen retrieval in sodium citrate buffer. Endogenous peroxidase activity was quenched with 3% H_2O_2 in methanol at room temperature for 5 minutes. Incubation with primary antibodies was performed overnight at 4°C in blocking buffer (TBS- Tween 1%), and chromogenic reactions were carried out. Automatic: sections were processed by automated staining using the automatic Discovery XT

(Ventana Systems) stainer, following preset protocols. Sections were subjected to ethylenediaminetetraacetic acid (EDTA) based antigen retrieval for 20 minutes. Sections were then examined under an Olympus microscope. The primary antibodies used were the following: H3K27me3 (Millipore 07-449), H3K27ac (Diagenode C15410196), TRA98 (Abcam Ab8252) in a dilution 1:1000. As secondary antibody the polyclonal anti-rabbit (Cell Signaling IgG #7074).

2.2.5.2 Evaluation of adipose tissue cellularity of histological sections

Visceral and subcutaneous fat sections from LFD/HFD challenged mice were imaged, after haematoxylin-eosin staining, at 20x magnification with an Olympus microscope and counted and analyzed using the Adiposoft software [300].

2.2.6 Cell sorting

2.2.6.1 Sperm isolation, count and developing germ cell isolation

Mouse sperm cells were collected from paired cauda epididymis C57BL/6J mice by using a swim-up procedure as described [215]. Mature spermatozoa of caudal epididymis were incubated for 1 h total at 37°C in sperm motility medium to let them swim. To avoid contamination of somatic cells, only top fractions containing about $5x10^6$ cells per mouse were used for further experiments and assays. The count was performed by microscopy through a Neubauer Chamber, this way, also the purity of the samples was investigated. Sperm concentration, motility and progressive motility have been calculated using an automated Computer Assisted Semen Analysis (CASA - Hamilton Thorn IVOS II) according to manufacturer's instructions. To purify developing germ cells, testes were manually decapsulated and sequentially digested with collagenase IV (4 mg/mL), hyaluronidase (0.66 mg/mL) and DNase I to digest the blood-testis-barrier and disperse the tubules. Developing sperm cells were isolated from the tubular fraction using the MACS system from Miltenyi Biotech through the positive selection of CD326 (EPCAM) expressing cells. Cells were magnetically labeled with MicroBeads conjugated to monoclonal CD326 antibody (Miltenyi Biotec), loaded into LS columns (Miltenyi Biotec) and separated using magnetic field of a MACS separator according to the manufacturer's instructions.

2.2.7 *In vitro* fertilization and embryo analysis

2.2.7.1 *In vitro* fertilization

Oocyte isolation and IVF were conducted following standardized procedures of the INFRAFRONTIER consortium as previously described [301]. To obtain morulae, male gamete donors were euthanized at 8 weeks of age, after the 2 weeks of LFD/HFD exposure. Mature sperm cells were obtained from cauda epididymis. Wild-type unexposed female oocyte donors were euthanized the same day at 10-11 weeks of age, after superovulation induced with 7.5 U of Pregnant Mare Serum Gonadotropin (PMSG) and 7.5 U of human Chorionic Gonadotropin (HCG) before sacrificed for oocyte collection. The sperm and the oocytes were co-cultured for 4–6 h. Subsequently, the fertilized oocytes were transferred and incubated for 72hrs in high-calcium human tubal fluid (HTF) culture medium at 37°C and 5% CO2 until they reached the morula differentiation stage. Proper embryonic development was microscopically checked before picking individual embryos for downstream analysis.

2.2.7.2 Embryo collection, microinjection and culture

Embryos were collected from 5-7-week-old F1 (C57BL/6J × CBA/H) superovulated females crossed with F1 males treated for 2 weeks with an HFD diet or control diet. Superovulation was induced by intraperitoneal injection of pregnant mare serum gonadotropin (PMSG) and human chorionic gonadotropin (HCG) 46-48 hours later. Zygotes were collected at 28h after HCG injection. All experiments were performed under the authorization of the Upper Bavarian authorities.

2.2.7.3 Immunostaining and confocal microscopy

Fixation of freshly collected embryos from CD1 natural mating or F1 superovulated, microinjected and cultured embryos was performed as described [302]. Briefly, the zona pellucida was removed with Acid Tyrode solution, followed by two washes in PBS and fixation in 4% paraformaldehyde, 0.04% triton, 0.3% tween-20, 0.2% sucrose at 37°C to ensure preservation of nuclear architecture. Embryos were then washed with PBS and permeabilized with 0.05% Triton-X100 for 20 minutes. After permeabilization, embryos were washed 3x in PBSt (0.1% Tween20 in PBS), quenched in 2.6 mg/ml freshly prepared ammonium chloride, washed 3x in PBSt and blocked for 3-4 hours at 4°C in blocking solution (BS: 3% BSA in PBSt) and incubated with anti-H3K27me3 (Millipore 07-449) in BS. After overnight incubation at 4°C embryos were washed 3x in PBSt,

blocked for 20 minutes in BSA and incubated for 3h at RT in BS containing secondary antibodies labelled with Alexa fluorophores (Invitrogen). After washing 3x in PBSt and 1x in PBS, embryos were mounted in Vectashield (Vector Laboratories) containing 4'-6-Diamidino-2-phenylindole (DAPI) for visualizing DNA. Confocal microscopy was performed on a 63x oil objective in a TCS SP8 inverted confocal microscope (Leica). Z-sections were taken every 0.5-1 µm. Image analysis was performed using the software LAS-AF (Leica) and Imaris (Bitplane). Acquisition parameters were set in order to obtain fluorescence intensity signal in the linear range of hybrid detectors throughout the manuscript. These detectors have negligible detector noise and linearly amplify incoming photons into photoelectrons, allowing the counting of measured photons as long as the detector is not saturated. Hence, given identical acquisition settings, the fluorescence signal recovered accurately reflects the level of antigen present in the system.

2.2.7.4 Quantification of fluorescence intensity

Confocal z-series stacks were reconstructed in 3D using Imaris software (Bitplane) and the pronuclei (zygote) or nuclei (2-cell stage) were segmented based on the DAPI channel. 3D images have been preferred because analysis of optical sections at 0.5 microns apart robustly reflects the intensity distribution throughout the nucleus more accurately than measuring a single confocal section alone. The fluorescence intensity for each embryo was normalized to the average of the non-injected control group. The data was found to be not normally distributed using the Kolmogorov-Smirnov test, therefore, the non-parametric two-tailed Mann-Whitney U-test was used for statistical analysis.

2.2.8 Molecular biology

2.2.8.1 EpCAM+ and morula RNA-sequencing

Total RNA was prepared from EpCAM+ spermatids and morula (50 morulae per condition per sample) using the RNeasy mini kit (QIAGEN) according to the manufacturer's instructions. RNA concentration and integrity were controlled on a Bioanalyzer system (Agilent) and only RNA samples with RIN (RNA Integrity Number) values > 7 were used for downstream applications. Library construction and sequencing was outsourced to IGA Technology Services Srl. Libraries were constructed using the NextEra Library Prep Kit (Illumina) according to the manufacturer's instructions and sequenced on an Illumina HiSeq 2500 at 150bp paired-ended, with a minimum output of

40 million reads per sample. Read mapping and differential expression analysis was performed using the A.I.R (Artificial Intelligence RNA-Seq) software from Sequentia Biotech with the following pipeline: BBDuk (reads trimming - http://jgi.doe.gov/data-and-tools/bbtools/bb-tools-user-guide/bbduk-guide/), STAR (reads mapping to the mouse genome GRCm38 [ENSEMBL] - https://github.com/alexdobin/STAR), featureCounts (gene expression quantification - http://bioinf.wehi.edu.au/featureCounts/), and EdgeR (liver) or NOISeq (statistical analysis of differentially expressed genes - http://bioinfo.cipf.es/noiseq/doku.php). Compared to other methods to calculate differential expression, NOISeq is a data adaptive non-parametric method specifically designed to account for high variability across replicates and genes with low expression levels [303], a feature of RNA-Seq datasets from both germ-cells and developing embryos. Heatmap and PCA analyses were performed with the web-application ClustVis using default parameters. KEGG analysis was performed with DAVID (https://david.ncifcrf.gov). GoPlot was used to visualize the results of the KEGG pathway analysis.

2.2.8.2 ChIP-seq and EpiCSeg chromatin segmentation analysis

Publicly available spermatids chip-seq datasets (GSE49624) [274] has been used for peak calling using MACS (version 2.0.9) following the parameters defined in published article [274]. Peak annotation has been performed using HOMER (http://homer.salk.edu/homer/).

For chromatin segmentation, we applied EpiCSeg [304] to the aforementioned dataset. We compartmentalized the genome into twenty chromatin states with different abundance and co-occurrence of H3K27me3, H3K4me1, H3K4me3, H3K27ac, H3K9ac, and H2A.Z histone marks together with Pol2. Chromatin states were assigned to genes according to individual and combinatory marks coverage over the gene body and at the TSS.

2.2.8.3 ATAC-sequencing

ATAC-seq was performed as described [305] on 100,000 sperm and 50,000 EpCAM+ cells. Cells were washed in PBS and centrifuged at 500g (EpCAM+) or 2500g (Sperm) in a pre-chilled (4°C) fixed-angle centrifuge for 5 minutes. To further prepare nuclei, pellet was resuspended in 50 µl of Cold Lysis Buffer and immediately spun for 10 minutes in a refrigerated centrifuge (500g for EpCAM+ and 2500g for Sperm). The nuclei pellet was then resuspended in the transposase reaction mix (FC-121-1030,

Illumina). The transposition was carried for 30 minutes at 37° C and DNA purified using a Qiagen MinElute kit (Cat # ID: 28004). Transposed DNA fragments were then amplified using NEBnext PCR master mix and 1.25 μM of Ad1_noMX and Ad2.1e2.4 bar-coded primers from [305] (Table) using the following conditions:

Cycle	Time	Degree
1x	5 minutes	72°C
	30 seconds	98°C
5x	10 seconds	98°C
	30 seconds	63°C
	1 minute	72 °C

qPCR was used to estimate the number of additional cycles needed to generate products at 25% saturation, this way the amplification could be stopped prior to saturation. Indeed, part of the previously amplified DNA was used to run a qPCR side reaction using SYBR Green I as dye and the instrument as follow:

Cycle	Time	Degree
1x	30 seconds	98°C
20x	10 seconds	98°C
	10 seconds	98°C
	30 seconds	63°C
	1 minute	72 °C

The additional number of cycles needed was calculated by referring to one-third of the maximum fluorescent intensity and the remaining product of PCR reaction was then further amplified for additional, determined, cycles.

Amplified libraries were purified with AMPure XP beads (Agencourt) to remove primer dimers. Library quality was assessed using the Agilent Bioanalyzer with the High Sensitivity DNA kit and a pool of libraries were sequenced on the illumina Hiseq 2500 with 125bp-PE. Paired end reads were adapter trimmed and quality filtered using "trim_galore", they were further aligned to the mouse reference genome mm10 using Bowtie2 version 2.3.4.3. Reads were aligned using default parameters expect -very-sensitive -X 2000. The unmapped and duplicate reads were filtered using "samtools".

ATAC-Seq peak regions of each sample were called using MACS2 version 2.1.2 with parameters --nomodel --shift 75 --extsize 150 -q 0.01. Blacklisted regions (http://mitra.stanford.edu/kundaje/akundaje/release/blacklists/mm10-mouse/mm10.blacklist.bed.gz) and mitochondrial chromosome were excluded from called peaks. The Irreproducible Discovery Rate (IDR) method was used to identify reproducible peaks between two technical replicates. Only peaks reproducible between the two technical replicates were retained for downstream analyses. "DiffBind" was used to identify differentially opened regions between samples. The peak regions were annotated using annotatePeaks.pl from HOMER. "Deeptools" was used to visualize density profiles.

2.2.8.4 Bulk tissue mRNA-sequencing

Total RNA was extracted from large lobe of liver, 20mg of eWAT and muscle (3 per group) isolated from 6h fasted mice. In brief, samples were homogenized in Trizol using a GentleMacs tissue homogenizer by Miltenyi Biotech in M-tubes (Cat#130-093-236, Miltenyi Biotech). Chloroform was added and the extract was vigorously shaken and centrifuged at 12,000 g to separate the organic and aqueous phases. Total RNA was further purified according Trizol instruction. RNA concentration was measured using Qubit RNA BR Assay (cat # Q10210, Thermo Fischer Scientific) and RNA integrity was measured with an Agilent Bioanalyzer (values > 7 were used for downstream applications). Libraries were prepared from the extracted RNA using the QuantSeq 3'mRNA-Seq Library Prep Kit (cat # 015, Lexogen). Indices from the first 54 i7 Index Plate for QuantSeq/SENSE for Illumina adapters 7001–7060 (cat # 044, Lexogen) were used, and 18 cycles of library amplification were performed. At the second strand synthesis UMI Second Strand synthesis Module were used to include identifiers in FWD libraries. Libraries were eluted in 20 µl of the kit's Elution Buffer. The double stranded DNA concentration was quantified using the Qubit dsDNA HS Assay Kit (cat # Q32854, Thermo Fischer Scientific). The region average size instead determined through analysis on Agilent Bioanalyzer instrument. Aliquots containing an equal number of nmoles of cDNA molecules from each library were pooled to obtain a pooled library with a concentration of 15 nM cDNA molecules. The pooled libraries were sequenced in an Illumina HiSeq2500 instrument (Illumina). Rapid Flow Cell 50bp-SR (300 million reads). The reads were mapped to the mouse genome (nm10/GRCm38) by making use of the online platform "Bluebee", as suggested from Lexogen (www.bluebee.com/lexogen).

To find differentially expressed genes DESeq2 was used. The FDR was adjusted to 0.05 and log fold changes considered.

2.3 Statistical analysis

All figures and statistical analyses were generated using GraphPad Prism 6 or 7. Statistical significance was tested by student's t-test, or ANOVA where appropriate. Correlations tested for linear regression. Odd ratios have been calculated using MedCalc. All data are expressed as mean ± SEM unless otherwise specified and a two-tailed p-value < 0.05 was considered to indicate statistical significance.

3. RESULTS

3.1 Paternal overweight correlates with children's body mass index and insulin resistance

Previous epidemiological studies have shown that parental overweight and obesity (mostly maternal) are the strongest risk factors for early onset obesity in children predisposing to metabolic disease in the adulthood [306, 307], and that paternal BMI, in particular, inversely correlates with offspring lipid homeostasis and cardiovascular health.

Paternal contribution to offspring health is a relatively new research topic and, despite the growing evidence, the influence of paternal metabolic health at conception on the progeny is still a point of discussion.

The LIFE Child study is a parents-child cohort made of more than 3000 trios (parents/children) generated by the Research Center for Civilization Disease at the University of Leipzig. Data have been analyzed with the aim of elucidating the parental role on metabolic health of children. The regional population-based project pointed at characterizing factors connected with diseases of civilization such as diet and lifestyles with impact on health by comprehensive phenotyping, including BMI and glucose homeostasis [295, 296]. Using available phenotypic data from the LIFE-Child cohort (parental phenotyping and conception and longitudinal offspring phenotyping), we aimed to study whether and how much paternal BMI at conception impacts on offspring BMI and glucose homeostasis.

The analysis showed that, despite the strong maternal association (Supplementary Figure 1A, B), paternal BMI correlated with children's BMI in an age dependent manner (Figure 1A, B). As expected, paternal effect was additive to the maternal overweight or obesity (lean - BMI < 24 Kg/m^2, overweight - BMI 24-30 Kg/m^2 and obese - BMI > 30 Kg/m^2) but, interestingly, independent (Figure 3.1A). Indeed, multiple regression analysis revealed an additional effect on children's BMI (6.5%), unrelated to maternal BMI (20.4%) and age of the child (2.3%) (Supplementary Table 1). Of note, in families with lean mothers, paternal BMI did not influence offspring birth weight (Supplementary Figure 2).

More precisely, the study revealed that the influence of paternal BMI on childhood obesity is first evident in prepubescent offspring (no longer under breastfeeding), with

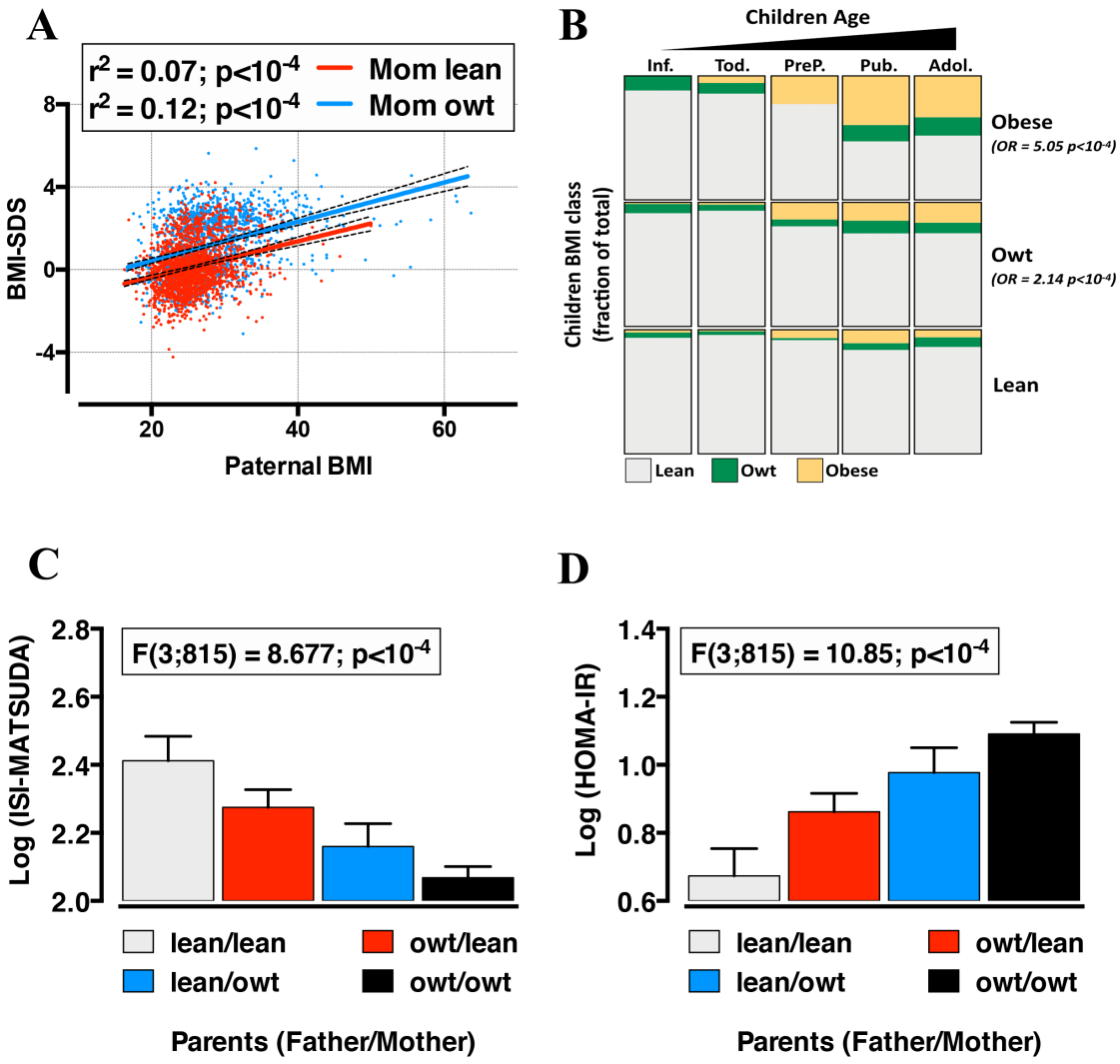

Figure 3.1 - Paternal weight influences offspring metabolic health
A. Correlation between paternal and children's BMI with lean or owerweight (owt) (BMI > 25) mothers. **B.** Children's weight status distribution according to paternal BMI and children's age in families with lean mothers. **C-D.** Children's insulin sensitivity in families with lean or overweight parents measured as ISI-Matsuda index (C) or HOMA-IR (D) (1-way ANOVA $p < 10^{-4}$). Inf. = Infants; Tod. = Toddlers; PreP. = Prepubescents; Pub. = Pubescents; Adol. = Adolescents.

overweight fathers doubling (BMI < 24 Kg/m^2) (pat. overweight vs lean OR = 2.14 $p < 10^{-4}$) and obese fathers quintuplicating offspring obesity risk (obese vs lean OR = 5.05 $p < 10^{-4}$) (Figure 3.1 B). In addition to the effect on childhood obesity, paternal BMI was also associated to reduced insulin sensitivity (showed as measurement of ISI-Matsuda index and HOMA-IR) in children, with both maternal and paternal BMI having independent and additive effects (Figure 3.1C, D; Supplementary figure 1 C, D). The

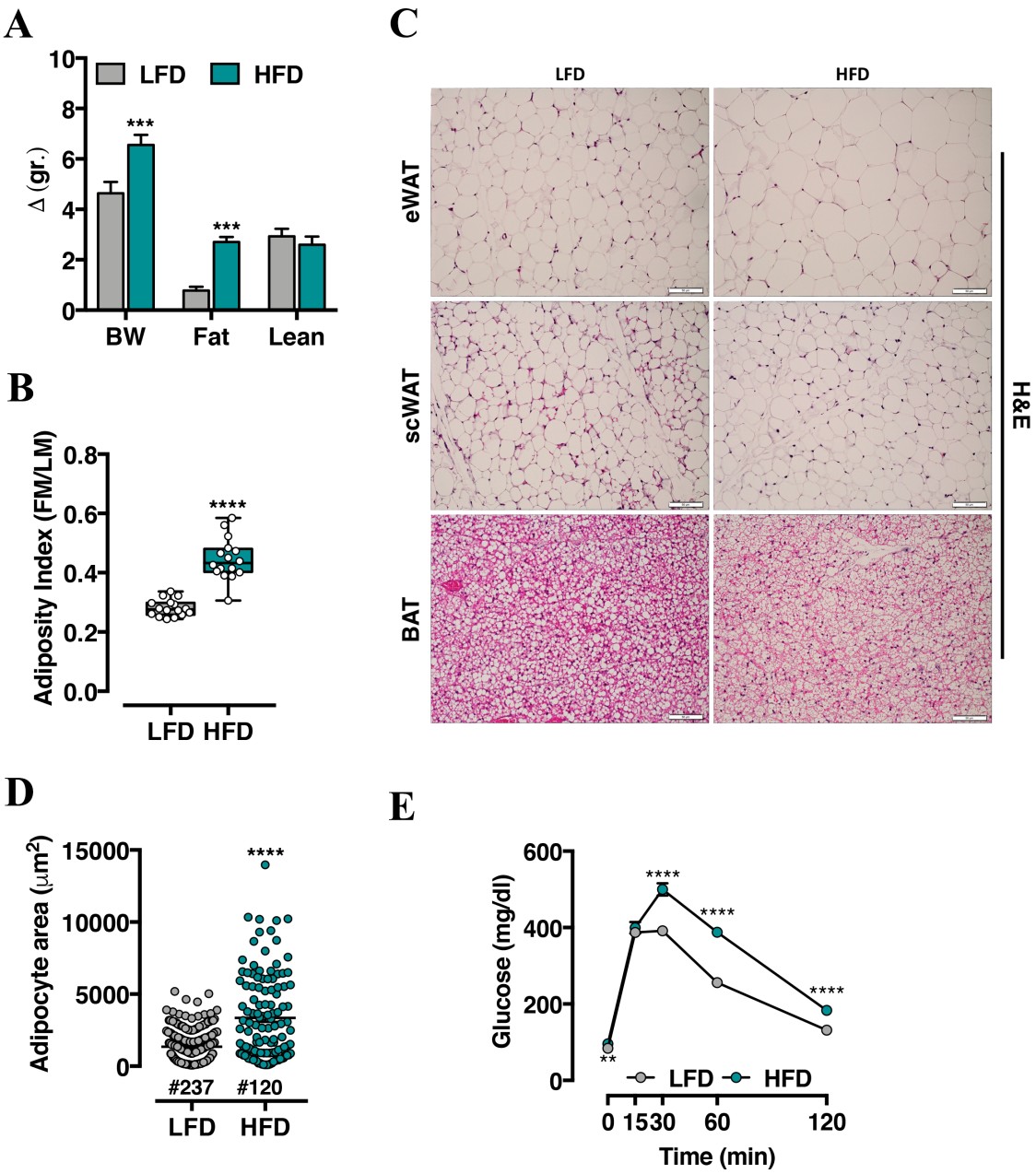

Figure 3.2 - Two weeks of high fat diet induce overweight and glucose intolerance in male mice

A. Increase in body weight, fat and lean mass after two weeks of high (HFD) or low (LFD) fat diets. **B.** Adiposity index (fat mass/lean mass). **C.** H&E staining of visceral white fat (eWAT) subcutaneous white fat (scWAT) and brown fat (BAT) on paraffin-embedded sections from LFD and HFD-fed mice. Scale bars: 50 μm. **D.** Cell numbers and adipocyte areas of visceral fat (eWAT) measured in μm^2. 237 and 120 cells were counted from IHC sections from representative LFD and HFD-fed mice respectively. **E.** Glucose tolerance test (GTT). Results expressed as mean ±SEM or ±SD (n = 6). *p < 0.05 by Student's t test or 1-way or 2-ways ANOVA where applicable.

results highlight a significant contribution of the father in influencing the metabolic health of the children and poses the question on the underlying mechanisms. Since this analysis

could not exclude the contribution of genetics, as well as of a shared familial environment, the next approach was to test the hypothesis of a role for acquired epigenetic inheritance. High-fat diet (HFD – 60% Kcal from fat) feeding in mice is a generally accepted model to study human obesity and its complications [308, 309]. A chronic HFD challenge (9 to 16 weeks) induces obesity with metabolic derangement, systemic inflammation and consequent alteration of male reproductive fitness [310]. These conditions, while not always associated to human obesity [311], represent strong confounding factors for the mechanistic dissection of epigenetic inheritance. Also, as shown before, paternal overweight is sufficient to double offspring obesity risk and to impair their metabolic homeostasis. That said, to mimic paternal overweight in mice, animals have been fed with HFD for two weeks, from 6 to 8 weeks of age (control animals were on a matched low-fat diet with 10% Kcal from fat). It is well established that two weeks of HFD are enough to induce glucose intolerance and significant body weight increase in mice [312]. In keeping with these published findings, in two weeks, HFD-fed males robustly gained significant weight and increased adiposity (Figure 3.2A, B), epididymal adipose tissue hypertrophy (eWAT) (Figure 3.2C, D), and presented with whole-body glucose intolerance (Figure 3.2E). Importantly, neither any marker of systemic inflammation in the plasma (Figure 3.3A), alteration of the male testis structure (measured also through the TRA98, testis-specific nuclear protein that marks all the germ cells, or tubule diameter) (Figure 3.3B, C), nor alteration of the male reproductive fitness (measured by sperm motility and rate of successful fertilization *in vitro*) (Figure 3.3D, E) have been detected in those mice, which instead represent all features of a chronic HFD feeding (> 6 weeks of HFD diet).

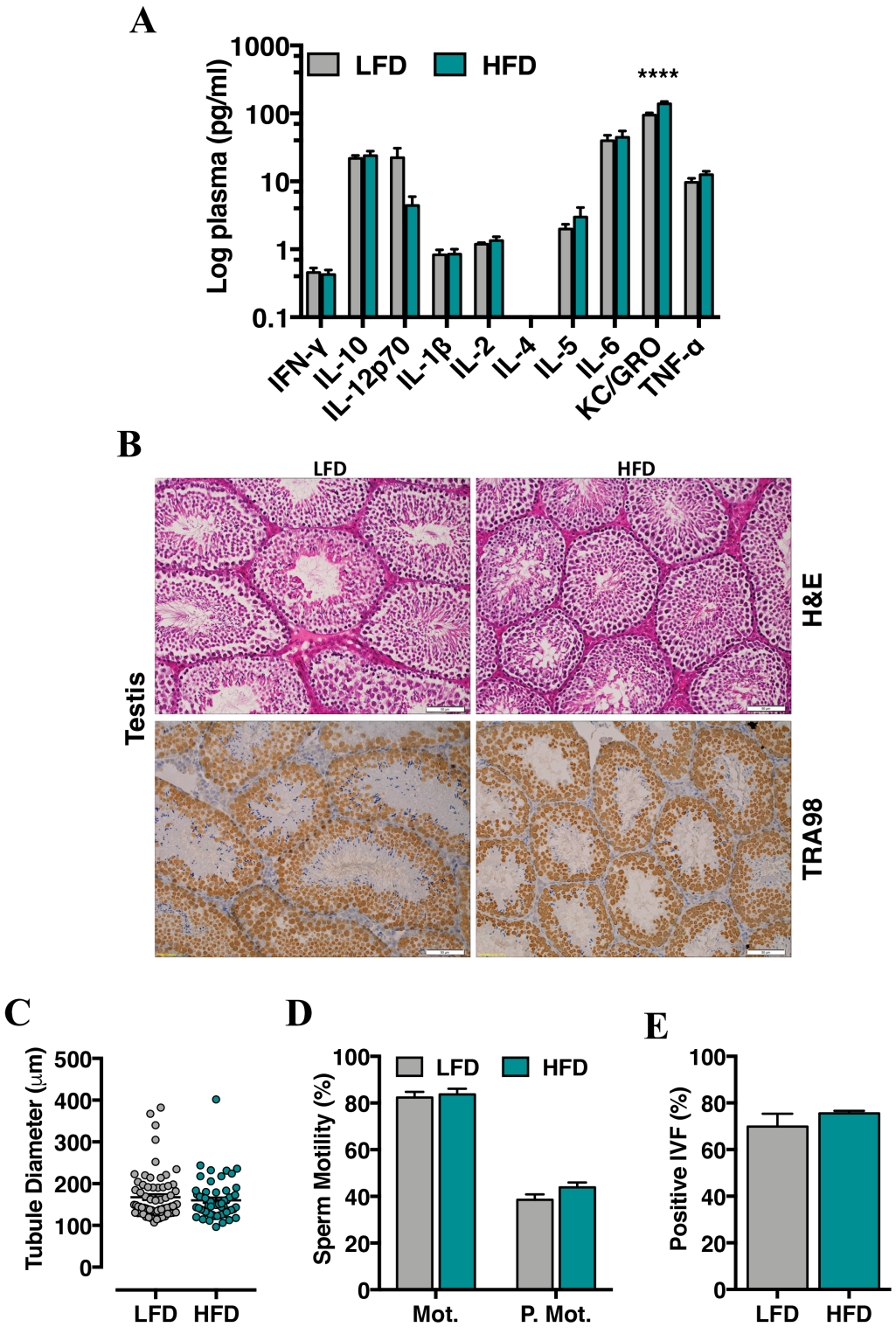

Figure 3.3 - HFD challenge does not induce inflammation or reduced fertility
A. Mesoscale Discovery analysis of cytokine levels in plasma of LFD and HFD-fed mice. **B.** H&E of testis from LFD and HFD-fed mice (upper panel) and immunostaining for the germ-cell specific antigen TRA98. Scale bar, 50μm. **C.** Measurement of tubule diameters showed in μm. 69 and 58 tubules were counted on TRA98-stained sections of LFD and HFD testis respectively. **D.** Sperm motility and progressive motility (% total live sperm cells). **E.** Fertility rate of sperm from LFD and HFD-fed mice (% of fertilized eggs successfully developed to blastocysts). Results expressed as mean ±SEM or ±SD ($n = 6$). *p < 0.05 by Student's t test or 1-way or 2-ways ANOVA where applicable.

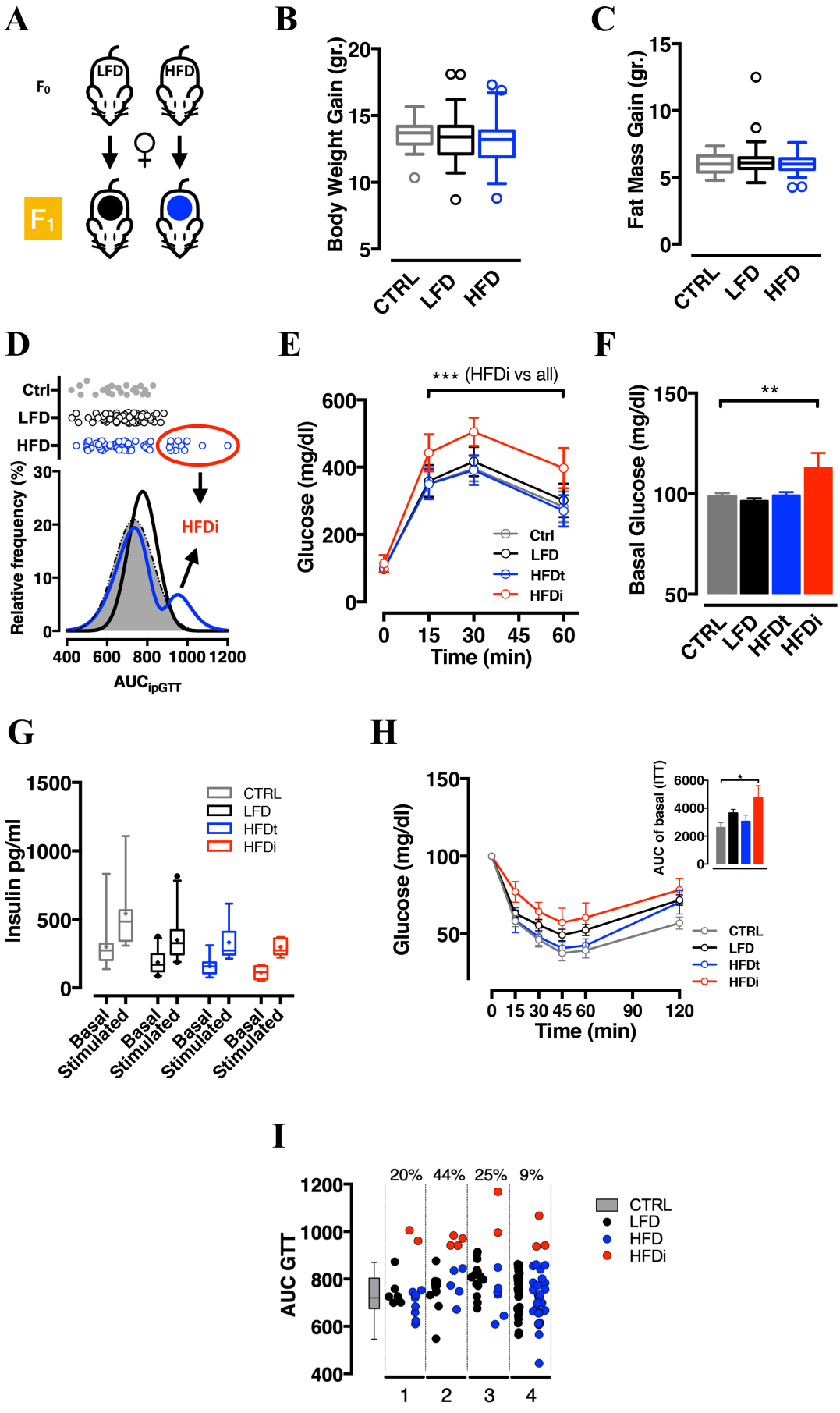

See legend on the next page

Figure 3.4 - Preconceptional paternal overweight induces glucose intolerance in male offspring

A. Schematic representation of paternal exposures and F1 generation. **B-C.** Body weight gain (4-14 weeks – B) and fat mass (4-14 weeks – C) of LFD and HFD-fed fathers' descendants and control (Ctrl – age-matched and kept on chow diet ad libitum for > 8 generations) animals used as reference. **D.** Area under the curve of glucose tolerance test (AUC – upper panel) and frequency distribution of AUC (lower panel) in F1 animals from CTRL, LFD or HFD-fed fathers. HFD intolerant (HFDi) mice are circled in red. **E.** Box plot representation of the AUC for Ctrl, LFD, HFDt and HFDi mice. **F.** Basal glucose measured in the fasting state (16h). **G.** Insulin measurement during GTT. **H.** Insulin tolerance tests of LFD, HFDt and HFDi mice with AUC plot (upper panel). **I.** Frequency distribution of HFDi animals across 4 independent cohorts, two different seasons and two different mouse rooms with a variable frequency ranging from 9 to 45%.

F1: four independent cohorts (from four founding fathers each) with 12-15 mice/group/cohort. F2: three independent cohorts (from four founding fathers each) with 10-12 mice/group/cohort. Results expressed as mean ±SD. *$p < 0.05$ by Student's t test or 1-way or 2-ways ANOVA where applicable.

After the 2 weeks of challenge, HFD and LFD-fed mice have been mated with unexposed and age-matched females to assess later consequences on the offspring (Figure 3.4A). To uncover truly paternal effects, progeny has been kept exclusively on chow diet for the entire life. While paternal HFD did not affect body weight and fat mass gain in the offspring (Figure 3.4B, C), when challenged for whole body glucose homeostasis with a GTT, males from HFD-fed fathers showed variation in the area under the curve (AUC) of the GTT highlighting a partial penetrant glucose intolerance. Offspring of HFD-fed fathers indeed clustered in two distinct subpopulations (Figure 3.4D): one with values falling in the range of the control groups (LFD and Chow) and the other with higher AUC, hence, with reduced glucose tolerance (HFDi). The HFDi subpopulation remained significantly intolerant and hyperglycemic when retested four weeks later (Figure 3.4E). The increased basal glucose (Figure 3.4F) and the glucose intolerance observed in the HFDi group did not reflect reduced insulin secretion, as no significant variation in basal and stimulated insulin (measured before and during GTT) was found (Figure 3.4G), however, a significantly higher AUC of ITT unveiled reduced insulin sensitivity (Figure 3.4H).

Importantly, the glucose homeostasis phenotype occurred in four independent F1 generations obtained from different and unrelated fathers, raised in two distinct mouse rooms and different seasons. The traits observed were therefore stable, nevertheless, partially penetrant (Figure 3.4I).

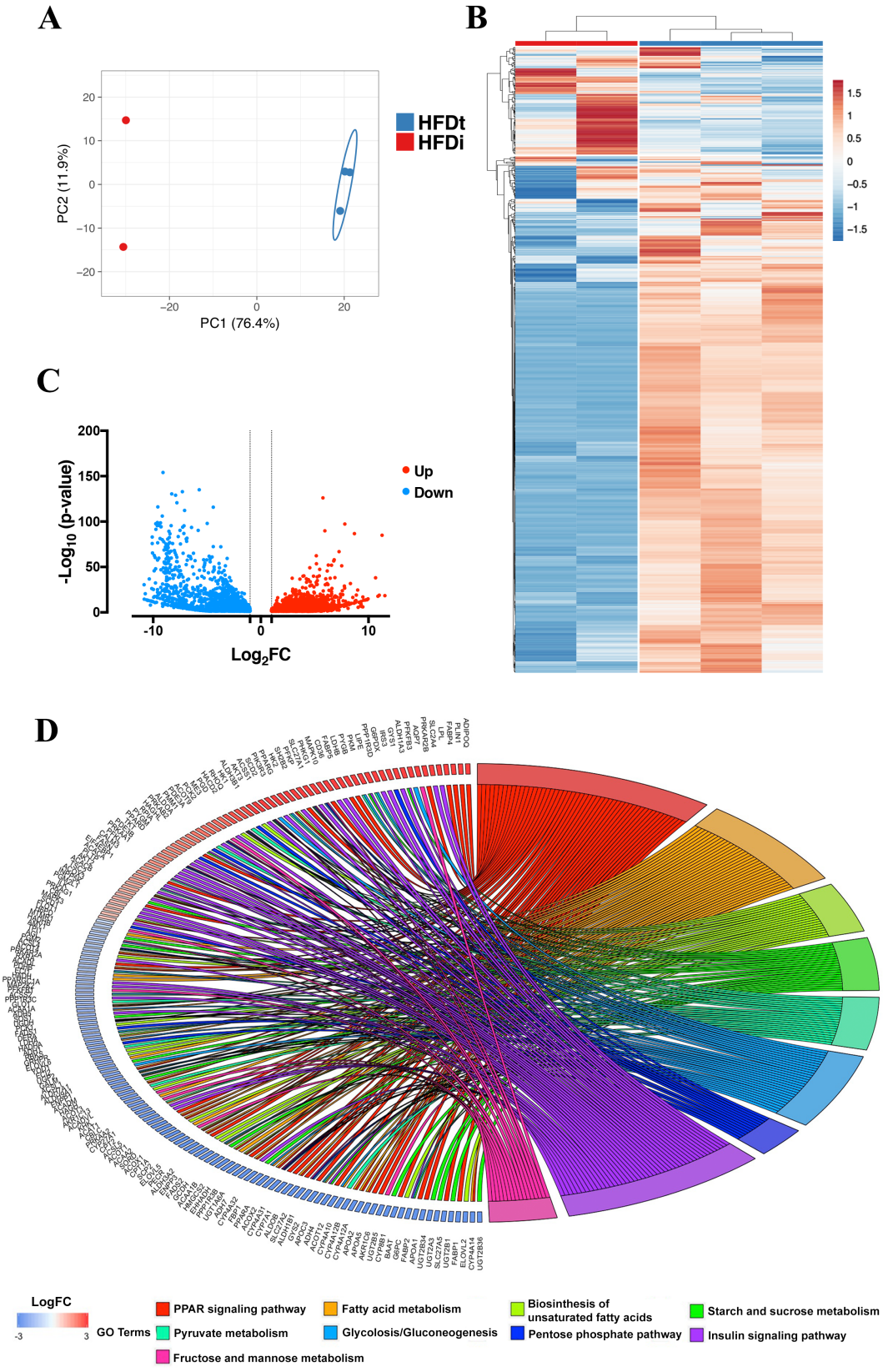

Figure 3.5 - Acute paternal HFD induce liver transcriptional reprogramming in the male progeny

A-B. PCA plot (A) and heatmap representation (B) showing the variation in gene expression in liver between HFDt and HFDi F1 male offspring. **C.** MA plot of expressed genes with the DEG genes FC ≥ 1 or ≤ -1 in HFDi/HFDt. **D.** KEGG pathway analysis of DEGs (HFDi/HFDt). HFDt group is represented by 3 different animals while the HFDi by 2.

RNA-seq performed in metabolic tissues further highlighted the differences between the HFDt and HFDi groups. More precisely, liver, eWAT and gastrocnemius have been taken into account for their role in glucose homeostasis, whole body-metabolism, blood glucose and energy balance respectively. Despite deriving from the same HFD challenged group of fathers, the glucose intolerant HFDi animals significantly differed from the HFDt in terms of transcriptional expression within liver (Figure 3.5) and eWAT (Figure 3.6) but not in skeletal muscle (Supplementary Figure 3). Critically, liver of HFDi significantly differed from the HFDt (Figure 3.5A, B), with more than 4000 genes differentially expressed between the conditions (Figure 3.5C) and enriched in pathways important for metabolism such as PPAR signaling, fatty acid metabolism, amino acid metabolism, starch and sucrose metabolism, pyruvate metabolism, glycolysis/gluconeogenesis, pentose phosphate and fructose and mannose metabolism pathways among others (Figure 3.5D). On the same line, adipose tissue of HFDi group clearly differed from the HFDt group (Figure 3.6A, B), with the majority of DEGs (Figure 3.6C) mostly downregulated and enriched in metabolic pathways as PPAR signaling, fatty acid metabolism, maturity onset diabetes of the young, starch and sucrose metabolism, biosynthesis of unsaturated fatty acids and glycolysis/gluconeogenesis pathways (Figure 3.6D).

Impressively, the analysis of differentially expressed genes within the liver and visceral adipose tissue revealed a drastic correlation between the two tissues in terms of transcriptional reprogramming, with the majority DEGs commonly downregulated (32.6% of DEGs) and enriched in similar metabolic pathways (Figure 3.7 A-C).

Of note, the additional analysis performed on the top 100 DEGs genes between liver and eWAT showed enrichment for fat (UP in Liver/eWAT) and liver specific genes (DOWN in Liver/eWAT), finally revealing their proper identity. In particular, functional annotation charts of tissue expression showed significant enrichment for adipose tissue and liver within the three groups (LFD, HFDt and HFDi) (Supplementary Table 3).

Skeletal muscle is a master organ for maintenance of blood glucose and energy balance. In the concrete, most of the glucose uptake by contraction or after insulin secretion occur in this tissue [313]. Consistent with a comparable lean mass proportion between the groups, no difference in gene expression has been detected within the gastrocnemius (Supplementary Figure 3) revealing that the paternal challenge did not affect muscle and that any dissimilarity found within the HFD-subpopulations was not driven by transcriptional differences in this tissue.

To determine whether the intolerance observed in the HFDi F1 group could be also transmitted to their progeny, F2 animals were generated from F1 fathers identified as

LFD, HFDt and HFDi by mating them with unexposed females (Figure 3.8A). Critically, F2 male animals born to F1 HFDi fathers, despite no significant change in body weight, fat and lean mass gain (Figure 3.8B, C), showed altered glucose tolerance (Figure 3.8D, E) when compared to both HFDt and control LFD groups, which instead remained phenotypically close.

The pathogenesis of complex diseases, like diabetes, is the result of an intricate interaction between several genes and environmental factors. Sexual dimorphism further complicates the picture influencing the development of many multifactorial diseases including diabetes [314]. Metabolically speaking, the biological differences observed between males and females in respect to lipid metabolism, glucose and energy balance suggest a mechanism in which sexual chromosomes and hormones drive and program adult physiology. In line with that and with the recently published findings [314, 315], female offspring of both F1 and F2 generations were found to be protected from the paternally induced metabolic reprogramming (Supplementary Figure 4) in a way that is still unknown.

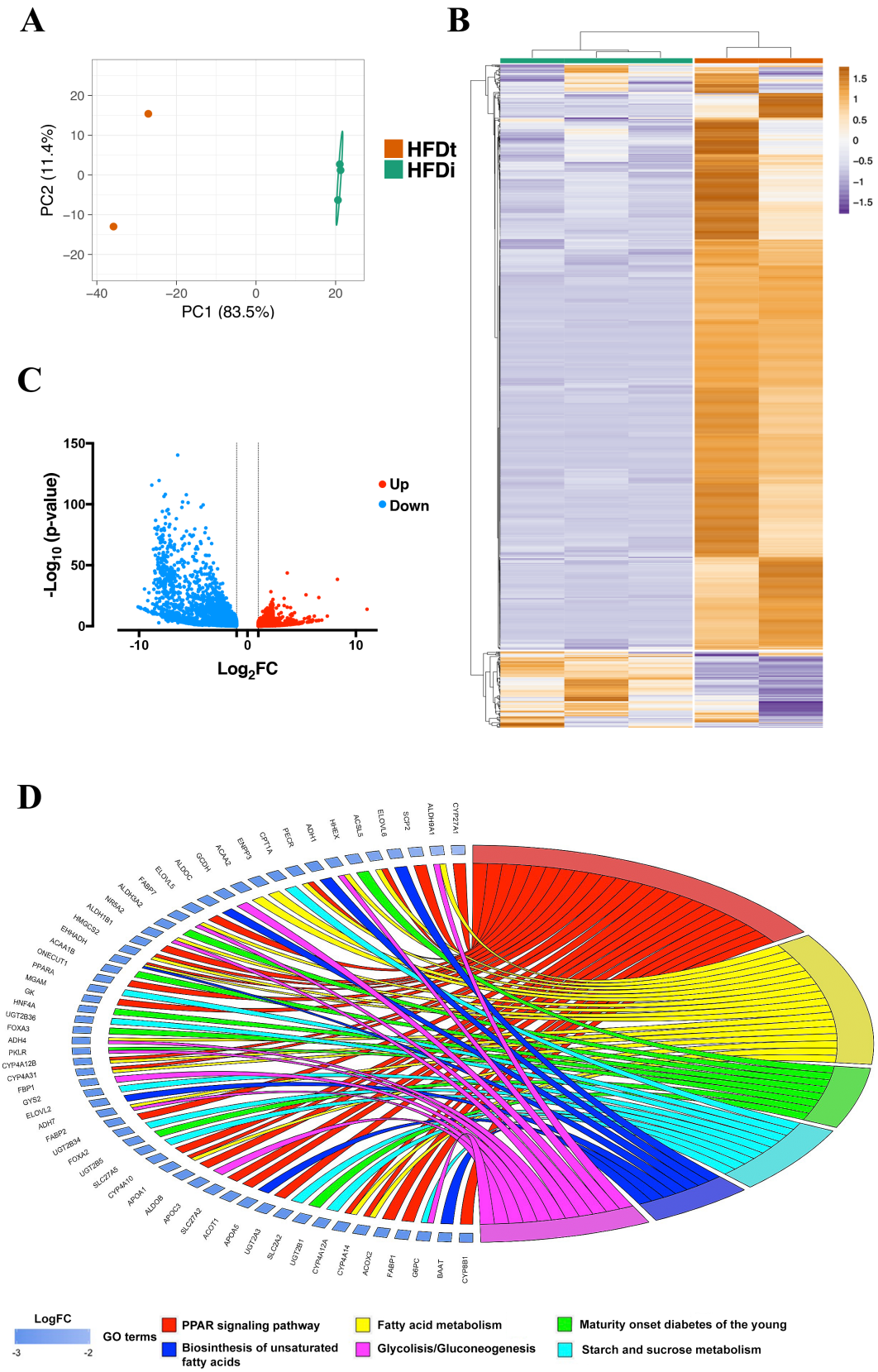

Figure 3.6 - Acute paternal HFD reprograms the eWAT in male progeny

A-B. PCA plot (A) and heatmap representation (B) showing the variation in gene expression in liver between HFDt and HFDi F1 male offspring. **C.** Volcano plot of expressed genes with the DEG genes (FC ≥1 and ≥-1) of HFDi/HFDt. **D.** KEGG pathway analysis of DEGs (HFDi/HFDt). HFDt group is represented by 2 different animals while the HFDi by 3.

A

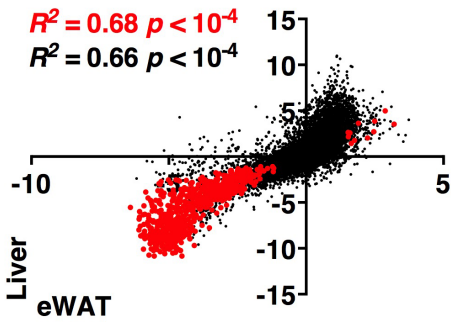

B

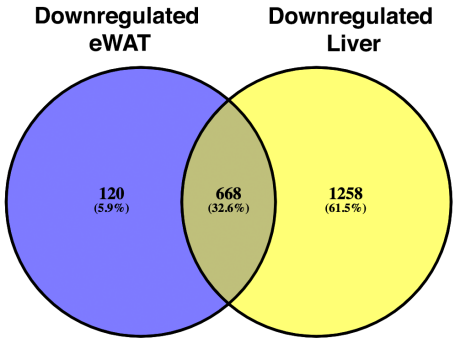

Term	PValue	Genes
mmu03320: **PPAR signaling pathway**	7.08E-10	*Slc27a2, Cyp4a12b, Cyp4a10, Cyp4a12a, Cyp4a31 Cpt1a, Cyp27a1, Pparα, Hmgcs2, Cyp4a14, Fabp2, Ehhadh, Apoa5, Acaa1b, Acsl5, Slc27a5, Acox2, Scp2, Fabp1, Apoc3, Apoa1, Cyp8b1*
mmu00071: **Fatty acid metabolism**	1.56E-09	*Gcdh, Aldh9a1, Cyp4a12b, Aldh3a2, Acaa2, Cyp4a10, Adh7, Cyp4a12a, Cyp4a31, Cpt1a, Aldh1b1, Cyp4a14, Adh1, Ehhadh, Acaa1b, Acsl5, Adh4*
mmu04950: **Maturity onset diabetes of the young**	0.00136044	*Hnf4a, Foxa3, Nr5a2, Slc2a2, Foxa2, Hhex, Onecut1*
mmu00500: **Starch and sucrose metabolism**	0.00160057	*Ugt2b1, Enpp3, Ugt2b36, Ugt2a3, Gys2, G6pc, Ugt2b5, Ugt2b34*
mmu00010: **Glycolysis / Gluconeogenesis**	0.01789302	*Aldh1b1, G6pc, Adh1, Aldh9a1, Aldh3a2, Fbp1, Adh4, Aldob, Adh7*

Figure 3.7 - Liver and eWAT in the HFDi are similarly reprogrammed
A-B. Common DEGs in liver and eWAT of HFDi/HFDt tissues. In red are indicated the DEGs in common (A), mostly downregulated (B). **C.** Table indicating KEGG pathways of common DEGs between liver and eWAT (HFDi/HFDt).

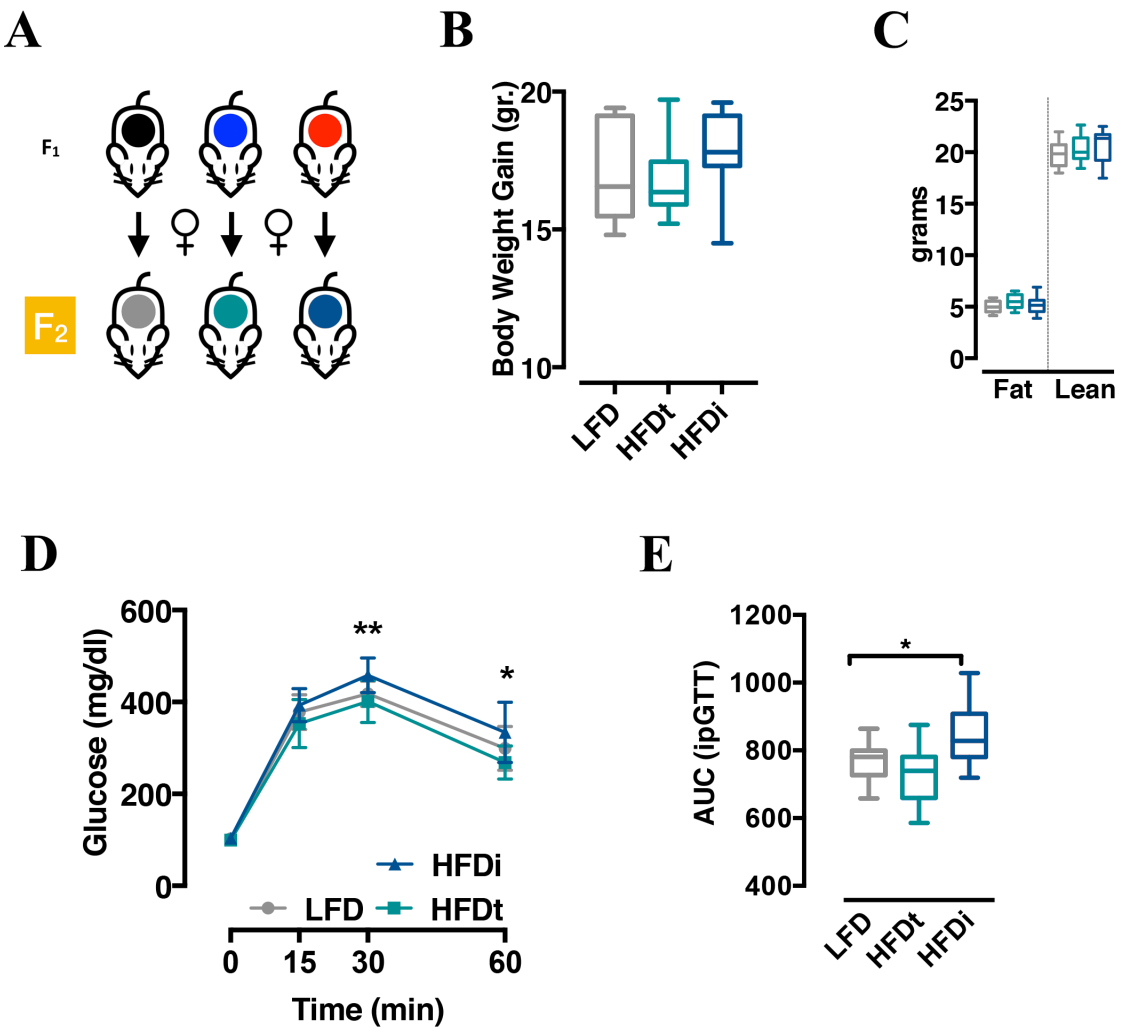

Figure 3.8 - Paternal overweight induces glucose intolerance up to the F2 generation
A. Schematic representation of F2 generation from LFD, HFDt and HFDi F1 males. **B-C.** Body weight gain (4-14 weeks – B) and body composition measured at 14 weeks (C) of F2 animals. **D.** Representation of glucose tolerance test. **E.** Box plot representation of the area under the curve (AUC) of glucose tolerance test. F2: three independent cohorts (from four founding fathers each) with 10-12 mice/group/cohort.
Results expressed as mean ±SD. *p < 0.05 by Student's t test or 1-way or 2-ways ANOVA where applicable.

3.2 Paternal HFD-induced overweight associates with altered Polycomb activity during spermatogenesis

Being overweight impacts intergenerationally on offspring metabolic health (Figure 3.1). Aiming at exploring the molecular bases of this inheritance, a step back to the founding fathers F0 was necessary.

Germ cells are the carriers of parental genetic, but also epigenetic information, to the progeny. During fertilization, gametes fuse to initiate the development of a new organism,

and recent experimental evidence demonstrated that intergenerational control of metabolic health (both maternal and paternal) is germline inherited [316]. Based on this, testicular germ cells from seminiferous tubules of males exposed to the 2 weeks of diet have been isolated and RNA-seq analysis performed. To obtain testicular germ cells, the membrane protein EpCAM (Epithelial Cell Adhesion Molecule) has been selected as a sorting marker. EpCAM stands for a homophilic, calcium-independent cell adhesion molecule expressed throughout spermatogenesis in cells that still adhere to each other (Supplementary Figure 5A-F) [317]. The top 2000 expressed genes in EpCAM$^+$ testicular germ cells were enriched for spermatogenesis-related gene ontology GO_terms, thus supporting the identity of the cells (Supplementary Figure 5).

The analysis revealed a global, although not drastic, de-repression of gene transcription. In particular, about 1000 genes have been found positively regulated (89 downregulated) in the testicular germ cells from HFD-fed mice compared to the LFD group (Figure 3.9A). The DEGs belong to pathways relevant for pentose phosphate, fructose and mannose metabolism, glycerolypid and glycerophospholipid metabolic processes and comprise master regulators of glucose in gluconeogenesis and glycogenolysis (eg. G6pd2, Fbp1, G6pc3, Aldoart1, Lpin1, Gapdhs, Ldha, Adh7, Tpi1) (Figure 3.9B).

The observed global upregulation of gene expression suggested diet-dependent impairment of a chromatin-based silencing system. To detect genomic chromatin accessibility and to discern active (open) and inactive (condensed) chromatin, the transposase-accessible chromatin has been prepared from EpCAM$^+$ germ cells and analyzed following sequencing (ATAC-Seq) (Figure 3.9C) [305]. The analysis revealed an increased global accessibility in the HFD-derived EpCAM+ cells (Figure 3.9C).

With the intent of mapping the transcriptional differences to specific chromatinic domains, a chromatin-state segmentation analysis has been performed by making use of publicly available spermatids ChIp-seq data [274] (Figure 3.9D left panel). Interestingly, the de-repression of gene transcription matched with a de-repression of Polycomb repressed (marked with H3K27me3) (states 4,11,15,16 – Figure 3.9D left panel) and bivalent domains (marked by H3K27me3 and H3K4me1 or H3Kme3) (states 5, 6, 10, 12-14 – Figure 3.9D left panel) in testicular germ cells from HFD animals (Figure 3.9D right panel). In line with this, a global reduction of H3K27me3 histone mark, as shown by immunohistochemistry (Figure 3.9E) performed in the testis, Western Blot (Figure 3.9F) and ELISA (Figure 3.9G), in sorted EpCAM$^+$ cells in the HFD condition suggested a PRC2 dysfunction.

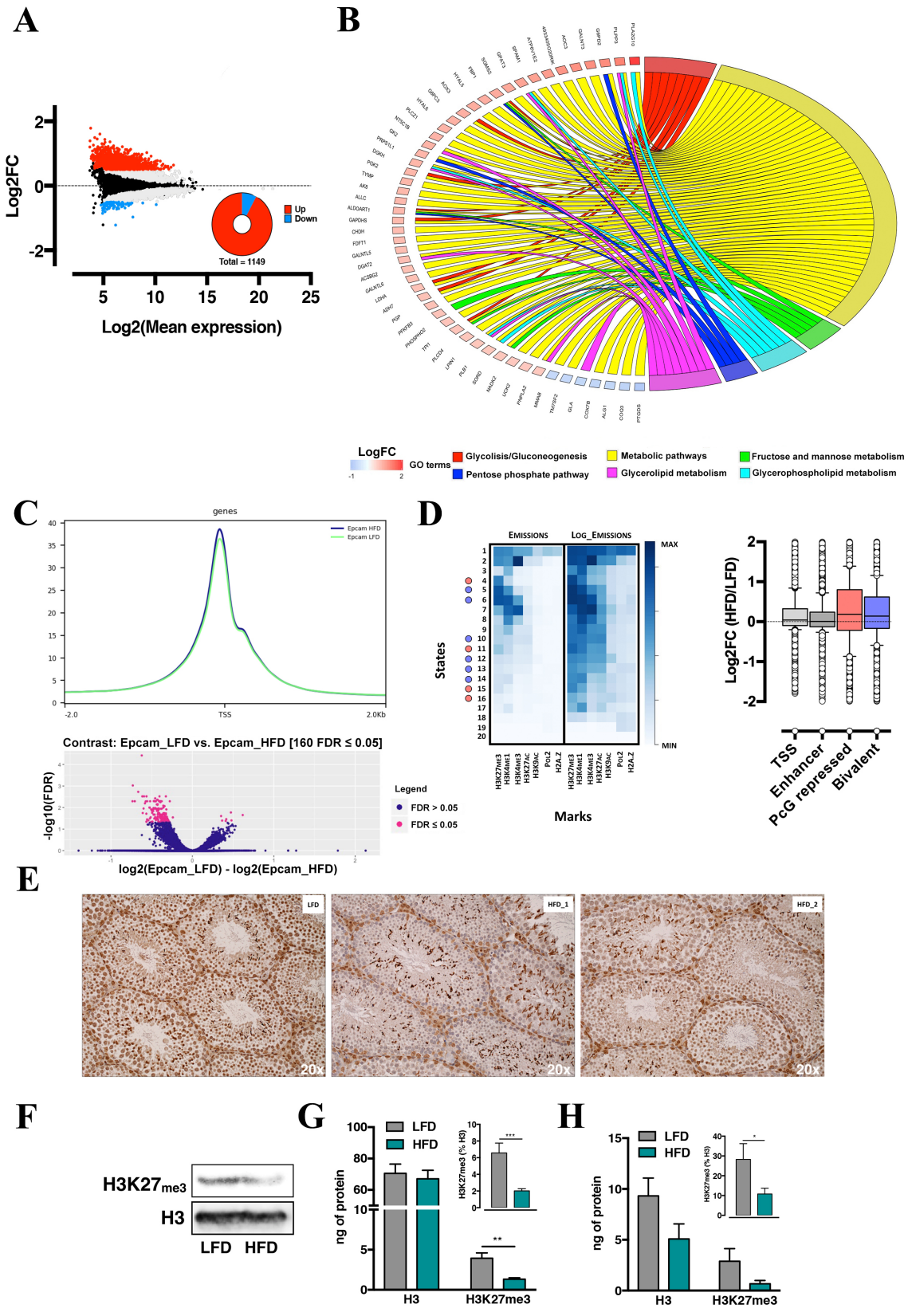

Figure 3.9 - Acute HFD impinges on PRC2 function during spermatogenesis

A. MA-plot representation of RNA-seq analysis of testicular germ cells sorted from LFD and HFD-fed mice. Red (FC ≥ 0.5) and blue (FC ≤ -0.5) dots are genes significantly up- and downregulated respectively (FC > 0.5 and < -0.5). **B.** KEGG pathway analysis of DEGs of HFD/LFD. **C.** ATAC-seq representation, expressed as FDR, showing rate of accessible chromatin

(upper panel) with volcano plot highlight significantly differentially bound sites showed as fold change (lower panel) **D.** EpiCSeg Chromatin state segmentation in wild-type spermatids (left panel) and expression levels at the indicated chromatin states expressed as Log2FC (HFD/LFD – right panel). **D.** H3K27me3 immunohistochemistry analysis on testis from LFD and HFD-fed mice. Scale bars: 50 μm. **E-H.** Western blot (E) and ELISA (F) determination of total H3 and H3K27me3 in testicular germ cells and mature sperm (H) sorted from LFD and HFD-fed mice. The inlet shows the relative abundance of H3K27me3 (% H3). Results expressed as mean ±SEM (n = 6). *p < 0.05 by Student's t test.

Given the global loss of H3K27me3, changes in the related H3K27 acetylation and DNA methylation have been also investigated. Surprisingly, no global alteration in either of them could be detected (Supplementary Figure 6), suggesting TrxG and DNA-methylation independent mechanisms involved in the transcriptional de-repression. To check whether the loss of H3K27 trimethylation in the HFD group was a common diet-induced mechanism, immunohistochemistry analysis has been performed as well in liver, a diet-sensitive peripheral tissue. Interestingly, neither acetylation (Supplementary Figure 6A, C) nor methylation of H3K27 (Supplementary Figure 6B, D) were changed in this organ upon HFD thus suggesting that – at least in the current experimental conditions – the diet-induced reduction of PRC2 activity was specific to spermatogenesis. Finally, the reduction in trimethylation on the K27 of the histone H3 detected in the testicular germ cells (Figure 3.9G) has been also confirmed in the mature spermatozoa (Figure 3.9H).

A complete wave of spermatogenesis in mice requires about 40 days, therefore two weeks of diet may appear as sufficient to affect either the developing germ cells or mature sperm released into the epididymis. Since the partial penetrance of the observed phenotypes may simply come from unaffected germ cells, a second group of mice has been challenged with the 2 weeks of diet followed by 4 weeks of normal chow diet to allow developing germ cells in the seminiferous tubule to complete their development to mature spermatozoa. The results of this experiment instruct on whether the diet has an effect uniquely on epididymal spermatozoa or it affects developing germ cells as well.

Of note, offspring generated with the above approach would either show a close to fully penetrant phenotype or nothing. Interestingly, male offspring of challenged fathers displayed, although not significant, an overall reduced glucose tolerance (Figure 3.10A, B) explained by a loss in insulin sensitivity, as shown by the significantly higher AUC of the second, but not the first, part of the glucose tolerance test (30-120') (Figure 3.10C,D). In keeping with this observation, offspring of HFD-fed fathers are hyperinsulinemic at fasting and remain hyperinsulinemic during the entire glucose challenge (Figure 3.10E-H) and show reduced response to external insulin in an insulin tolerance test (Figure

3.10I). Interestingly, and contrary to the F1 directly derived from the two weeks of challenge, the intergenerational effect was close to full penetrance in males (as population-based analysis reached statistically significant values) with also the females partially affected, as hyperinsulinemic and insulin resistant (Supplementary Figure 8).

These findings suggest that 2 weeks of HFD induce intergenerational inheritance of metabolic phenotypes by acting on both epididymal spermatozoa (2 weeks-direct experiment) and testicular germ cells during spermatogenesis (2+4 weeks experiment).

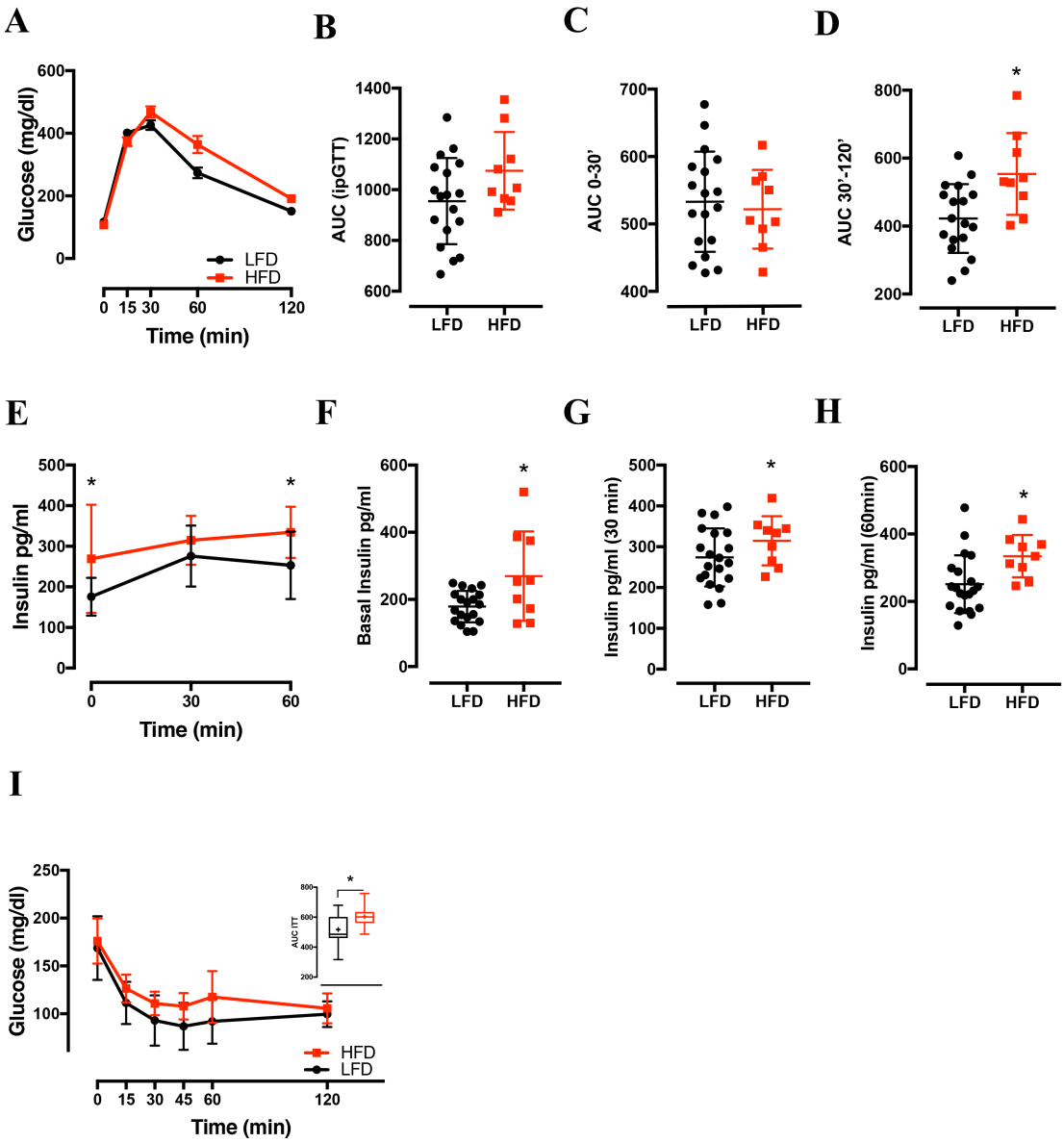

Figure 3.10 - Acute high fat diet impacts on developing germ cells and mediates metabolic phenotypes

A-B. Representation of glucose tolerance test and relative box plot showing the AUC (B). **C-D.** Representation of AUC of individual mice in the first 30 minutes (C) and after 30 minutes (D) of glucose challenge. **E-H.** Insulin measurement during GTT with representation of individual values for basal (F), 30 (G) and 60 minutes (H) after the glucose injection. **I.** Insulin tolerance test with the AUC represented as box plot (upper panel). Results expressed as mean ±SD (LFD = 18, HFD = 9). *p < 0.05 by Student's t test.

3.3 Reduced Polycomb function during spermatogenesis is associated with altered transcriptional programs in pre-implantation embryos

Being haploid, spermatozoa contribute half of the heritable information to the next generation. Given that the alterations detected in spermatozoa could prime the development of the observed adult phenotype, signatures in pre-implantation embryos have also been investigated. To this aim, LFD and HFD sperm have been used to *in vitro*

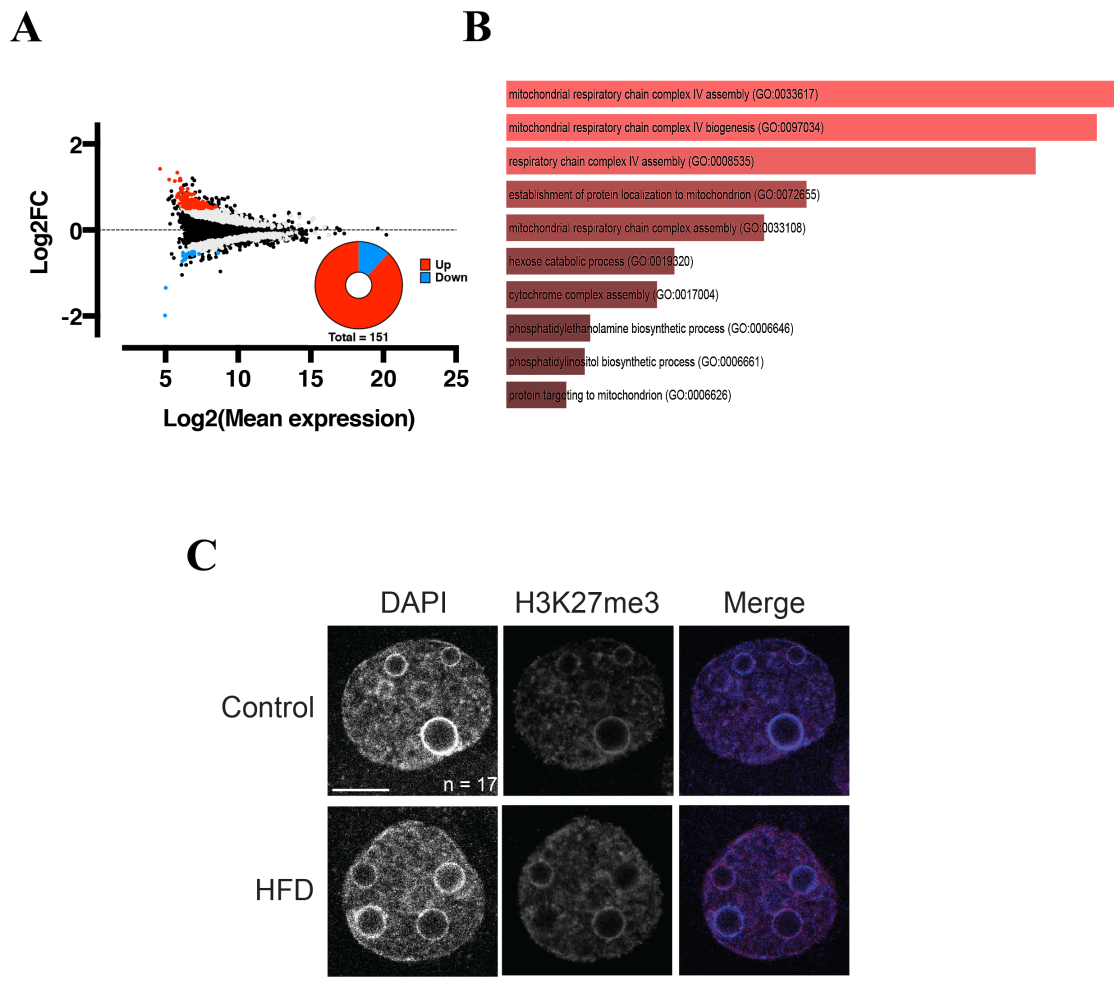

Figure 3.11 - Paternal overweight alters embryo transcriptional programs
A. MA-plot representation of RNA-seq analysis of morula generated via IVF from sperm of LFD and HFD-fed mice. Red (FC ≥ 0.5) and blue (FC ≤ -0.5) dots are genes significantly up- and downregulated respectively. **B.** GO_term analysis of DEGs (HFD/LFD). **C.** Representative single confocal section of the paternal pronucleus from confocal stacks of zygotes derived from control or HFD-treated fathers, stained for H3K27me3 from 2 independent experiments. n = total number of embryos analyzed in each group. Scale bar 10 µm.

fertilize (IVF) oocytes from unexposed females and performed RNA-Seq analysis on

morulae, which are late enough in pre-implantation development to detect embryo-borne phenotypes and transcriptional signatures. In this stage indeed, the maternal and paternal pronuclei are fused and the reprogramming and zygotic genome activation have already taken place [318]. In line with the post fertilization epigenetic reprogramming, no sign of global de-repression has been found, however, a bias towards transcriptional de-repression among DEGs was detectable (Figure 3.11A). GO_term analysis of differentially expressed genes revealed a significant enrichment for mitochondrial functions and cytochrome complex (Figure 3.11B) (e.g. Surf1, Ndufb8, Cox18, Cox17, Timm21), thus for genes important for aerobic respiration, a fundamental function for correct embryonic development [319].

Fertilized oocytes, obtained from a natural mating of HFD mice with unexposed females, have been tested for H3K27me3 to examine whether the alteration was maintained at the early post-fertilization embryonic stage when the maternal and paternal pronuclei are still distinct and clearly visible (Figure 3.11).

The analysis revealed that at this stage of embryonic development, despite the alteration of Polycomb during spermatogenesis, H3K27me3 levels were not altered (Figure 3.11C and Supplementary Figure 7), indicating that any probable alteration during development does not directly rely on the H3K27me3 marks.

3.4 H3K27me3 levels in mature sperm inversely correlate with BMI in humans

The human LIFE Child cohort has revealed that paternal overweight correlates with childhood obesity and insulin resistance (Figure 3.1). To understand whether the changes observed in the epigenetic architecture in the mouse were also occurring for humans, histone H3, together with H3K27 and H3K9 trimethylation were measured in mature sperm cells obtained from healthy human donors stratified per BMI and WC. Methylation of both lysines 9 and 27 of the histone H3 are heterochromatin hallmarks and label transcriptionally inactive promoters. In human germ cells in particular, the trimethylation of the Lys9 gains relevance as it persists during fertilization and is required for the formation of embryonic heterochromatin [294, 320].

While H3K9me3 levels in human sperm were unrelated to BMI, total H3 and H3K27me3 were found to inversely correlate with it (Figure 3.12A). Of note, despite the lower H3 levels in the obese group ($p = 0.054$), the reduction H3K27me3, but not H3K9me3, levels

were significantly reduced in human mature sperm of overweight donors (BMI ≥ 25) when adjusted for total H3 levels (Figure 3.12C,D). Although not yet conclusive, these data suggested that the heterochromatin alteration in mature germ cells could be a common feature of paternal inheritance of obesity and diabetes in mammals.

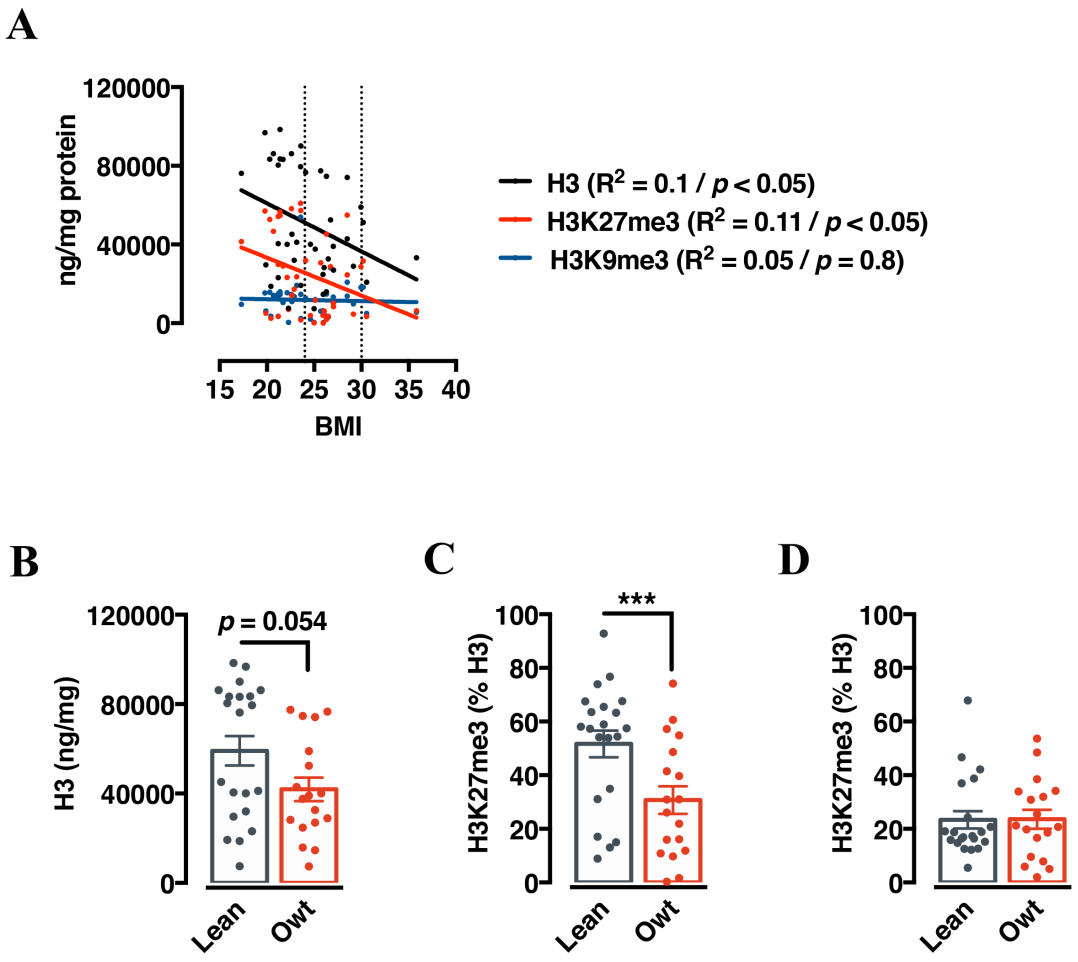

Figure 3.12 - Heterochromatin marks are reduced in sperm from human obese individuals
A. Scatterplot with fitted regression line showing the correlation between BMI and ng for mg of protein for total histone H3 (r^2 = 0.01 p < 0.05), H3K27me3 (r^2 = 0.11 p < 0.05), H3K9me3 (r^2 = 0.05 p = 0.8). B. H3 levels plotted as ng for mg of protein (p = 0.054). C. H3K27me3 plotted as percentage of total H3. D. H3K27me3 ng in mg of protein measured by ELISA. $n = 44$. Results are expressed as mean ±SD. *p < 0.05 by Student's t test.

3.5 Paternal genetic disruption of PRC2 phenocopies the HFD induced overweight in wild-type isogenic offspring

Increased BMI in fathers (Figure 3.1), as well as increased body weight by short HFD feeding in mice (Figure 3.4) have shown transgenerational effect on metabolic homeostasis, linked with reduced PRC2 activity in germ cells. To investigate whether the

reduced PRC2 activity during spermatogenesis was directly causing or it was simply associated to the paternal inheritance, a genetic approach has been chosen. To this purpose, male heterozygous mutants for the Embryonic Ectoderm Development (Eed-het) -core subunit of the PRC2 [321]- have been used to recreate Polycomb disruption.

To validate the model, testicular germ cells from Eed-het mice have been sorted and analyzed. As expected, the RNA-Seq performed in $EpCAM^+$ germ cells showed reduced expression of Eed (Supplementary Figure 9A) and global reduction of H3K27me3 by ELISA assay (Supplementary Figure 9B). Samples clustered accordingly to genotype (Supplementary Figure 9C) with substantial derangement of gene expression at PRC2 target genes such as SMAD1-5, 7, CBX4, 5, 7, FGF11 and H19 among the DEGs (Supplementary Figure 9D). Moreover, DEGs grouped to metabolically relevant pathways such as the MAPK, TGF-β, fructose and mannose metabolism and insulin signaling (Supplementary Figure 9E). Importantly, mature spermatozoa also showed a global reduction of H3K27me3 (Supplementary Figure 9F).

To check whether Polycomb was directly causing the observed paternal effects, wild-type C57BL6/J control mice were compared with co-housed and isogenic wild-type animals coming from Eed-het fathers (Figure 3.13A). In this respect, wild-type offspring of PRC2 mutant fathers would show impaired glucose homeostasis. A comparison between the two groups for several metabolic parameters (Figure 3.13B, C) indeed revealed that, despite the same genetic background, wild-type descendants of heterozygous fathers were discernible from the C57BL6/J controls in terms of metabolic homeostasis. In particular, wild-type offspring of Eed-het fathers increased fat mass when compared with the control group and were hyperinsulinemic and insulin resistant (Figure 3.13D-F). The above results confirmed the idea that a paternal genetic disruption of PRC2 activity phenocopies the overweight-induced intergenerational inheritance of glucose intolerance in a germline dependent manner.

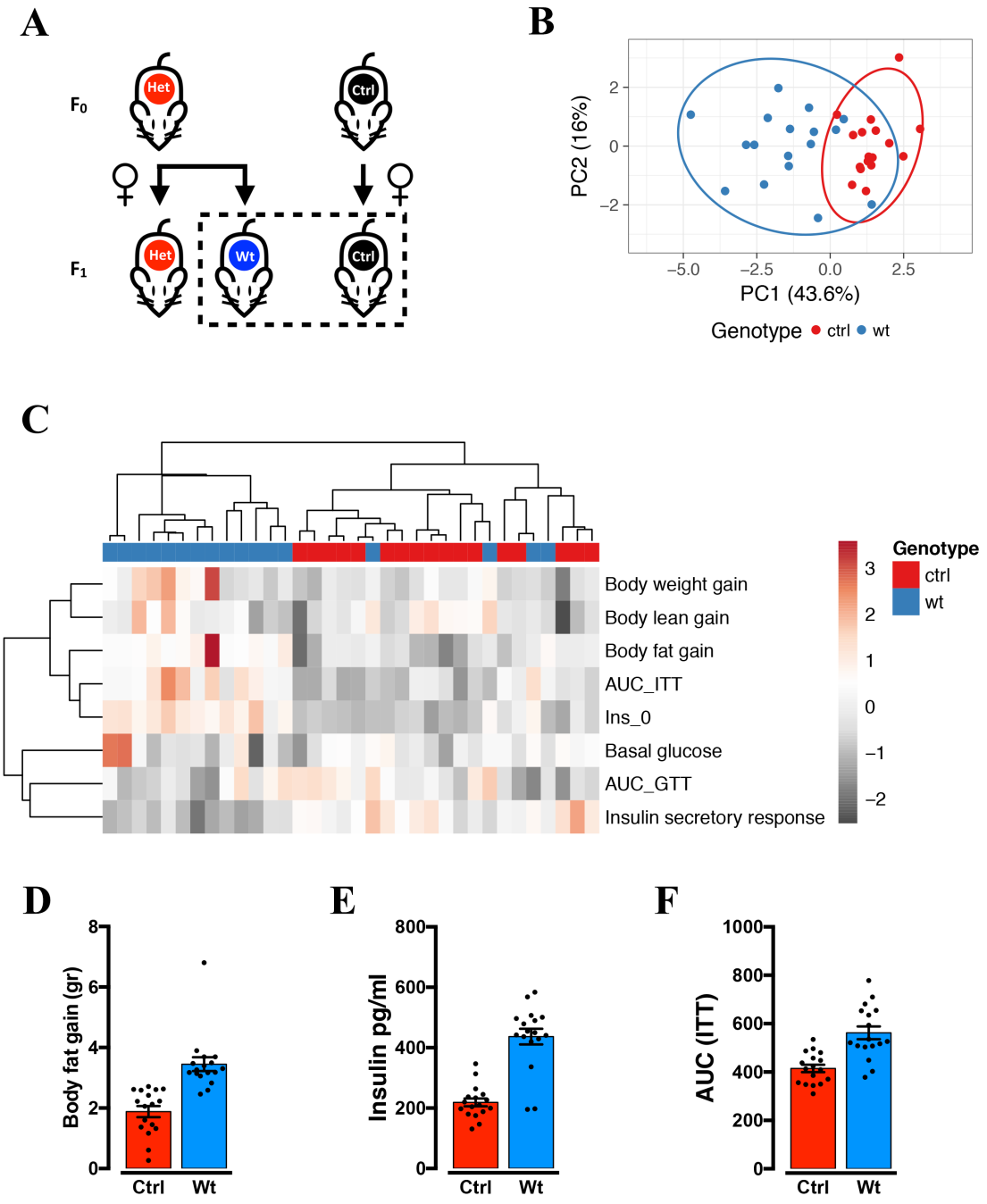

Figure 3.13 - Paternal PRC2 disruption affects the metabolic health of wild-type offspring
A. Schematic representation of F1 generation from Eed heterozygous and control fathers. **B-C**. PCA plot (B) and Heatmap representation (C) of phenotypic results for several metabolic parameters in F1 animals [body weight gain between the 4th to 14th week of age; lean mass gain between the 4th to 14th week of age; body fat gain between the 4th to 14th week of age; area under the curve of ITT (AUC_ITT); basal insulin level (6h fasted Ins_0); fasted blood glucose; area under the curve of the GTT (AUC_GTT); Insulin secretory response (IS_response). **D-F.** Representation of individual values for fat mass gain (D), basal insulin (E) and AUC_ITT (F). Results are representative of two independent cohorts (from four founding fathers each) with 8-10 mice/sex/genotype/cohort. Results are expressed as mean ±SD. *p < 0.05 by Student's t test.

4. DISCUSSION

4.1 Parental influence on offspring BMI

While maternal influence on offspring health has been largely studied and well established, paternal influence is still controversial and requires more evidence. The mother, besides the half DNA supply, directly supports the needs of the embryo until it can acquire food on its own, therefore, both mother and fetus remain directly connected during gestation.

In the last years, progress in this field has seen the father strongly influencing embryonic development and adult health. To further explore the paternal contribution to offspring metabolic control, we used data from a cross-sectional longitudinal human study and analyzed health parameters of more than 3000 children born to parents characterized for metabolic parameters. While we confirmed the critical role of maternal health on offspring BMI, we show paternal weight status as a strong and independent determinant of offspring obesity and metabolic health (Figure 3.1, Supplementary Figure 1), with children having higher chance of developing obesity and insulin resistant in an age-dependent manner. Strikingly, having an overweight father is sufficient to significantly increase the risk of childhood obesity predisposing children to obesity later in life.

Noteworthy, high birth weight increases the risk of type 2 diabetes in males and obesity in both genders [322] and results in higher chance of suffering from atherosclerosis and cardiovascular disease [323]. We observed that the mother, but not the father, influenced the offspring weight at birth confirming that it is a maternal prerogative (Supplementary Figure 2).

Of note, one of the most relevant studies relates to the Dutch famine in 1944. In this study, pregnant women who experienced the famine during pregnancy influenced birth weight and risk of metabolic derangement in adulthood. In particular, famine during the last trimester of pregnancy induced obesity, whereas exposure in the first half of pregnancy resulted in the opposite outcome [324]. This study conducted by Ravelli *et al.* was among the first to reveal an acquired inheritance in humans that was later associated with epigenetic mechanisms. The famine exposure in the early pregnancy, indeed, has been found related to hypermethylation of the imprinted IGF2 receptor [325].

Perhaps, the most famous study focusing on the paternal effects refers to Överkalix population in Sweden. Here, paternal overnutrition during childhood (in the slow growth

phase period) has been found to correlate with increased risk of metabolic and cardiovascular defects in grandsons, revealing paternal relevance and suggesting a specific age (prepubertal) as a sensitive period for transgenerational phenotype transfer. Indeed, when accounting for this kind of inheritance, the time and duration of environmental exposure must be always taken into account. Research in rodents have corroborated findings in humans allowing the dissection of molecular mechanisms mediating the epigenetic inheritance. In the same way, we modeled paternal overweight in mice to further study the underlying mechanism of the observed paternal effects.

4.2 Paternal overweight and partially penetrant glucose intolerance

Our findings show that paternal overweight induces transgenerational glucose intolerance in the BL6J male progeny, which is partially penetrant in the F1 and completely penetrant in the F2 generated from affected F1 males. The choice of using the C57BL6/J strain to model the paternal overweight derived from its recognition as appropriate for the study of human metabolic syndrome. Similar to humans, BL6J are sensitive to dietary challenges. Indeed, they remain lean on standard chow diet and develop obesity, hyperinsulinemia, hyperglycemia and hypertension on high fat diet [326]. In agreement with this, mice challenged with 2 weeks of HFD gained significant weight and showed reduced glucose tolerance (Figure 3.2).

Importantly and differently from other models commonly used, two weeks of high fat diet do not add comorbidities (Figure 3.3), such as inflammation and reduced fertility, that are very commonly seen upon chronic high fat diet feeding. This model thus allows better discrimination of dietary direct and indirect effects and – especially for epigenetic inheritance studies like this – clearer dissection of the underlying molecular mechanisms. The phenotype observed in the F1 males coming from challenged fathers appeared as not completely penetrant, showing two normally distributed populations arising from the same exposed fathers, with discordant glucose tolerance and insulin sensitivity (Figure 3.4). While on the one hand this phenotype could appear as an example of bi-modality (or polyphenism) as shown by Dalgaard *et al.* [327] in the case of Trim28 mutants, on the other hand, it could simply be the result of a partial reprogramming of the paternal epigenome. Evidence supporting this hypothesis come from our and independently published data. As pointed out throughout the thesis, to mimic paternal overweight, we challenge 6 weeks old animals with HFD for 2 weeks. While this recapitulates to many

extents human overweight, it does not cover a sufficient amount of time to robustly induce reprogramming during spermatogenesis and in mature sperm. Spermatogenesis in mice lasts 6 weeks (almost 40 days) [268], and mature spermatozoa released from the seminiferous tubule spend roughly two weeks in the epididymis. The same two weeks are sufficient for spermatogonia to differentiate into round spermatids [268]. In other words, the 2-week HFD challenge, while potentially impacting both developing and mature spermatozoa, is not sufficient to robustly induce full reprogramming in mature spermatozoa, a likely explanation for the partial penetrant intergenerational phenotype. Stemming from these pieces of evidence and to challenge this theory, we have modified our dietary paradigm into a 2+4 challenge, where animals are exposed to the diet for 2 weeks (between 6 and 8 week of age) and are only mated 4 weeks later. This would hypothetically allow reprogrammed developing germ cells to fully mature and complete their epididymal transit. In keeping with this hypothesis, our data show a fully penetrant glucose intolerance and insulin resistance in F1 animals generated from fathers exposed to the 2+4 paradigm (Figure 3.10 and Supplementary Figure 8). These data imply that the partially penetrant phenotype observed upon 2-week exposure is the result of partial germline reprogramming and that – most likely – the first site of action of the HFD is the seminiferous tubule and the developing germ cells.

4.3 Paternal overweight impact on liver and eWAT transcriptional programs

The phenotypic variation observed between HFDt and HFDi F1 males sired from challenged mice was also emphasized by different transcriptional program in liver (Figure 3.5) and visceral white fat (Figure 3.6), important metabolic organs involved in glucose homeostasis and energy balance. Analysis of gene transcription in liver and eWAT revealed that the two tissues are programmed in the same direction maintaining, however, their identity (Supplementary Table 3). Indeed, more than 30% of DEGs in the tissues are commonly downregulated and involved in fundamental metabolic pathways (Figure 3.7) confirming that intolerant and tolerant males are mechanistically different. In line with no variation in lean mass or fat content between the F1 groups, skeletal muscle appeared as similar between the HFD and control groups (Supplementary Figure 3). Muscle is the largest insulin-sensitive tissue, primary site for insulin stimulated glucose utilization where the insulin resistance and altered mitochondrial oxidative capacity are usually

associated with obesity and drive the metabolic dysregulation. Finally, the absence of transcriptional differences suggests unaltered insulin signaling in this tissue, not responsible for the phenotypes observed in the model.

4.4 Sexual dimorphism and female protection

Metabolism is known to be sex-specific in mice and humans [314, 315]. Hormones and chromosomes drive the physiological differences observed between genders. Sexual dimorphism characterizes many phenotypes and disease susceptibilities and it must be always considered in metabolic diseases. In particular, sex in mice has an impact on more than 50% of quantitative traits, such as body weight and morphology [315]. Importantly, we did not observe sexual dimorphism in children with respect to metabolic parameters in response to paternal weight status (Figure 3.1). Conversely, and as expected, we found drastic sexual dimorphism in mice (Supplementary Figure 4). Females F1 are indeed protected from any metabolic alteration induced by paternal overweight; they remain lean, glucose tolerant and insulin sensitive across two generations. The reasons for this observation are yet to be clarified, but our findings are in line with recent actions in biomedical research inclined at considering sex as a biological variable [328, 329].

4.5 Polycomb disruption as mechanism of epigenetic inheritance in mammals

Paternal overweight in mice correlates with reduced PRC2 activity during spermatogenesis (Figure 3.9). Polycomb dysregulation in germ cells associates with transcriptional alterations in the pre-implantation embryos (Figure 3.10), impaired metabolic homeostasis and transcriptional reprogramming in adult F1 animals (Figure 3.4). The alteration of H3K27me3 observed in human mature sperm suggests that this could be a common feature of obesity in mammals (Figure 3.12). Lastly, paternal genetic disruption of PRC2 activity affects metabolic health of the wild-type progeny (Figure 3.13) thus supporting, for the first time, a mechanistic role of PRC2 in paternal intergenerational effects on offspring metabolic health in mammals.

Maintenance of H3K27 methylation and Polycomb-dependent repression across cellular division and generations has been shown in plants, *C. Elegans* and *D. Melanogaster* and

is dependent on self-propagation of the H3K27me3 mark through PRE-mediated Polycomb recruitment to DNA [233, 330-332].

Crucially, embryonic staining (Figure 3.10, Supplementary Figure 7) and further analysis of publicly available H3K27me3 Chip-seq data in morula (not shown) have revealed that H3K27me3 marks and Polycomb target genes were not de-repressed in the HFD condition, thus suggesting Polycomb disruption limited to the F0 and, as expected, most likely reset at fertilization [239, 277, 289].

These results, therefore, propose a mechanism of inheritance that starts with a reduction of PRC2 activity during spermatogenesis, but does not rely on H3K27me3 histone mark during embryogenesis.

Importantly, wild-type offspring of Eed mutant fathers (which therefore carry a genetic disruption of the PRC2 complex) generated via either natural mating or in-vitro fertilization show alterations in metabolic homeostasis (Figure 3.13), similar to offspring of HFD-fed fathers. Altogether, our results show that proper Polycomb functioning in the paternal germline is critical to offspring metabolic health and suggest Polycomb as an important player in paternal control of intergenerational metabolic health.

4.6 Conclusions and critical points

This work reinforces the interrelationships between energy metabolism and epigenetic control of transcriptional program, within and across generations, observed in several species and humans [333-336] and opens new perspectives to fight the rising global epidemic of metabolic disorders.

However, the exact molecular mechanisms of the observed paternal inheritance are yet to be investigated more deeply. Indeed, this study ends up with two main open questions:

- *What controls Polycomb activity during spermatogenesis?*
- *How does a Polycomb-defective germline affect embryonic development and developmental programming of adult metabolism?*

Despite DNA and chromatin borne factors [337, 338], not much is known about the upstream regulation of Polycomb activity and, by similarity with other chromatin modifiers [339], to answer these questions metabolic intermediates are currently being explored.

Polycomb importance during spermatogenesis is well accepted. The repressive complexes are both required for maintenance of undifferentiated spermatogonial stem

cell, progression of meiosis and suppression of somatic genes [340]. Indeed, Eed depletion in mice exhibits infertility as a result of drastic decrease in spermatocytes, post-pachytene spermatocytes and spermatids as consequence of nuclei abnormalities and apoptosis [341].

Bivalent domains are chromatin feature that persist into sperm without being replaced by protamines, this way genes critical for somatic development remain silent throughout the spermatogenesis and, at the same time, allow the establishment of totipotency in the next generation [341]. H3K27me3 has been detected at poised developmental gene promoters in mature sperm [342].

Additionally, PRC2 regulates transposable elements during germ-line reprogramming, indicating that those regions may resist the reprogramming and influence embryonic development [343]. Importantly, the majority of PcG proteins bind to non-coding DNA and repetitive elements. Those interspersed repeats represent mobile genetic elements generators of genetic diversity and drivers of evolution. Retrotransposons belong to the mobile elements and are known to vary in different tissues of soma. A specific regulation of such elements is fundamental in the germline and during embryonic development to avoid their expression and consequent insertional mutations [344, 345]. In this regard, germ-line specific Eed deletion causes increased expression of transposable elements in the germ cells together with alteration of the early embryonic development [291]. This evidence further supports the role of Polycomb in regulating germline reprogramming. Given this, a valid approach would be the investigation of the repetitive element fraction to verify whether their expression change during spermatogenesis of HFD challenged mice. Indeed, dysregulation of repetitive elements may directly affect embryonic development and give rise to metabolic phenotypes in the adulthood.

Together with DNA methylation and histone alteration, ncRNAs participate in many important biological processes and have been also found associated with intergenerational epigenetic inheritance. A large number of ncRNAs have been identified in testis and epididymis important for the regulation of gene expression, for protamine exchange during spermatogenesis [343] and for the correct embryonic development, therefore fundamental to mediate the paternal epigenetic information transfer [346]. Furthermore, several ncRNAs have been linked to PRC2 targeting and found able to directly recruit the complex [347], thus linking histone modification to chromatin conformation and remodeling to inheritance [348], and revealing the non-coding portion of the genome as undoubtedly relevant for epigenetic inheritance. As previously

observed, these mechanisms may all work together to facilitate the transgenerational effect and impact on disease etiology and evolution [349].

The transmission of the environmental information between generations may canalize the development of the offspring in a specific direction. Epigenetic mechanisms may help to prepare the new generation to the parental environment to easily adapt and survive. However, humans more than animals are likely to experience several environments during their life, thus the anticipated environment (as information derived from parents to offspring) could not match with the progeny living environment and give rise to maladapted individuals who show reduced reproductive fitness.

Finally, these findings show that paternal weight in humans influences offspring metabolic health and this is, at least in mice, associated to diet-dependent reduction of Polycomb activity during spermatogenesis. In addition to recently published finding [291], this work reveals for the first time, in mammals, that paternal Polycomb controls offspring metabolic health epigenetically.

5. SUPPLEMENTARY MATERIAL

5.1 Supplementary Figures

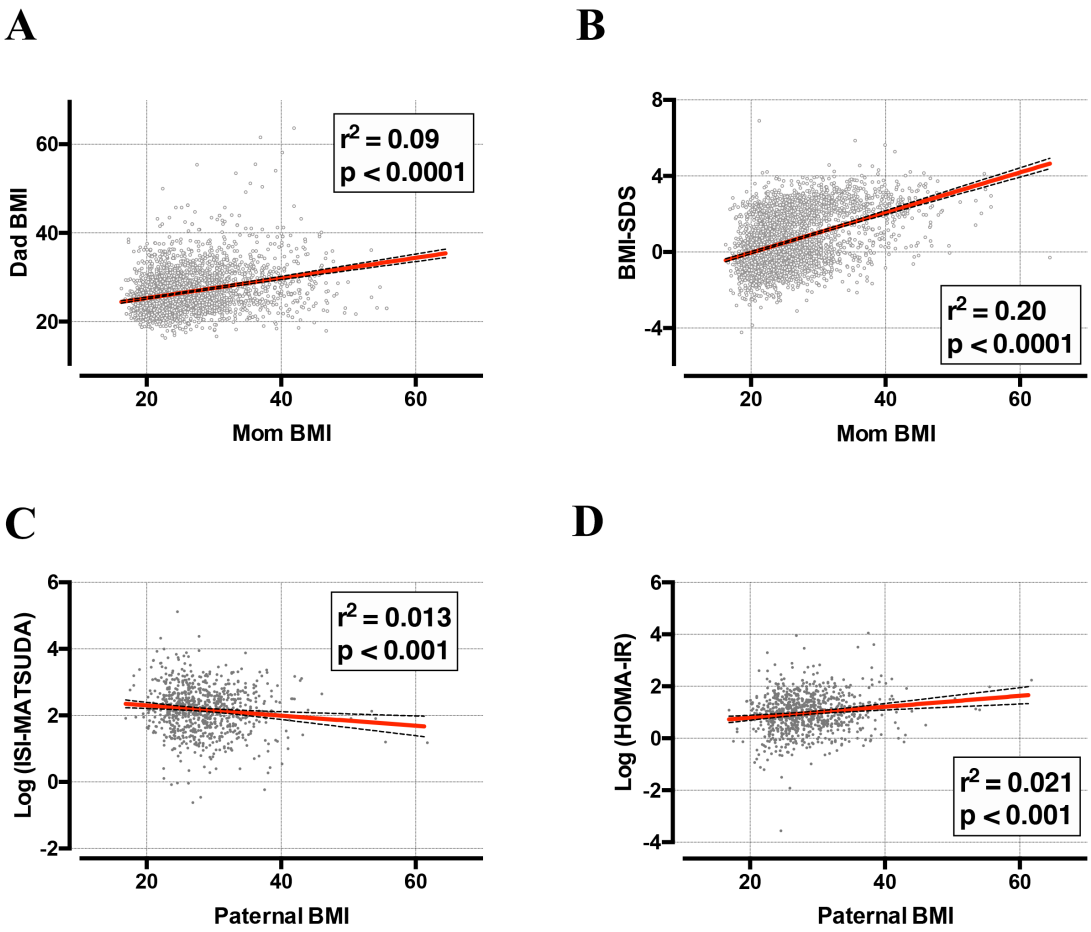

Supplementary Figure 1 - Parental BMI is intercorrelated and correlated to offspring metabolic health

A. Correlation between maternal and paternal BMI; **B.** Correlation between maternal and kids BMI as standard deviation score (SDS). **C-D.** Correlation between paternal BMI and children's insulin sensitivity measured as ISI-Matsuda index (C) or HOMA-IR (D).

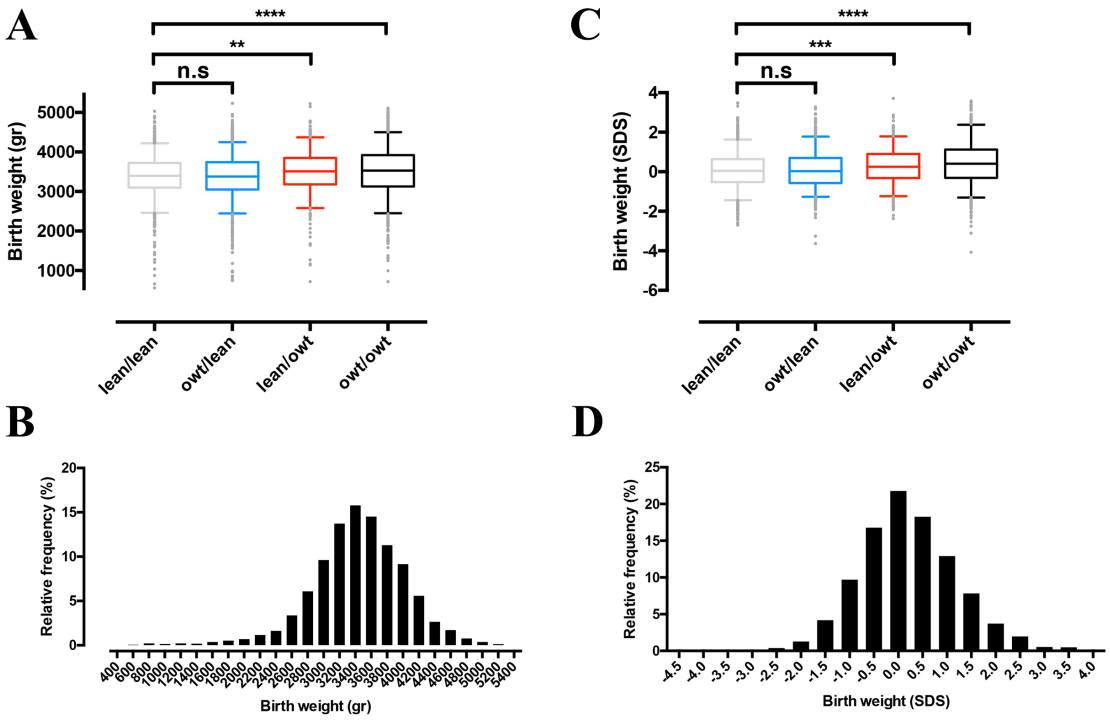

Supplementary Figure 2 - Maternal influence on birth weight

A-D. Birth weight in grams (A) with relative frequency distribution (B); birth weight SDS (C) with relative frequency distribution (D) of children separated by paternal/maternal status of the Life Child cohort.

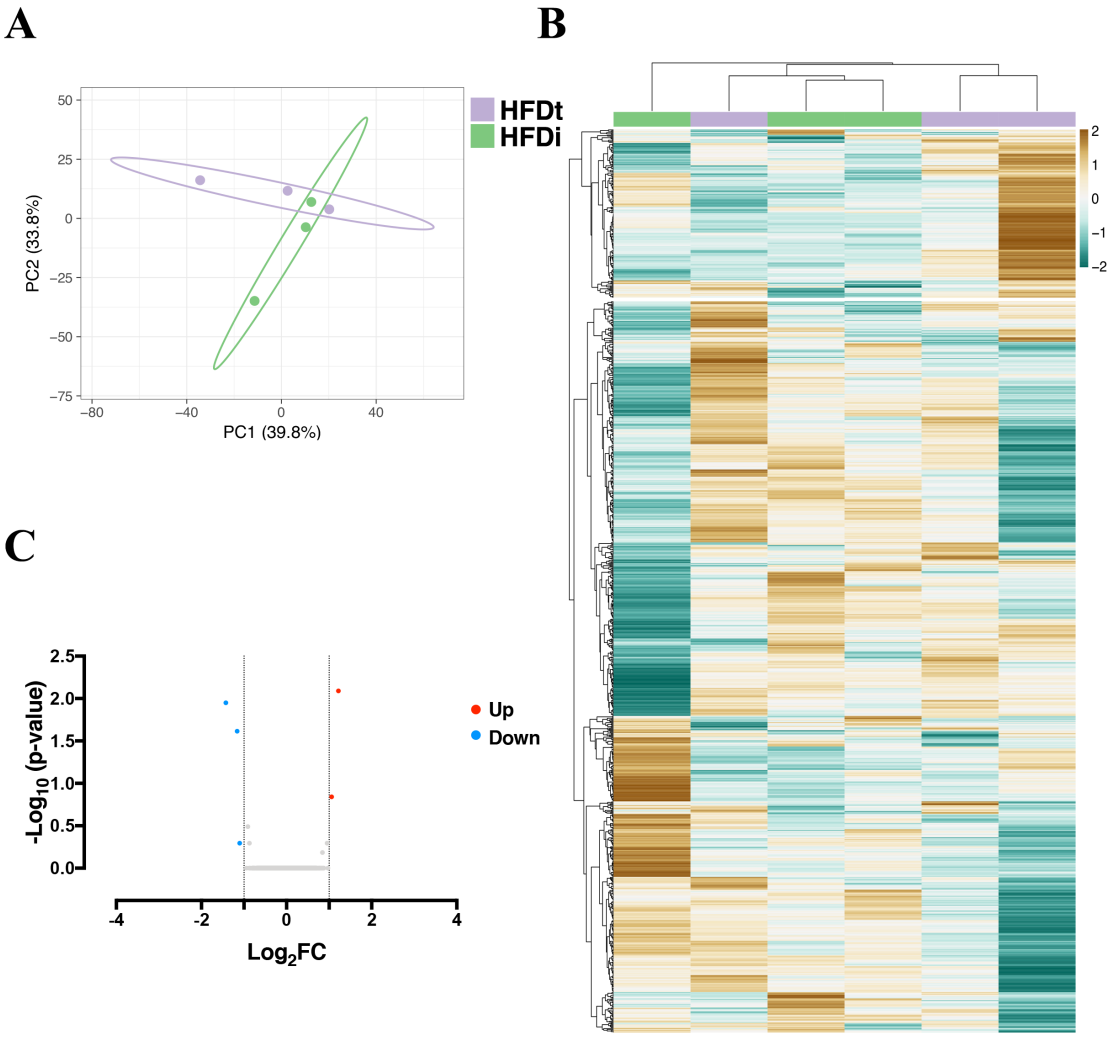

Supplementary Figure 3 - Acute paternal HFD does not affect skeletal muscle transcriptional reprogramming in the F1 progeny

A-B. PCA plot (A) and heatmap representation (B) showing the variation in gene expression in gastrocnemius muscle between HFDt and HFDi F1 male offspring. **C.** MA plot of expressed genes with the DEG genes with FC ≥ 0.5 or ≤ -0.5 in HFDi/HFDt in red.

HFDt and HFDi groups are composed of 3 animals.

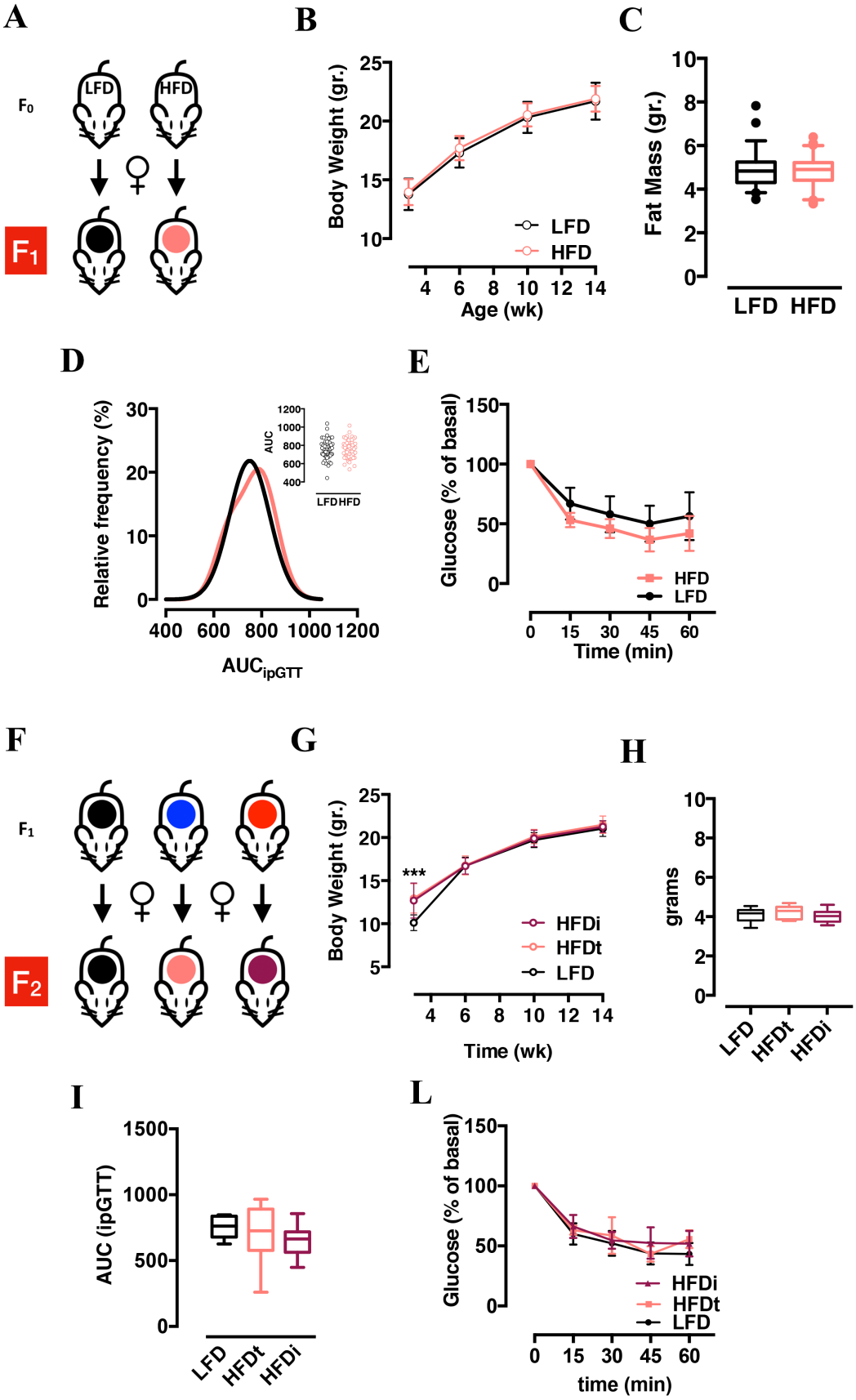

Supplementary Figure 4 - F1 and F2 phenotypes are gender specific

A. Schematic representation of paternal exposures and F1 female generation. **B-C.** Body weight curve (4-14 weeks – B) and fat mass (measured at 14 weeks – C) of LFD and HFD-fed fathers'

descendants. **D.** Frequency distribution and box plot representation (upper panel) of the AUC of glucose tolerance test in F1 animals from LFD or HFD-fed fathers. **E.** Insulin tolerance test with glucose values expressed as percent of basal. **F.** Schematic representation of F2 female generation from LFD, HFDt and HFDi F1 males. **G-H.** Body weight curve (4-14 weeks – G) and fat mass (measured at 14 weeks – H) of F2 animals. **I.** Box plot representation of the area under the curve (AUC) of glucose tolerance test. **L.** Insulin tolerance test of F2 with glucose values expressed as percent of basal.
F1: four independent cohorts (from four founding fathers each) with 12-15 mice/group/cohort.
F2: three independent cohorts (from four founding fathers each) with 10-12 mice/group/cohort.
Results expressed as mean ±SD. *$p < 0.05$ by Student's t test or 1-way or 2-ways ANOVA where applicable.

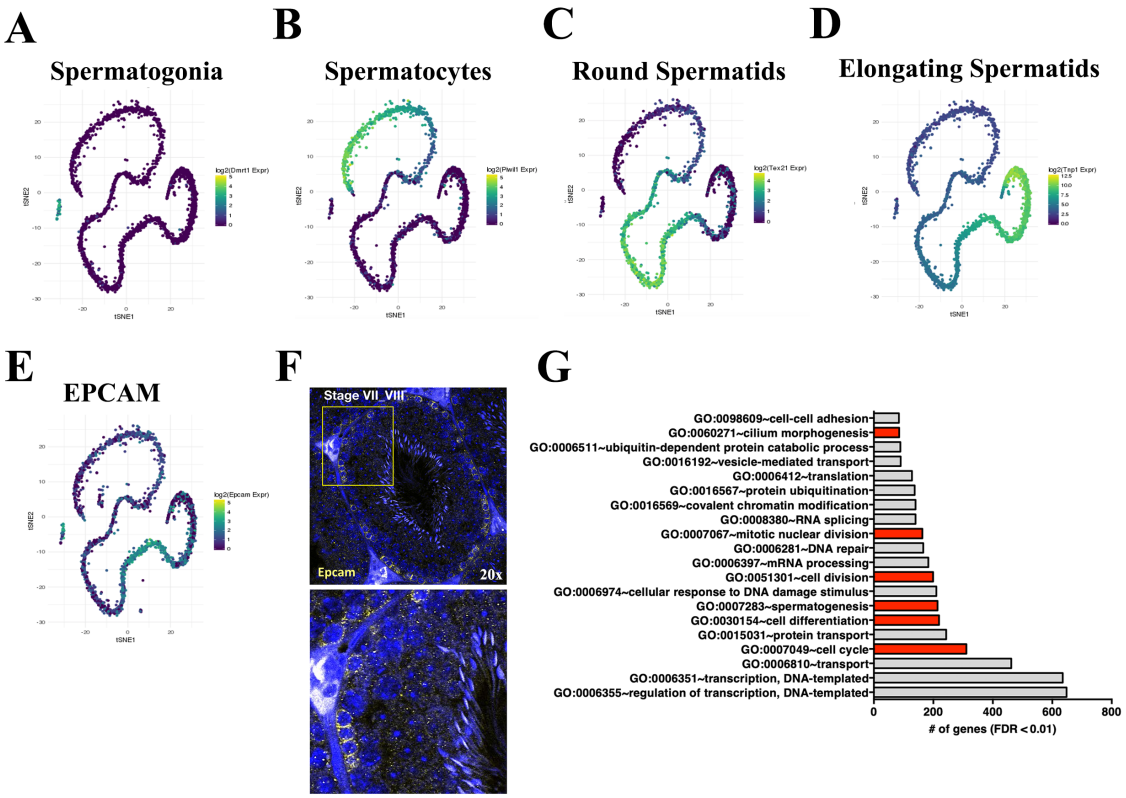

Supplementary Figure 5 - EpCAM labels testicular germ cells

A-C. Graphical representation of different stage of spermatogenesis according to specific markers for Spermatogonia (A), Spermatocytes (B), Round Spermatids (C) and Elongating Spermatids (D). **E.** EpCAM expression within the sperm cell precursors. **F.** Immunofluorescence staining for EpCAM in seminiferous tubules (stage VII-VIII) of wild type animal. Nuclei were stained with DAPI; scale bar: 100 µm. **B.** Gene Ontology Analysis of the top 2000 expressed genes in $EpCAM^{+}$ testicular germ cells isolated from wild-type seminiferous tubules.

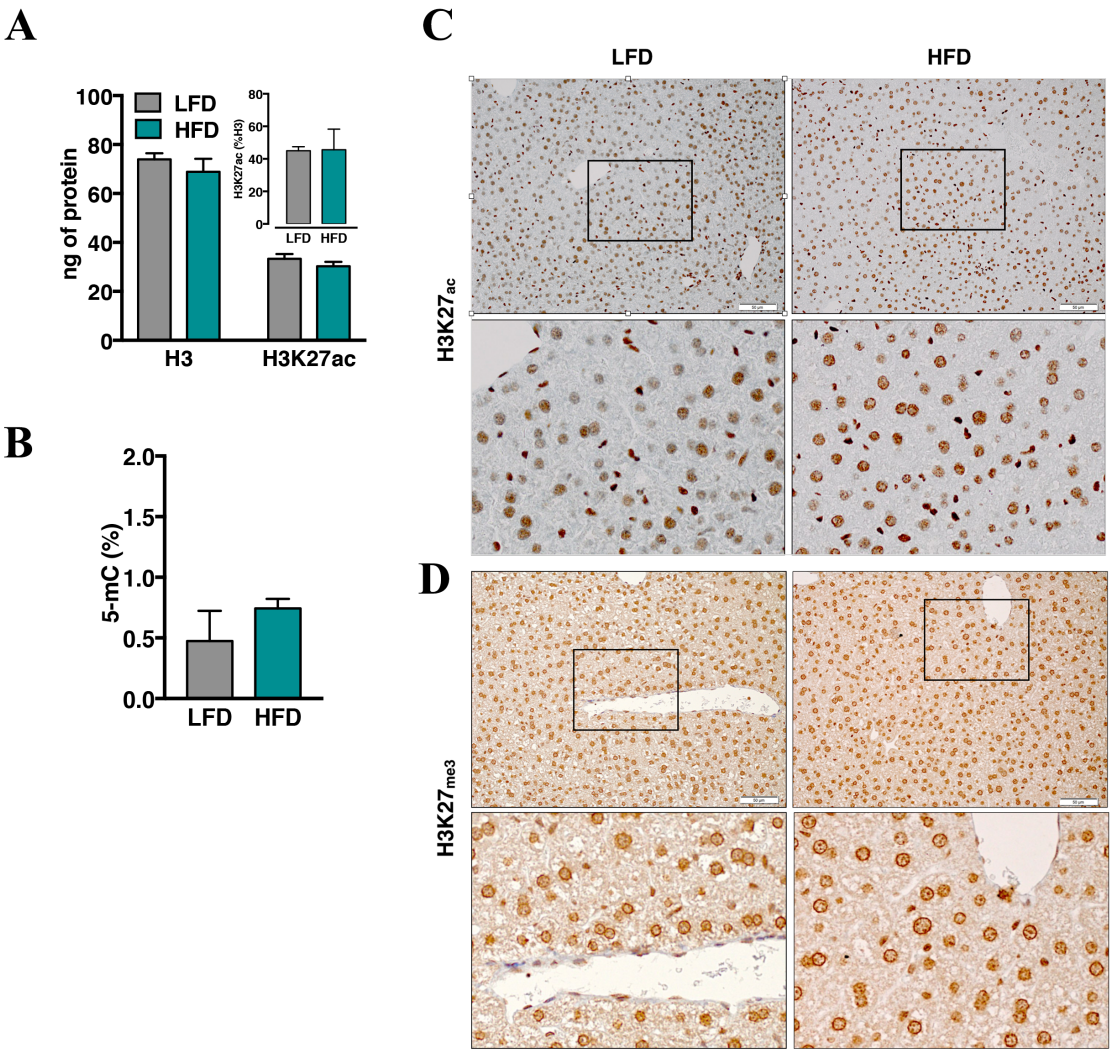

Supplementary Figure 6 - PRC2 impairment in HFD-fed animals is specific to spermatogenesis

A. Quantitative ELISA of total H3 and H3K27ac with relative percentage of H3K27ac over total histone H3 (upper panel) from histones purified from sorted testicular germ cells. **B.** Global DNA Methylation (5-methylcytosine - % total DNA) in sorted testicular germ cells. **C-D.** Immunohistochemistry for H3K27ac (C) and H3k27dme3 (D) in liver from LFD and HFD-fed mice. Scale bars: 50 µm.

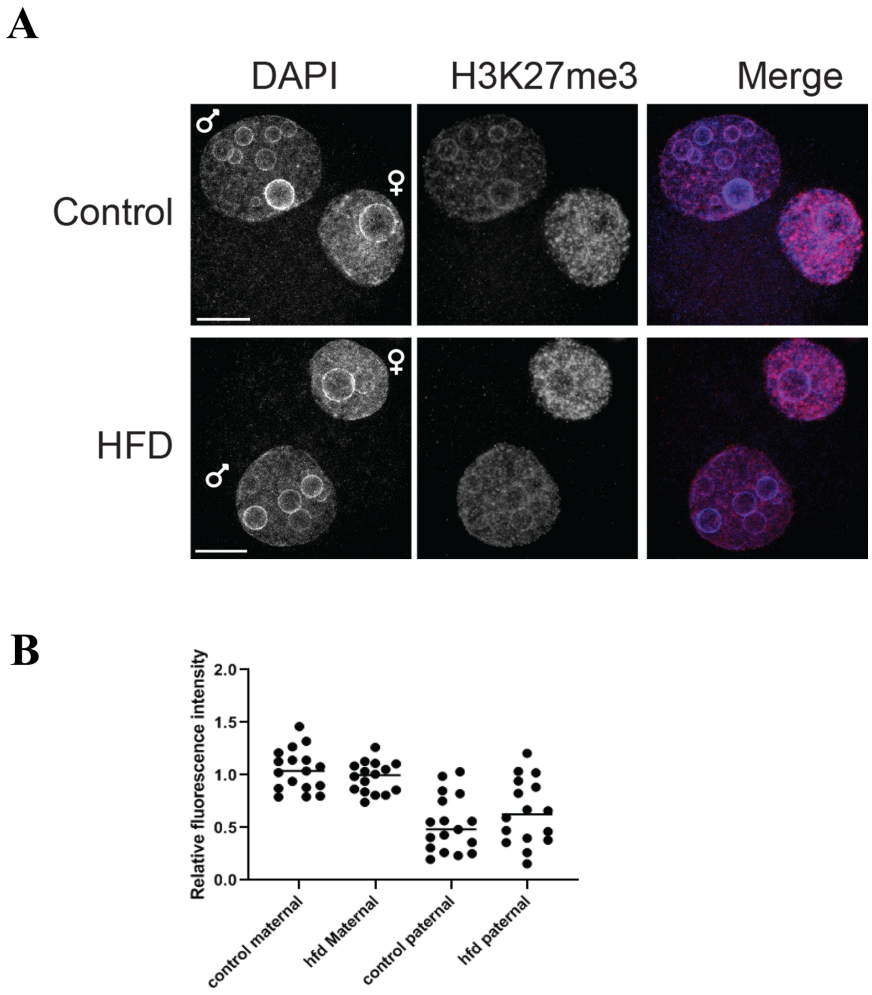

Supplementary Figure 7 - Polycomb dysregulation is not transmitted to the embryo
A. Representative single confocal section of the paternal pronucleus from confocal stacks of zygotes derived from control or HFD-treated fathers, stained for H3K27me3 from 2 independent experiments. $n = 17$ (total number of embryos analyzed in each group). Scale bar 10 μm. **B.** Quantification of the levels of H3K27me3 staining in the maternal and paternal pronuclei across zygotes derived from HFD-treated or control-fed fathers. Confocal stacks were subjected to 3D image reconstruction using IMARIS software and the maternal and paternal pronuclei were segmented using the DAPI channel. The average levels of H3K27me3 staining in the maternal and paternal pronucleus were quantified and normalized to the maternal levels in the control group. The error bars represent the S.E.M. Statistical analysis was performed using the Mann-Whitney U test for comparing nonparametric distributions and no significant difference between control and HFD groups in either maternal or paternal signal was detected.

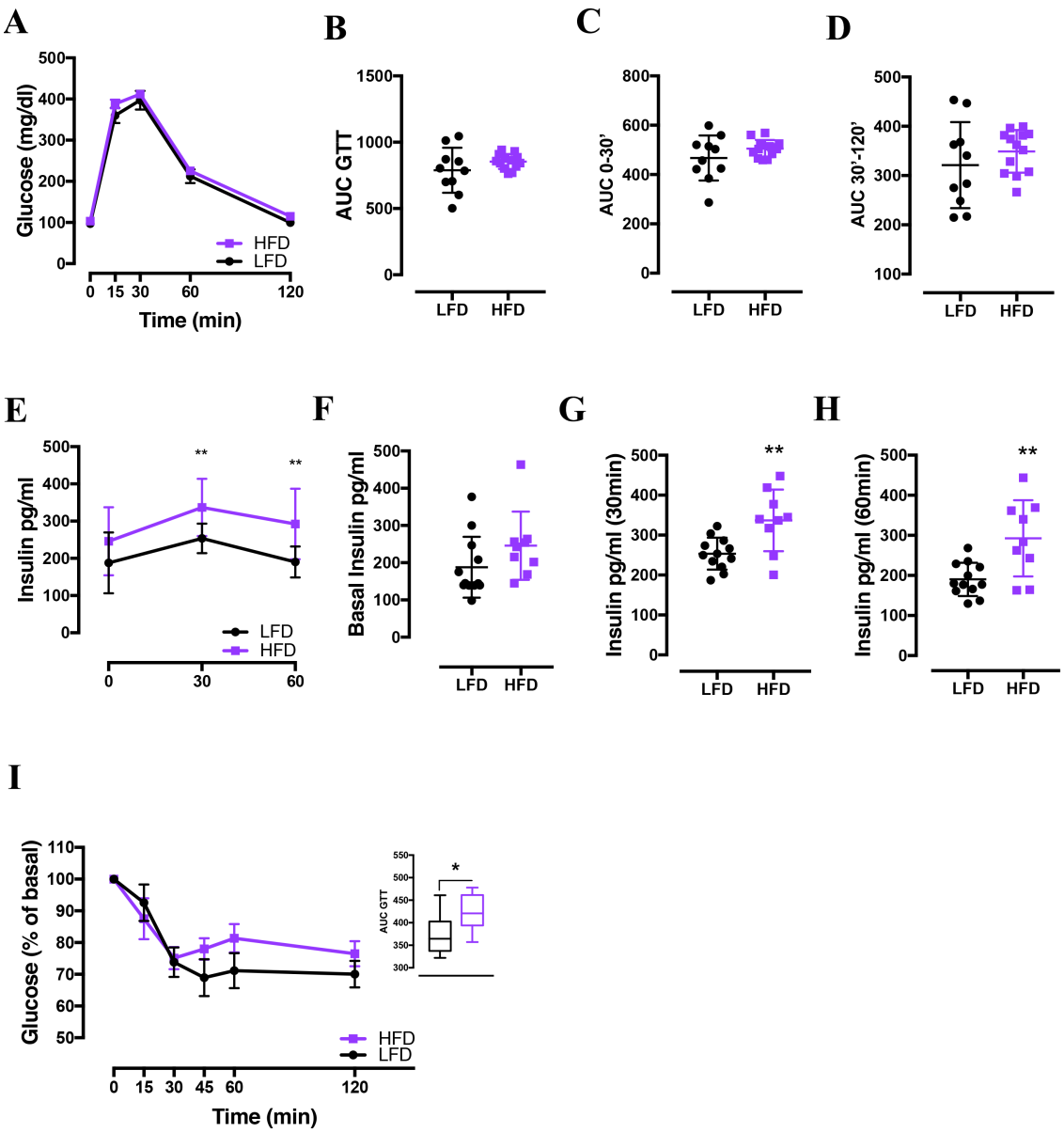

Supplementary Figure 8 - Acute high fat diet impacts on developing germ cells and mediates metabolic phenotypes also in the female offspring

A-B. Representation of glucose tolerance test and relative box plot showing the AUC (B). **C-D.** Representation of AUC of individual mice in the first 30 minutes (C) and after 30 minutes (D) of glucose challenge. **E-H.** Insulin measurement during GTT with representation of individual values for basal (F), 30 (G) and 60 minutes (H) after the glucose injection. **I.** Insulin tolerance test with the AUC represented as box plot (upper panel). Results expressed as mean ±SD (LFD=10, HFD=13). *p < 0.05 by Student's t test.

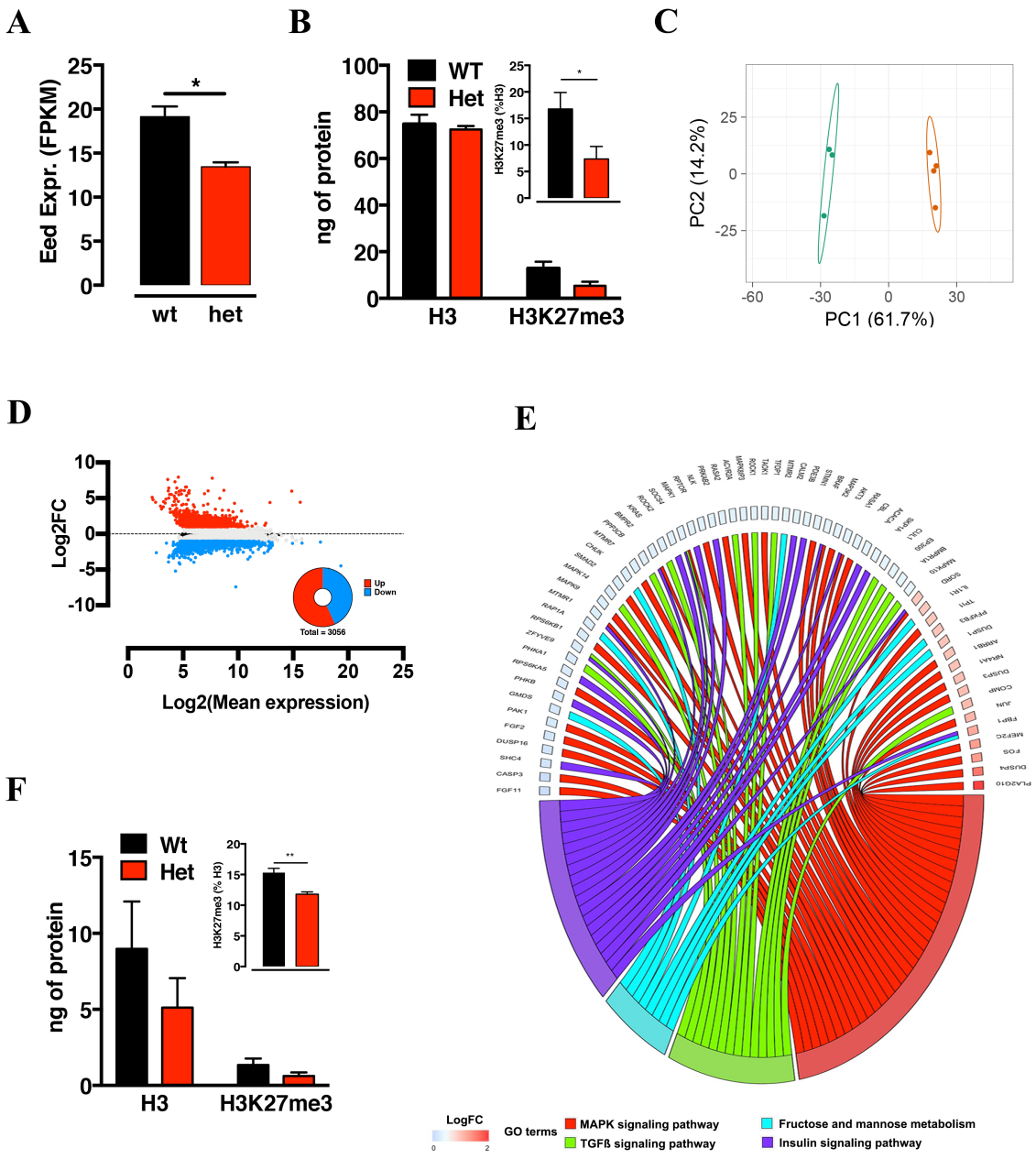

Supplementary Figure 9 - Heterozygous loss of Eed alters transcriptional programs during spermatogenesis

A. Eed expression (FPKM) in testicular germ cells sorted from wild-type and Eed-het testis. **B.** ELISA quantification of total H3 and H3K27me3 with relative percentage of H3K27me3 over total histone H3 (upper panel) of histones isolated from wild-type and Eed heterozygous testicular germ cells. **C-D.** Principal Component Analysis (PCA – C) and MA-plot (D) representation of RNA-Seq analysis performed in testicular germ cells sorted from wild-type and Eed-het testis. Red and blue dots are genes significantly up- and downregulated respectively. Inlet cake plot represent the DEGs. **E.** KEGG pathway analysis of DEGs (Eed-het/wt). **F.** ELISA quantification of total H3 and H3K27me3 with relative percentage of H3K27me3 over total histone H3 (upper panel) of histones isolated from wild-type and Eed-het mature sperm cells. Results expressed as mean ±SEM. *p < 0.05 by Student's t test.

5.2 Supplementary Tables

	Mean	SD	Min	Max
Age	9.3	5.18	0.1	24.0
BMI SDS	0.58	1.40	-4.22	5.86
BMI	20.4	6.60	11.3	65.1
Maternal BMI	25.8	5.99	16.2	64.5
Paternal BMI	26.6	4.58	16.3	63.7

Supplementary Table 1 - Characterization of study population
Data from children/parents trios ($n = 3431$).

Ad1_noMX:	**AATGATACGGCGACCACCGAGATCTACACTCGTCGGCAGCGTCAGATGTG**
Ad2.1_TAAGGCGA	CAAGCAGAAGACGGCATACGAGATTCGCCTTAGTCTCGTGGGCTCGGAGATGT
Ad2.2_CGTACTAG	CAAGCAGAAGACGGCATACGAGATCTAGTACGGTCTCGTGGGCTCGGAGATGT
Ad2.3_AGGCAGAA	CAAGCAGAAGACGGCATACGAGATTTCTGCCTGTCTCGTGGGCTCGGAGATGT
Ad2.4_TCCTGAGC	CAAGCAGAAGACGGCATACGAGATGCTCAGGAGTCTCGTGGGCTCGGAGATGT
Ad2.5_GGACTCCT	CAAGCAGAAGACGGCATACGAGATAGGAGTCCGTCTCGTGGGCTCGGAGATGT
Ad2.6_TAGGCATG	CAAGCAGAAGACGGCATACGAGATCATGCCTAGTCTCGTGGGCTCGGAGATGT
Ad2.7_CTCTCTAC	CAAGCAGAAGACGGCATACGAGATGTAGAGAGGTCTCGTGGGCTCGGAGATGT
Ad2.8_CAGAGAGG	CAAGCAGAAGACGGCATACGAGATCCTCTCTGGTCTCGTGGGCTCGGAGATGT
Ad2.9_GCTACGCT	CAAGCAGAAGACGGCATACGAGATAGCGTAGCGTCTCGTGGGCTCGGAGATGT
Ad2.10_CGAGGCTG	CAAGCAGAAGACGGCATACGAGATCAGCCTCGGTCTCGTGGGCTCGGAGATGT
Ad2.11_AAGAGGCA	CAAGCAGAAGACGGCATACGAGATTGCCTCTTGTCTCGTGGGCTCGGAGATGT
Ad2.12_GTAGAGGA	CAAGCAGAAGACGGCATACGAGATTCCTCTACGTCTCGTGGGCTCGGAGATGT

Supplementary Table 2 - List of ATAC-seq oligos used for PCR

	LFD	HFDt	HFDi	
UP eWAT/Liver p-value	8.48E-26	1.8E-6	1.2E-71	*Fat-specific genes*
DOWN eWAT/Liver p-value	1.02E-04	5.0E-7	2.1E-68	*Liver-specific genes*

Supplementary Table 3 - Functional annotation charts of tissue expression
Top 100 DEGs (Log2FC cutoff = 1 or -1) in eWAT/Liver within the three groups (LFD, HFDt and HFDi). UP DEGs describe Fat specific genes, while DOWN DEGs the liver specific ones, the enrichment score is expressed as p-value.

III. REFERENCES

1. Khan, S.S., et al., *Association of Body Mass Index With Lifetime Risk of Cardiovascular Disease and Compression of Morbidity.*, in *JAMA Cardiol*. 2018, American Medical Association. p. 280-287.
2. Ferraro, K.F., et al., *Body mass index and disability in adulthood: a 20-year panel study.*, in *Am J Public Health*. 2002, American Public Health Association. p. 834-840.
3. Seo, D.-C., S. Choe, and M.R. Torabi, *Is waist circumference ≥102/88cm better than body mass index ≥30 to predict hypertension and diabetes development regardless of gender, age group, and race/ethnicity? Meta-analysis.*, in *Prev Med*. 2017. p. 100-108.
4. Sahakyan, K.R., et al., *Normal-Weight Central Obesity: Implications for Total and Cardiovascular Mortality.*, in *Ann. Intern. Med.* 2015, American College of Physicians. p. 827-835.
5. Cote, A.T., et al., *Childhood obesity and cardiovascular dysfunction.*, in *J. Am. Coll. Cardiol.* 2013. p. 1309-1319.
6. Pollock, N.K., *Childhood obesity, bone development, and cardiometabolic risk factors.*, in *Mol. Cell. Endocrinol.* 2015. p. 52-63.
7. Africa, J.A., K.P. Newton, and J.B. Schwimmer, *Lifestyle Interventions Including Nutrition, Exercise, and Supplements for Nonalcoholic Fatty Liver Disease in Children.*, in *Dig. Dis. Sci.* 2016, Springer US. p. 1375-1386.
8. Biro, F.M. and M. Wien, *Childhood obesity and adult morbidities*, in *Am. J. Clin. Nutr.* 2010. p. 1499S-1505S.
9. Sampson, R.J., S.W. Raudenbush, and F. Earls, *Neighborhoods and violent crime: a multilevel study of collective efficacy.*, in *Science*. 1997. p. 918-924.
10. Bjerregaard, L.G., et al., *Change in Overweight from Childhood to Early Adulthood and Risk of Type 2 Diabetes.* N Engl J Med, 2018. **378**(14): p. 1302-1312.
11. Tirosh, A., et al., *Adolescent BMI trajectory and risk of diabetes versus coronary disease.*, in *N. Engl. J. Med.* 2011, Massachusetts Medical Society. p. 1315-1325.
12. Twig, G., et al., *Body-Mass Index in 2.3 Million Adolescents and Cardiovascular Death in Adulthood.*, in *N. Engl. J. Med.* 2016, Massachusetts Medical Society. p. 2430-2440.
13. Simmonds, M., et al., *Predicting adult obesity from childhood obesity: a systematic review and meta-analysis*, in *Obesity Reviews*. 2015. p. 95-107.
14. Geserick, M., et al., *Acceleration of BMI in Early Childhood and Risk of Sustained Obesity.*, in *N. Engl. J. Med.* 2018. p. 1303-1312.
15. Baker, J.L., L.W. Olsen, and T.I.A. Sørensen, *Childhood body-mass index and the risk of coronary heart disease in adulthood.*, in *N. Engl. J. Med.* 2007, Massachusetts Medical Society. p. 2329-2337.

16. Llewellyn, A., et al., *Childhood obesity as a predictor of morbidity in adulthood: a systematic review and meta-analysis.*, in *Obes Rev*. 2016, Wiley/Blackwell (10.1111). p. 56-67.
17. Bassali, R., et al., *Utility of waist circumference percentile for risk evaluation in obese children.*, in *Int J Pediatr Obes*. 2010, Taylor & Francis. p. 97-101.
18. Fisher, K.J., et al., *Neighborhood-Level Influences on Physical Activity among Older Adults: A Multilevel Analysis*, in *Journal of Aging and Physical Activity*. 2004. p. 45-63.
19. Kubota, T., N. Kubota, and T. Kadowaki, *Imbalanced Insulin Actions in Obesity and Type 2 Diabetes: Key Mouse Models of Insulin Signaling Pathway*, in *Cell Metabolism*. 2017, Elsevier Inc. p. 797-810.
20. Iguacel, I., et al., *Prospective associations between socioeconomically disadvantaged groups and metabolic syndrome risk in European children. Results from the IDEFICS study.*, in *Int. J. Cardiol.* 2018. p. 333-340.
21. Burke, V., et al., *Predictors of body mass index and associations with cardiovascular risk factors in Australian children: a prospective cohort study.*, in *Int J Obes (Lond)*. 2005, Nature Publishing Group. p. 15-23.
22. Semmler, C., et al., *Development of overweight in children in relation to parental weight and socioeconomic status.*, in *Obesity (Silver Spring)*. 2009, John Wiley & Sons, Ltd. p. 814-820.
23. Freeman, E., et al., *Preventing and treating childhood obesity: time to target fathers.*, in *Int J Obes (Lond)*. 2012, Nature Publishing Group. p. 12-15.
24. Carlsen, E.M., et al., *Newborn regional body composition is influenced by maternal obesity, gestational weight gain and the birthweight standard score*, in *Acta Paediatr*. 2014. p. 939-945.
25. Rhee, K.E., et al., *Warm Parenting Associated with Decreasing or Stable Child BMI during Treatment.*, in *Child Obes*. 2016, Mary Ann Liebert, Inc. 140 Huguenot Street, 3rd Floor New Rochelle, NY 10801 USA. p. 94-102.
26. Saltiel, A.R. and C.R. Kahn, *Insulin signalling and the regulation of glucose and lipid metabolism.*, in *Nature*. 2001, Nature Publishing Group. p. 799-806.
27. Graves, L.E. and K.C. Donaghue, *Management of diabetes complications in youth.*, in *Ther Adv Endocrinol Metab*. 2019. p. 2042018819863226.
28. Thomas, M.C., J.M. Forbes, and M.E. Cooper, *Advanced glycation end products and diabetic nephropathy.* Am J Ther, 2005. **12**(6): p. 562-72.
29. Stitt, A.W. and T.M. Curtis, *Advanced glycation and retinal pathology during diabetes.* Pharmacol Rep, 2005. **57 Suppl**: p. 156-68.
30. Yan, S.F., R. Ramasamy, and A.M. Schmidt, *Receptor for AGE (RAGE) and its ligands-cast into leading roles in diabetes and the inflammatory response.* J Mol Med (Berl), 2009. **87**(3): p. 235-47.
31. Association, A.D., *Diagnosis and classification of diabetes mellitus.*, in *Diabetes Care*. 2009, American Diabetes Association. p. S62-7.
32. Weir, G.C. and S. Bonner-Weir, *Five stages of evolving beta-cell dysfunction during progression to diabetes.*, in *Diabetes*. 2004, American Diabetes Association. p. S16-21.

33. Haeusler, R.A., T.E. McGraw, and D. Accili, *Biochemical and cellular properties of insulin receptor signalling.*, in *Nature Reviews Molecular Cell Biology*. 2018, Nature Publishing Group. p. 31-44.
34. Jones, A.G. and A.T. Hattersley, *The clinical utility of C-peptide measurement in the care of patients with diabetes.* Diabet Med, 2013. **30**(7): p. 803-17.
35. Unger, R.H., *Glucoregulatory hormones in health and disease. A teleologic model.* Diabetes, 1966. **15**(7): p. 500-6.
36. Da Silva Xavier, G., *The Cells of the Islets of Langerhans.* J Clin Med, 2018. **7**(3).
37. Rich, S.S., *The Promise and Practice of Genetics on Diabetes Care: The Fog Rises to Reveal a Field of Genetic Complexity in HNF1B.*, in *Diabetes Care*. 2017, American Diabetes Association. p. 1433-1435.
38. Borchers, A.T., R. Uibo, and M.E. Gershwin, *The geoepidemiology of type 1 diabetes.*, in *Autoimmun Rev*. 2010. p. A355-65.
39. Katsarou, A., et al., *Type 1 diabetes mellitus.*, in *Nat Rev Dis Primers*. 2017, Nature Publishing Group. p. 17016.
40. Paschou, S.A., et al., *On type 1 diabetes mellitus pathogenesis.*, in *Endocr Connect*. 2018, Bioscientifica Ltd. p. R38-R46.
41. Pociot, F., et al., *Genetics of type 1 diabetes: what's next?*, in *Diabetes*. 2010, American Diabetes Association. p. 1561-1571.
42. Bensellam, M., J.-C. Jonas, and D.R. Laybutt, *Mechanisms of β-cell dedifferentiation in diabetes: recent findings and future research directions.*, in *J. Endocrinol.* 2018, Bioscientifica Ltd. p. R109-R143.
43. Cerf, M.E., *Beta cell dysfunction and insulin resistance.*, in *Front Endocrinol (Lausanne)*. 2013, Frontiers. p. 37.
44. Huang, X., et al., *The PI3K/AKT pathway in obesity and type 2 diabetes.*, in *Int. J. Biol. Sci.* 2018. p. 1483-1496.
45. Dimitriadis, G., et al., *Insulin effects in muscle and adipose tissue.* Diabetes Res Clin Pract, 2011. **93 Suppl 1**: p. S52-9.
46. Lewis, G.F., et al., *Disordered fat storage and mobilization in the pathogenesis of insulin resistance and type 2 diabetes.*, in *Endocr. Rev.* 2002. p. 201-229.
47. Guh, D.P., et al., *The incidence of co-morbidities related to obesity and overweight: A systematic review and meta-analysis*, in *BMC Public Health*. 2009, BioMed Central. p. 1197-20.
48. Matsuzawa, Y., et al., *Pathophysiology and pathogenesis of visceral fat obesity.*, in *Obes. Res.* 1995. p. 187S-194S.
49. Fujimoto, W.Y., et al., *The visceral adiposity syndrome in Japanese-American men.*, in *Obes. Res.* 1994. p. 364-371.
50. Banerji, M.A., et al., *Body composition, visceral fat, leptin, and insulin resistance in Asian Indian men.*, in *The Journal of Clinical Endocrinology & Metabolism*. 1999. p. 137-144.
51. Gerlini, R., et al., *Glucose tolerance and insulin sensitivity define adipocyte transcriptional programs in human obesity.*, in *Molecular Metabolism*. 2018.
52. Corbin, K.D., et al., *Obesity in Type 1 Diabetes: Pathophysiology, Clinical Impact, and Mechanisms.*, in *Endocr. Rev.* 2018. p. 629-663.

53. Conway, B., et al., *Temporal patterns in overweight and obesity in Type 1 diabetes.*, in *Diabet. Med.* 2010, John Wiley & Sons, Ltd (10.1111). p. 398-404.
54. Flegal, K.M., et al., *Prevalence and trends in obesity among US adults, 1999-2008.* JAMA, 2010. **303**(3): p. 235-41.
55. Minges, K.E., et al., *Correlates of overweight and obesity in 5529 adolescents with type 1 diabetes: The T1D Exchange Clinic Registry.* Diabetes Res Clin Pract, 2017. **126**: p. 68-78.
56. DuBose, S.N., et al., *Obesity in Youth with Type 1 Diabetes in Germany, Austria, and the United States.* J Pediatr, 2015. **167**(3): p. 627-32 e1-4.
57. Bellos, I., et al., *Serum levels of adipokines in gestational diabetes: a systematic review.*, in *J. Endocrinol. Invest.* 2019. p. 621-631.
58. Billionnet, C., et al., *Gestational diabetes and adverse perinatal outcomes from 716,152 births in France in 2012.*, in *Diabetologia*. 2017, Springer Berlin Heidelberg. p. 636-644.
59. Jensen, J., et al., *The role of skeletal muscle glycogen breakdown for regulation of insulin sensitivity by exercise.*, in *Front. Physiol.* 2011, Frontiers. p. 112.
60. Gallwitz, B., *[Type 2 diabetes: Metformin: first choice at the start of therapy].* Dtsch Med Wochenschr, 2015. **140**(4): p. 236.
61. Ryden, M., *[Metformin in type 2 diabetes. An extensive observational study confirms the agent as first choice--so far].* Lakartidningen, 2011. **108**(4): p. 136.
62. Elbein, S.C., *The genetics of human noninsulin-dependent (Type 2) diabetes mellitus*, in *Journal of Nutrition*. 1997. p. 1891S-1896S.
63. Bouchard, C., et al., *The response to long-term overfeeding in identical twins.*, in *N. Engl. J. Med.* 1990, Massachusetts Medical Society. p. 1477-1482.
64. Hainer, V., et al., *A twin study of weight loss and metabolic efficiency.*, in *Int. J. Obes. Relat. Metab. Disord.* 2001. p. 533-537.
65. Stunkard, A.J., et al., *An adoption study of human obesity.*, in *N. Engl. J. Med.* 1986. p. 193-198.
66. Wardle, J., et al., *Evidence for a strong genetic influence on childhood adiposity despite the force of the obesogenic environment.*, in *Am. J. Clin. Nutr.* 2008. p. 398-404.
67. Newman, B., et al., *Concordance for type 2 (non-insulin-dependent) diabetes mellitus in male twins.*, in *Diabetologia*. 1987. p. 763-768.
68. Barnett, A.H., et al., *Diabetes in identical twins - A study of 200 pairs*, in *Diabetologia*. 1981. p. 87-93.
69. Medici, F., et al., *Concordance rate for type II diabetes mellitus in monozygotic twins: actuarial analysis.*, in *Diabetologia*. 1999. p. 146-150.
70. Poulsen, P., et al., *Heritability of type II (non-insulin-dependent) diabetes mellitus and abnormal glucose tolerance--a population-based twin study.*, in *Diabetologia*. 1999. p. 139-145.
71. Gloyn, A.L. and M.I. McCarthy, *The genetics of type 2 diabetes.*, in *Best Pract. Res. Clin. Endocrinol. Metab.* 2001. p. 293-308.
72. Meigs, J.B., L.A. Cupples, and P.W. Wilson, *Parental transmission of type 2 diabetes: the Framingham Offspring Study.*, in *Diabetes*. 2000. p. 2201-2207.
73. Diamond, J., *The double puzzle of diabetes.*, in *Nature*. 2003. p. 599-602.

74. Serjeantson, S.W., et al., *Genetics of diabetes in Nauru: effects of foreign admixture, HLA antigens and the insulin-gene-linked polymorphism.*, in *Diabetologia*. 1983. p. 13-17.
75. Lee, S.H., et al., *Estimating missing heritability for disease from genome-wide association studies.*, in *Am. J. Hum. Genet.* 2011. p. 294-305.
76. Pigeyre, M., et al., *Recent progress in genetics, epigenetics and metagenomics unveils the pathophysiology of human obesity.*, in *Clin. Sci.* 2016, Portland Press Limited. p. 943-986.
77. Goodarzi, M.O., *Genetics of obesity: what genetic association studies have taught us about the biology of obesity and its complications.* Lancet Diabetes Endocrinol, 2018. **6**(3): p. 223-236.
78. Basile, K.J., et al., *Genetic susceptibility to type 2 diabetes and obesity: follow-up of findings from genome-wide association studies.* Int J Endocrinol, 2014. **2014**: p. 769671.
79. Fuchsberger, C., et al., *The genetic architecture of type 2 diabetes.* Nature, 2016. **536**(7614): p. 41-47.
80. Schwenk, R.W., H. Vogel, and A. Schürmann, *Genetic and epigenetic control of metabolic health.*, in *Molecular Metabolism*. 2013. p. 337-347.
81. Lyssenko, V., et al., *Mechanisms by which common variants in the TCF7L2 gene increase risk of type 2 diabetes*, in *J. Clin. Invest.* 2007. p. 2155-2163.
82. Schäfer, S.A., et al., *Impaired glucagon-like peptide-1-induced insulin secretion in carriers of transcription factor 7-like 2 (TCF7L2) gene polymorphisms*, in *Diabetologia*. 2007. p. 2443-2450.
83. Qi, Q. and F.B. Hu, *Genetics of type 2 diabetes in European populations.*, in *J Diabetes*. 2012, John Wiley & Sons, Ltd (10.1111). p. 203-212.
84. Grant, S.F.A., et al., *Variant of transcription factor 7-like 2 (TCF7L2) gene confers risk of type 2 diabetes.*, in *Nature Genetics*. 2006, Nature Publishing Group. p. 320-323.
85. Zeggini, E., et al., *Meta-analysis of genome-wide association data and large-scale replication identifies additional susceptibility loci for type 2 diabetes*, in *Nature Genetics*. 2008. p. 638-645.
86. Scott, R.A., et al., *An Expanded Genome-Wide Association Study of Type 2 Diabetes in Europeans.*, in *Diabetes*. 2017. p. 2888-2902.
87. Saxena, R., et al., *Genome-wide association analysis identifies loci for type 2 diabetes and triglyceride levels*, in *Science*. 2007. p. 1331-1336.
88. Wellcome Trust Case Control, C., *Genome-wide association study of 14,000 cases of seven common diseases and 3,000 shared controls.* Nature, 2007. **447**(7145): p. 661-78.
89. Sladek, R., et al., *A genome-wide association study identifies novel risk loci for type 2 diabetes.*, in *Nature*. 2007, Nature Publishing Group. p. 881-885.
90. Steinthorsdottir, V., et al., *A variant in CDKAL1 influences insulin response and risk of type 2 diabetes.*, in *Nature Genetics*. 2007, Nature Publishing Group. p. 770-775.

91. Dupuis, J., et al., *New genetic loci implicated in fasting glucose homeostasis and their impact on type 2 diabetes risk.*, in *Nature Genetics*. 2010, Nature Publishing Group. p. 105-116.
92. Rung, J., et al., *Genetic variant near IRS1 is associated with type 2 diabetes, insulin resistance and hyperinsulinemia.*, in *Nature Genetics*. 2009, Nature Publishing Group. p. 1110-1115.
93. Wheeler, E. and I. Barroso, *Genome-wide association studies and type 2 diabetes.*, in *Brief Funct Genomics*. 2011. p. 52-60.
94. Scott, R.A., et al., *Large-scale association analyses identify new loci influencing glycemic traits and provide insight into the underlying biological pathways.*, in *Nature Genetics*. 2012, Nature Publishing Group. p. 991-1005.
95. Locke, A.E., et al., *Genetic studies of body mass index yield new insights for obesity biology.*, in *Nature*. 2015, Nature Publishing Group. p. 197-206.
96. Klarin, D., et al., *Genetics of blood lipids among ~300,000 multi-ethnic participants of the Million Veteran Program.*, in *Nature Genetics*. 2018, Nature Publishing Group. p. 1514-1523.
97. Mahajan, A., et al., *Fine-mapping type 2 diabetes loci to single-variant resolution using high-density imputation and islet-specific epigenome maps.*, in *Nature Genetics*. 2018, Nature Publishing Group. p. 1505-1513.
98. Stutzmann, F., et al., *Non-synonymous polymorphisms in melanocortin-4 receptor protect against obesity: the two facets of a Janus obesity gene*, in *Hum. Mol. Genet.* 2007. p. 1837-1844.
99. Dina, C., et al., *Variation in FTO contributes to childhood obesity and severe adult obesity.*, in *Nature Genetics*. 2007, Nature Publishing Group. p. 724-726.
100. Wabitsch, M., et al., *Biologically inactive leptin and early-onset extreme obesity.* N Engl J Med, 2015. **372**(1): p. 48-54.
101. Farooqi, I.S., et al., *Clinical and molecular genetic spectrum of congenital deficiency of the leptin receptor.*, in *N. Engl. J. Med.* 2007, Massachusetts Medical Society. p. 237-247.
102. Krude, H., H. Biebermann, and A. Gruters, *Mutations in the human proopiomelanocortin gene.*, in *Ann. N. Y. Acad. Sci.* 2003. p. 233-239.
103. Özen, S., et al., *Unexpected clinical features in a female patient with proopiomelanocortin (POMC) deficiency.*, in *J. Pediatr. Endocrinol. Metab.* 2015. p. 691-694.
104. Thorleifsson, G., et al., *Genome-wide association yields new sequence variants at seven loci that associate with measures of obesity.*, in *Nature Genetics*. 2009, Nature Publishing Group. p. 18-24.
105. Fall, T. and E. Ingelsson, *Genome-wide association studies of obesity and metabolic syndrome.*, in *Mol. Cell. Endocrinol.* 2014. p. 740-757.
106. Shungin, D., et al., *New genetic loci link adipose and insulin biology to body fat distribution.*, in *Nature*. 2015, Nature Publishing Group. p. 187-196.
107. Consortium, D.G.R.A.M.-a.D., et al., *Genome-wide trans-ancestry meta-analysis provides insight into the genetic architecture of type 2 diabetes susceptibility.*, in *Nature Genetics*. 2014, Nature Publishing Group. p. 234-244.

108. Maher, B., *Personal genomes: The case of the missing heritability.*, in *Nature*. 2008, Nature Publishing Group. p. 18-21.
109. Manolio, T.A., et al., *Finding the missing heritability of complex diseases.*, in *Nature*. 2009, Nature Publishing Group. p. 747-753.
110. Dickson, S.P., et al., *Rare variants create synthetic genome-wide associations.*, in *PLoS Biol.* 2010, Public Library of Science. p. e1000294.
111. Anderson, C.A., et al., *Synthetic associations are unlikely to account for many common disease genome-wide association signals.*, in *PLoS Biol.* 2011, Public Library of Science. p. e1000580.
112. Wray, N.R., S.M. Purcell, and P.M. Visscher, *Synthetic associations created by rare variants do not explain most GWAS results.*, in *PLoS Biol.* 2011, Public Library of Science. p. e1000579.
113. Elks, C.E., et al., *Variability in the heritability of body mass index: a systematic review and meta-regression.*, in *Front Endocrinol (Lausanne)*. 2012, Frontiers. p. 29.
114. Burkhardt, R.W., *Lamarck, evolution, and the inheritance of acquired characters.*, in *Genetics*. 2013, Genetics. p. 793-805.
115. Szyf, M., *Nongenetic inheritance and transgenerational epigenetics*, in *Trends in Molecular Medicine*. 2015, Elsevier Ltd. p. 1-11.
116. Wang, D.D. and F.B. Hu, *Precision nutrition for prevention and management of type 2 diabetes.*, in *Lancet Diabetes Endocrinol*. 2018. p. 416-426.
117. Jirtle, R.L. and M.K. Skinner, *Environmental epigenomics and disease susceptibility.* Nat Rev Genet, 2007. **8**(4): p. 253-62.
118. Holliday, R., *Epigenetics: a historical overview.*, in *Epigenetics*. 2006. p. 76-80.
119. Egger, G., et al., *Epigenetics in human disease and prospects for epigenetic therapy.*, in *Nature*. 2004, Nature Publishing Group. p. 457-463.
120. Klose, R.J. and A.P. Bird, *Genomic DNA methylation: the mark and its mediators.*, in *Trends Biochem. Sci.* 2006. p. 89-97.
121. Bird, A., *DNA methylation patterns and epigenetic memory.*, in *Genes Dev.* 2002, Cold Spring Harbor Lab. p. 6-21.
122. Tahiliani, M., et al., *Conversion of 5-methylcytosine to 5-hydroxymethylcytosine in mammalian DNA by MLL partner TET1.*, in *Science*. 2009, American Association for the Advancement of Science. p. 930-935.
123. Ito, S., et al., *Role of Tet proteins in 5mC to 5hmC conversion, ES-cell self-renewal and inner cell mass specification.*, in *Nature*. 2010, Nature Publishing Group. p. 1129-1133.
124. Wu, S.C. and Y. Zhang, *Active DNA demethylation: many roads lead to Rome.*, in *Nature Reviews Molecular Cell Biology*. 2010, Nature Publishing Group. p. 607-620.
125. Payer, B. and J.T. Lee, *X chromosome dosage compensation: how mammals keep the balance.*, in *Annu. Rev. Genet.* 2008, Annual Reviews. p. 733-772.
126. Kim, M. and J. Costello, *DNA methylation: an epigenetic mark of cellular memory.*, in *Exp. Mol. Med.* 2017, Nature Publishing Group. p. e322-e322.

127. Zamudio, N., et al., *DNA methylation restrains transposons from adopting a chromatin signature permissive for meiotic recombination.*, in *Genes Dev.* 2015, Cold Spring Harbor Lab. p. 1256-1270.
128. Galupa, R. and E. Heard, *X-Chromosome Inactivation: A Crossroads Between Chromosome Architecture and Gene Regulation.*, in *Annu. Rev. Genet.* 2018.
129. Ferguson-Smith, A.C. and D. Bourc'his, *The discovery and importance of genomic imprinting.*, in *Elife*. 2018. p. 84.
130. Smith, Z.D. and A. Meissner, *DNA methylation: roles in mammalian development.*, in *Nat. Rev. Genet.* 2013, Nature Publishing Group. p. 204-220.
131. Mohn, F., et al., *Lineage-specific polycomb targets and de novo DNA methylation define restriction and potential of neuronal progenitors.*, in *Molecular Cell*. 2008. p. 755-766.
132. Luger, K., et al., *Crystal structure of the nucleosome core particle at 2.8 A resolution.*, in *Nature*. 1997, Nature Publishing Group. p. 251-260.
133. Davey, C.A., et al., *Solvent mediated interactions in the structure of the nucleosome core particle at 1.9 a resolution.*, in *J. Mol. Biol.* 2002. p. 1097-1113.
134. Dorigo, B., et al., *Nucleosome arrays reveal the two-start organization of the chromatin fiber.*, in *Science*. 2004, American Association for the Advancement of Science. p. 1571-1573.
135. Duan, Y., et al., *Inflammatory Links Between High Fat Diets and Diseases.*, in *Front Immunol*. 2018, Frontiers. p. 2649.
136. Peterson, C.L. and M.-A. Laniel, *Histones and histone modifications.*, in *Curr. Biol.* 2004. p. R546-51.
137. Bannister, A.J. and T. Kouzarides, *Regulation of chromatin by histone modifications.*, in *Cell Res.* 2011, Nature Publishing Group. p. 381-395.
138. Lawrence, M., S. Daujat, and R. Schneider, *Lateral Thinking: How Histone Modifications Regulate Gene Expression.*, in *Trends Genet.* 2016. p. 42-56.
139. Bernstein, B.E., et al., *Methylation of histone H3 Lys 4 in coding regions of active genes.* Proc Natl Acad Sci U S A, 2002. **99**(13): p. 8695-700.
140. Lachner, M., R.J. O'Sullivan, and T. Jenuwein, *An epigenetic road map for histone lysine methylation.* J Cell Sci, 2003. **116**(Pt 11): p. 2117-24.
141. Cao, R., et al., *Role of histone H3 lysine 27 methylation in Polycomb-group silencing.*, in *Science*. 2002, American Association for the Advancement of Science. p. 1039-1043.
142. O'Meara, M.M. and J.A. Simon, *Inner workings and regulatory inputs that control Polycomb repressive complex 2.*, in *Chromosoma*. 2012. p. 221-234.
143. Murdoch, B.M., et al., *Nutritional Influence on Epigenetic Marks and Effect on Livestock Production.*, in *Front Genet*. 2016. p. 182.
144. van der Knaap, J.A. and C.P. Verrijzer, *Undercover: gene control by metabolites and metabolic enzymes.*, in *Genes Dev.* 2016. p. 2345-2369.
145. Anderson, O.S., K.E. Sant, and D.C. Dolinoy, *Nutrition and epigenetics: an interplay of dietary methyl donors, one-carbon metabolism and DNA methylation.*, in *J. Nutr. Biochem.* 2012. p. 853-859.
146. Ulrey, C.L., et al., *The impact of metabolism on DNA methylation.*, in *Hum. Mol. Genet.* 2005. p. R139-47.

147. Peters, A.H., et al., *Loss of the Suv39h histone methyltransferases impairs mammalian heterochromatin and genome stability.*, in *Cell*. 2001. p. 323-337.
148. Bu, P., et al., *Loss of Gcn5 acetyltransferase activity leads to neural tube closure defects and exencephaly in mouse embryos.*, in *Mol Cell Biol*. 2007. p. 3405-3416.
149. Lyons, S.M., M.M. Fay, and P. Ivanov, *The role of RNA modifications in the regulation of tRNA cleavage.*, in *FEBS Letters*. 2018. p. 2828-2844.
150. Fatica, A. and I. Bozzoni, *Long non-coding RNAs: new players in cell differentiation and development.*, in *Nature Publishing Group*. 2014, Nature Publishing Group. p. 7-21.
151. Alvarez-Dominguez, J.R. and H.F. Lodish, *Emerging mechanisms of long noncoding RNA function during normal and malignant hematopoiesis.*, in *Blood*. 2017. p. 1965-1975.
152. Gu, K., L. Mok, and M.M.W. Chong, *Regulating gene expression in animals through RNA endonucleolytic cleavage.*, in *Heliyon*. 2018. p. e00908.
153. He, L. and G.J. Hannon, *MicroRNAs: small RNAs with a big role in gene regulation.*, in *Nat. Rev. Genet.* 2004, Nature Publishing Group. p. 522-531.
154. Malone, C.D. and G.J. Hannon, *Small RNAs as guardians of the genome.*, in *Cell*. 2009. p. 656-668.
155. Aravin, A.A., et al., *Double-stranded RNA-mediated silencing of genomic tandem repeats and transposable elements in the D. melanogaster germline.*, in *Curr. Biol.* 2001. p. 1017-1027.
156. Inagaki, T., et al., *The FBXL10/KDM2B scaffolding protein associates with novel polycomb repressive complex-1 to regulate adipogenesis.*, in *J. Biol. Chem.* 2015. p. 4163-4177.
157. Watanabe, T., et al., *Retrotransposons and pseudogenes regulate mRNAs and lncRNAs via the piRNA pathway in the germline.*, in *Genome Res.* 2015. p. 368-380.
158. Ozata, D.M., et al., *PIWI-interacting RNAs: small RNAs with big functions*, in *Nature Publishing Group*. 2019, Springer US. p. 1-20.
159. Post, C., et al., *The capacity of target silencing by Drosophila PIWI and piRNAs.*, in *RNA*. 2014, Cold Spring Harbor Lab. p. 1977-1986.
160. Grimson, A., et al., *Early origins and evolution of microRNAs and Piwi-interacting RNAs in animals.*, in *Nature*. 2008, Nature Publishing Group. p. 1193-1197.
161. Girard, A., et al., *A germline-specific class of small RNAs binds mammalian Piwi proteins.*, in *Nature*. 2006. p. 199-202.
162. Rouget, C., et al., *Maternal mRNA deadenylation and decay by the piRNA pathway in the early Drosophila embryo.*, in *Nature*. 2010, Nature Publishing Group. p. 1128-1132.
163. Gou, L.-T., et al., *Pachytene piRNAs instruct massive mRNA elimination during late spermiogenesis.*, in *Cell Res.* 2014, Nature Publishing Group. p. 680-700.
164. Ross, R.J., M.M. Weiner, and H. Lin, *PIWI proteins and PIWI-interacting RNAs in the soma.*, in *Nature*. 2014, Nature Publishing Group. p. 353-359.

165. Pillai, R.S. and S. Chuma, *piRNAs and their involvement in male germline development in mice.*, in *Dev. Growth Differ.* 2012, John Wiley & Sons, Ltd (10.1111). p. 78-92.
166. Aravin, A.A. and D. Bourc'his, *Small RNA guides for de novo DNA methylation in mammalian germ cells.*, in *Genes Dev.* 2008, Cold Spring Harbor Lab. p. 970-975.
167. Kuramochi-Miyagawa, S., et al., *Mili, a mammalian member of piwi family gene, is essential for spermatogenesis.*, in *Development*. 2004, The Company of Biologists Ltd. p. 839-849.
168. Robine, N., et al., *A broadly conserved pathway generates 3'UTR-directed primary piRNAs.*, in *Curr. Biol.* 2009. p. 2066-2076.
169. Beyret, E., N. Liu, and H. Lin, *piRNA biogenesis during adult spermatogenesis in mice is independent of the ping-pong mechanism.*, in *Cell Res.* 2012, Nature Publishing Group. p. 1429-1439.
170. Yamamoto, Y., et al., *Targeted gene silencing in mouse germ cells by insertion of a homologous DNA into a piRNA generating locus.*, in *Genome Res.* 2013, Cold Spring Harbor Lab. p. 292-299.
171. Xu, M., et al., *Mice deficient for a small cluster of Piwi-interacting RNAs implicate Piwi-interacting RNAs in transposon control.*, in *Biology of Reproduction*. 2008. p. 51-57.
172. Rodnina, M.V. and W. Wintermeyer, *The ribosome as a molecular machine: The mechanism of tRNA-mRNA movement in translocation*, in *Biochem. Soc. Trans.* 2011. p. 658-662.
173. Borek, E., et al., *High turnover rate of transfer RNA in tumor tissue.*, in *Cancer Res*. 1977. p. 3362-3366.
174. Gehrke, L., R.E. Bast, and J. Ilan, *An analysis of rates of polypeptide chain elongation in avian liver explants following in vivo estrogen treatment. II. Determination of the specific rates of elongation of serum albumin and vitellogenin nascent chains.*, in *J. Biol. Chem.* 1981. p. 2522-2530.
175. Saikia, M. and M. Hatzoglou, *The Many Virtues of tRNA-derived Stress-induced RNAs (tiRNAs): Discovering Novel Mechanisms of Stress Response and Effect on Human Health.* J Biol Chem, 2015. **290**(50): p. 29761-8.
176. Kumar, P., et al., *Meta-analysis of tRNA derived RNA fragments reveals that they are evolutionarily conserved and associate with AGO proteins to recognize specific RNA targets.*, in *BMC Biol.* 2014, BioMed Central. p. 78.
177. Chen, Q., et al., *Sperm tsRNAs contribute to intergenerational inheritance of an acquired metabolic disorder.*, in *Science*. 2016. p. 397-400.
178. Sharma, U., et al., *Biogenesis and function of tRNA fragments during sperm maturation and fertilization in mammals.*, in *Science*. 2016, American Association for the Advancement of Science. p. 391-396.
179. Kirchner, S. and Z. Ignatova, *Emerging roles of tRNA in adaptive translation, signalling dynamics and disease.*, in *Nature Publishing Group*. 2015, Nature Publishing Group. p. 98-112.
180. Ulitsky, I. and D.P. Bartel, *lincRNAs: genomics, evolution, and mechanisms.*, in *Cell*. 2013. p. 26-46.

181. Ravasi, T., et al., *Experimental validation of the regulated expression of large numbers of non-coding RNAs from the mouse genome.*, in *Genome Res.* 2006. p. 11-19.
182. Cabili, M.N., et al., *Integrative annotation of human large intergenic noncoding RNAs reveals global properties and specific subclasses.*, in *Genes Dev.* 2011. p. 1915-1927.
183. DiStefano, J.K., *The Emerging Role of Long Noncoding RNAs in Human Disease*, in *Spermatogenesis*. 2018, Springer New York. p. 91-110.
184. Bhan, A. and S.S. Mandal, *Long Noncoding RNAs: Emerging Stars in Gene Regulation, Epigenetics and Human Disease*, in *ChemMedChem*. 2014, John Wiley & Sons, Ltd. p. 1932-1956.
185. Wapinski, O. and H.Y. Chang, *Long noncoding RNAs and human disease*, in *Trends in Cell Biology*. 2011, Elsevier Current Trends. p. 354-361.
186. Zhao, J., et al., *Polycomb proteins targeted by a short repeat RNA to the mouse X chromosome.*, in *Science*. 2008. p. 750-756.
187. Tsai, M.C., et al., *Long Noncoding RNA as Modular Scaffold of Histone Modification Complexes*, in *Science*. 2010. p. 689-693.
188. Martianov, I., et al., *Repression of the human dihydrofolate reductase gene by a non-coding interfering transcript*, in *Nature*. 2007, Nature Publishing Group. p. 666-670.
189. Sibbritt, T., H.R. Patel, and T. Preiss, *Mapping and significance of the mRNA methylome.*, in *Wiley Interdiscip Rev RNA*. 2013. p. 397-422.
190. Yue, Y., J. Liu, and C. He, *RNA N6-methyladenosine methylation in post-transcriptional gene expression regulation*, in *Genes Dev.* 2015. p. 1343-1355.
191. Fu, Y., et al., *Gene expression regulation mediated through reversible m6A RNA methylation*, in *Nature Publishing Group*. 2014, Nature Publishing Group. p. 293-306.
192. Shanmugam, R., et al., *Cytosine methylation of tRNA-Asp by DNMT2 has a role in translation of proteins containing poly-Asp sequences.*, in *Cell Discovery*. 2015. p. 15010.
193. Arroyo, J.D., et al., *Argonaute2 complexes carry a population of circulating microRNAs independent of vesicles in human plasma*, in *Proc Natl Acad Sci USA*. 2011. p. 5003-5008.
194. Turchinovich, A., et al., *Characterization of extracellular circulating microRNA*, in *Nucleic Acids Res.* 2011. p. 7223-7233.
195. Tabet, F., et al., *HDL-transferred microRNA-223 regulates ICAM-1 expression in endothelial cells*, in *Nature Communications*. 2014, Nature Publishing Group. p. 11L.
196. Vickers, K.C., et al., *MicroRNAs are transported in plasma and delivered to recipient cells by high-density lipoproteins*, in *Nat. Cell Biol.* 2011, Nature Publishing Group. p. 423-433.
197. Valadi, H., et al., *Exosome-mediated transfer of mRNAs and microRNAs is a novel mechanism of genetic exchange between cells*, in *Nat. Cell Biol.* 2007, Nature Publishing Group. p. 654-659.

198. Caby, M.-P., et al., *Exosomal-like vesicles are present in human blood plasma.*, in *Int. Immunol.* 2005. p. 879-887.
199. Admyre, C., et al., *Exosomes with immune modulatory features are present in human breast milk.*, in *J.I.* 2007. p. 1969-1978.
200. Ogawa, Y., et al., *Exosome-like vesicles with dipeptidyl peptidase IV in human saliva.*, in *Biol. Pharm. Bull.* 2008. p. 1059-1062.
201. Di Carlo, V., I. Mocavini, and L. Di Croce, *Polycomb complexes in normal and malignant hematopoiesis.*, in *J. Cell Biol.* 2019, Rockefeller University Press. p. 55-69.
202. Ferrari, K.J., et al., *Polycomb-dependent H3K27me1 and H3K27me2 regulate active transcription and enhancer fidelity.*, in *Molecular Cell*. 2014. p. 49-62.
203. Margueron, R. and D. Reinberg, *The Polycomb complex PRC2 and its mark in life.* Nature, 2011. **469**(7330): p. 343-9.
204. Pengelly, A.R., et al., *Transcriptional repression by PRC1 in the absence of H2A monoubiquitylation.*, in *Genes Dev.* 2015. p. 1487-1492.
205. Illingworth, R.S., et al., *The E3 ubiquitin ligase activity of RING1B is not essential for early mouse development.*, in *Genes Dev.* 2015. p. 1897-1902.
206. Simon, J.A. and R.E. Kingston, *Occupying chromatin: Polycomb mechanisms for getting to genomic targets, stopping transcriptional traffic, and staying put.*, in *Molecular Cell*. 2013. p. 808-824.
207. Kassis, J.A., J.A. Kennison, and J.W. Tamkun, *Polycomb and Trithorax Group Genes in Drosophila.*, in *Genetics*. 2017. p. 1699-1725.
208. Zee, B.M., et al., *In vivo residue-specific histone methylation dynamics.*, in *J. Biol. Chem.* 2010. p. 3341-3350.
209. Schuettengruber, B., et al., *Genome Regulation by Polycomb and Trithorax: 70 Years and Counting.*, in *Cell*. 2017. p. 34-57.
210. Luo, M., et al., *Polycomb protein SCML2 associates with USP7 and counteracts histone H2A ubiquitination in the XY chromatin during male meiosis.*, in *PLoS Genet*. 2015, Public Library of Science. p. e1004954.
211. Takada, Y., et al., *Mammalian Polycomb Scmh1 mediates exclusion of Polycomb complexes from the XY body in the pachytene spermatocytes.*, in *Development*. 2007. p. 579-590.
212. Hasegawa, K., et al., *SCML2 establishes the male germline epigenome through regulation of histone H2A ubiquitination.*, in *Developmental Cell*. 2015. p. 574-588.
213. Lesch, B.J., et al., *A set of genes critical to development is epigenetically poised in mouse germ cells from fetal stages through completion of meiosis.*, in *Proc. Natl. Acad. Sci. U.S.A.* 2013. p. 16061-16066.
214. Vavouri, T. and B. Lehner, *Chromatin organization in sperm may be the major functional consequence of base composition variation in the human genome.*, in *PLoS Genet*. 2011, Public Library of Science. p. e1002036.
215. Brykczynska, U., et al., *Repressive and active histone methylation mark distinct promoters in human and mouse spermatozoa.* Nat Struct Mol Biol, 2010. **17**(6): p. 679-87.

216. Hammoud, S.S., et al., *Transcription and imprinting dynamics in developing postnatal male germline stem cells.* Genes Dev, 2015. **29**(21): p. 2312-24.
217. Berry, S. and C. Dean, *Environmental perception and epigenetic memory: mechanistic insight through FLC.*, in *Plant J.* 2015. p. 133-148.
218. Stern, S., et al., *Epigenetically heritable alteration of fly development in response to toxic challenge.*, in *CellReports*. 2012. p. 528-542.
219. Cannon, C.E., et al., *The Polycomb protein, Bmi1, regulates insulin sensitivity.*, in *Molecular Metabolism*. 2014. p. 794-802.
220. Wang, L., et al., *Histone H3K27 methyltransferase Ezh2 represses Wnt genes to facilitate adipogenesis.*, in *Proc. Natl. Acad. Sci. U.S.A.* 2010, National Academy of Sciences. p. 7317-7322.
221. Mikkelsen, T.S., et al., *Comparative epigenomic analysis of murine and human adipogenesis.*, in *Cell*. 2010. p. 156-169.
222. Jamieson, K., et al., *Regional control of histone H3 lysine 27 methylation in Neurospora.*, in *Proc. Natl. Acad. Sci. U.S.A.* 2013. p. 6027-6032.
223. Dumesic, P.A., et al., *Product binding enforces the genomic specificity of a yeast polycomb repressive complex.*, in *Cell*. 2015. p. 204-218.
224. van Mierlo, G., et al., *The Complexity of PRC2 Subcomplexes.*, in *Trends in Cell Biology*. 2019. p. 660-671.
225. Hauri, S., et al., *A High-Density Map for Navigating the Human Polycomb Complexome.*, in *CellReports*. 2016. p. 583-595.
226. Dorafshan, E., T.G. Kahn, and Y.B. Schwartz, *Hierarchical recruitment of Polycomb complexes revisited.*, in *Nucleus*. 2017, Taylor & Francis. p. 496-505.
227. Guertin, M.J. and J.T. Lis, *Chromatin landscape dictates HSF binding to target DNA elements.*, in *PLoS Genet*. 2010, Public Library of Science. p. e1001114.
228. Yuan, W., et al., *Dense chromatin activates Polycomb repressive complex 2 to regulate H3 lysine 27 methylation.*, in *Science*. 2012. p. 971-975.
229. Klose, R.J., et al., *Chromatin sampling--an emerging perspective on targeting polycomb repressor proteins.*, in *PLoS Genet*. 2013. p. e1003717.
230. Frey, F., et al., *Molecular basis of PRC1 targeting to Polycomb response elements by PhoRC.*, in *Genes Dev.* 2016. p. 1116-1127.
231. Jepsen, K., et al., *SMRT-mediated repression of an H3K27 demethylase in progression from neural stem cell to neuron.*, in *Nature*. 2007, Nature Publishing Group. p. 415-419.
232. Alhaj Abed, J., et al., *De novo recruitment of Polycomb-group proteins in Drosophila embryos.*, in *Development*. 2018. p. dev165027.
233. Steffen, P.A. and L. Ringrose, *What are memories made of? How Polycomb and Trithorax proteins mediate epigenetic memory.* Nat Rev Mol Cell Biol, 2014. **15**(5): p. 340-56.
234. Rickels, R., et al., *An Evolutionary Conserved Epigenetic Mark of Polycomb Response Elements Implemented by Trx/MLL/COMPASS.*, in *Molecular Cell*. 2016. p. 318-328.
235. Denissov, S., et al., *Mll2 is required for H3K4 trimethylation on bivalent promoters in embryonic stem cells, whereas Mll1 is redundant.*, in *Development*. 2014. p. 526-537.

236. Sachs, M., et al., *Bivalent chromatin marks developmental regulatory genes in the mouse embryonic germline in vivo.*, in *CellReports*. 2013. p. 1777-1784.
237. Hammoud, S.S., et al., *Distinctive chromatin in human sperm packages genes for embryo development.*, in *Nature*. 2009, Nature Publishing Group. p. 473-478.
238. Bernstein, B.E., et al., *A bivalent chromatin structure marks key developmental genes in embryonic stem cells.*, in *Cell*. 2006. p. 315-326.
239. Liu, X., et al., *Distinct features of H3K4me3 and H3K27me3 chromatin domains in pre-implantation embryos.* Nature, 2016. **537**(7621): p. 558-562.
240. Cui, K., et al., *Chromatin signatures in multipotent human hematopoietic stem cells indicate the fate of bivalent genes during differentiation.*, in *Cell Stem Cell*. 2009. p. 80-93.
241. Cui, P., et al., *Comparative analyses of H3K4 and H3K27 trimethylations between the mouse cerebrum and testis.*, in *Genomics Proteomics Bioinformatics*. 2012. p. 82-93.
242. Kinkley, S., et al., *reChIP-seq reveals widespread bivalency of H3K4me3 and H3K27me3 in CD4(+) memory T cells.*, in *Nature Communications*. 2016, Nature Publishing Group. p. 12514.
243. Mikkelsen, T.S., et al., *Genome-wide maps of chromatin state in pluripotent and lineage-committed cells.*, in *Nature*. 2007, Nature Publishing Group. p. 553-560.
244. Liu, J., et al., *Dynamics of RNA Polymerase II Pausing and Bivalent Histone H3 Methylation during Neuronal Differentiation in Brain Development.*, in *CellReports*. 2017. p. 1307-1318.
245. Lesch, B.J. and D.C. Page, *Poised chromatin in the mammalian germ line.*, in *Development*. 2014. p. 3619-3626.
246. Wei, Y., H. Schatten, and Q.-Y. Sun, *Environmental epigenetic inheritance through gametes and implications for human reproduction*. 2014. p. 194-208.
247. Schagdarsurengin, U. and K. Steger, *Epigenetics in male reproduction: effect of paternal diet on sperm quality and offspring health*, in *Nature Publishing Group*. 2016, Nature Publishing Group. p. 584-595.
248. Perez, M.F. and B. Lehner, *Intergenerational and transgenerational epigenetic inheritance in animals.*, in *Nat. Cell Biol.* 2019. p. 143-151.
249. Skinner, M.K., *What is an epigenetic transgenerational phenotype? F3 or F2.*, in *Reprod. Toxicol.* 2008. p. 2-6.
250. Dias, B.G. and K.J. Ressler, *Experimental evidence needed to demonstrate inter- and trans-generational effects of ancestral experiences in mammals.*, in *Bioessays*. 2014. p. 919-923.
251. Hayashi, K., et al., *Reconstitution of the mouse germ cell specification pathway in culture by pluripotent stem cells.* Cell, 2011. **146**(4): p. 519-32.
252. Wells, J.C.K., *Commentary: Paternal and maternal influences on offspring phenotype: the same, only different.*, in *Int J Epidemiol*. 2014. p. 772-774.
253. Rando, O.J. and R.A. Simmons, *I'm Eating for Two: Parental Dietary Effects on Offspring Metabolism*, in *Cell*. 2015. p. 93-105.
254. Sharma, A., *Transgenerational epigenetics: Integrating soma to germline communication with gametic inheritance*, in *Mechanisms of Ageing and Development*. 2017, Elsevier Ireland Ltd. p. 1-8.

255. Victora, C.G., et al., *Maternal and child undernutrition: consequences for adult health and human capital.*, in *Lancet*. 2008. p. 340-357.
256. Melaku, Y.A., et al., *Trends of mortality attributable to child and maternal undernutrition, overweight/obesity and dietary risk factors of non-communicable diseases in sub-Saharan Africa, 1990-2015: findings from the Global Burden of Disease Study 2015.*, in *Public Health Nutr*. 2018, Cambridge University Press. p. 1-14.
257. Limones, M., et al., *Metabolic alterations associated with maternal undernutrition during the first half of gestation lead to a diabetogenic state in the rat.*, in *Eur J Nutr*. 2018, Springer Berlin Heidelberg. p. 450-13.
258. Gutiérrez-Arzapalo, P.Y., et al., *Role of fetal nutrient restriction and postnatal catch-up growth on structural and mechanical alterations of rat aorta.*, in *The Journal of Physiology*. 2018. p. 5791-5806.
259. Ashorn, P., et al., *Co-causation of reduced newborn size by maternal undernutrition, infections, and inflammation.*, in *Matern Child Nutr*. 2018. p. e12585.
260. Fleming, T.P., et al., *Origins of lifetime health around the time of conception: causes and consequences.*, in *Lancet*. 2018. p. 1842-1852.
261. Pereira, T.J., et al., *Influence of maternal overnutrition and gestational diabetes on the programming of metabolic health outcomes in the offspring: experimental evidence.*, in *Biochem. Cell Biol.* 2015. p. 438-451.
262. Veena, S.R., et al., *Testing the fetal overnutrition hypothesis; the relationship of maternal and paternal adiposity to adiposity, insulin resistance and cardiovascular risk factors in Indian children.*, in *Public Health Nutr*. 2013, Cambridge University Press. p. 1656-1666.
263. Kaati, G., L.O. Bygren, and S. Edvinsson, *Cardiovascular and diabetes mortality determined by nutrition during parents' and grandparents' slow growth period*, in *Eur J Hum Genet*. 2002, Nature Publishing Group. p. 682-688.
264. Donkin, I. and R. Barres, *Sperm epigenetics and influence of environmental factors.*, in *Molecular Metabolism*. 2018. p. 1-11.
265. Carone, B.R., et al., *Paternally induced transgenerational environmental reprogramming of metabolic gene expression in mammals.*, in *Cell*. 2010. p. 1084-1096.
266. Ng, S.-F., et al., *Paternal high-fat diet consumption induces common changes in the transcriptomes of retroperitoneal adipose and pancreatic islet tissues in female rat offspring.*, in *FASEB J.* 2014, Federation of American Societies for Experimental Biology Bethesda, MD, USA. p. 1830-1841.
267. de Castro Barbosa, T., et al., *High-fat diet reprograms the epigenome of rat spermatozoa and transgenerationally affects metabolism of the offspring.* Mol Metab, 2016. **5**(3): p. 184-197.
268. Griswold, M.D., *Spermatogenesis: The Commitment to Meiosis*, in *Physiological Reviews*. 2016. p. 1-17.
269. Heller, C.G. and Y. Clermont, *Spermatogenesis in man: an estimate of its duration.* Science, 1963. **140**(3563): p. 184-6.

270. Clermont, Y., *Kinetics of spermatogenesis in mammals: seminiferous epithelium cycle and spermatogonial renewal.*, in *Physiological Reviews*. 1972. p. 198-236.
271. de Rooij, D.G., *Proliferation and differentiation of spermatogonial stem cells.*, in *Reproduction*. 2001. p. 347-354.
272. Rathke, C., et al., *Chromatin dynamics during spermiogenesis.*, in *Biochimica et biophysica acta*. 2014. p. 155-168.
273. Balhorn, R., *The protamine family of sperm nuclear proteins.*, in *Genome Biol.* 2007, BioMed Central. p. 227.
274. Hammoud, S.S., et al., *Chromatin and transcription transitions of mammalian adult germline stem cells and spermatogenesis.* Cell Stem Cell, 2014. **15**(2): p. 239-53.
275. Gold, H.B., Y.H. Jung, and V.G. Corces, *Not just heads and tails: The complexity of the sperm epigenome.*, in *J. Biol. Chem.* 2018. p. 13815-13820.
276. Champroux, A., et al., *A Decade of Exploring the Mammalian Sperm Epigenome: Paternal Epigenetic and Transgenerational Inheritance*, in *Front. Cell Dev. Biol.* 2018. p. 4615-19.
277. Zheng, H., et al., *Resetting Epigenetic Memory by Reprogramming of Histone Modifications in Mammals.* Mol Cell, 2016. **63**(6): p. 1066-79.
278. Lee, H.J., T.A. Hore, and W. Reik, *Reprogramming the methylome: erasing memory and creating diversity.*, in *Cell Stem Cell*. 2014. p. 710-719.
279. Gapp, K., et al., *Implication of sperm RNAs in transgenerational inheritance of the effects of early trauma in mice.*, in *Nat Neurosci*. 2014, Nature Publishing Group. p. 667-669.
280. Chen, Q., W. Yan, and E. Duan, *Epigenetic inheritance of acquired traits through sperm RNAs and sperm RNA modifications.* Nat Rev Genet, 2016. **17**(12): p. 733-743.
281. Schuster, A., et al., *SpermBase: A Database for Sperm-Borne RNA Contents.*, in *Biology of Reproduction*. 2016. p. 99.
282. Sharma, U., et al., *Small RNAs Are Trafficked from the Epididymis to Developing Mammalian Sperm.*, in *Developmental Cell*. 2018. p. 481-494.e6.
283. Cropley, J.E., et al., *Male-lineage transmission of an acquired metabolic phenotype induced by grand-paternal obesity.*, in *Molecular Metabolism*. 2016, Elsevier Ltd. p. 699-708.
284. Zhang, Y., et al., *Dnmt2 mediates intergenerational transmission of paternally acquired metabolic disorders through sperm small non-coding RNAs.*, in *Nat. Cell Biol.* 2018, Nature Publishing Group. p. 535-540.
285. Radford, E.J., et al., *In utero undernourishment perturbs the adult sperm methylome and intergenerational metabolism*, in *Science*. 2014. p. 1255903-1255903.
286. Sun, W., et al., *Publisher Correction: Cold-induced epigenetic programming of the sperm enhances brown adipose tissue activity in the offspring.*, in *Nature Medicine*. 2018, Nature Publishing Group. p. 1777-1777.
287. Inoue, A., et al., *Maternal H3K27me3 controls DNA methylation-independent imprinting.*, in *Nature*. 2017, Nature Publishing Group. p. 419-424.

288. Dahl, J.A., et al., *Broad histone H3K4me3 domains in mouse oocytes modulate maternal-to-zygotic transition.*, in *Nature*. 2016, Nature Publishing Group. p. 548-552.
289. Zhang, B., et al., *Allelic reprogramming of the histone modification H3K4me3 in early mammalian development.* Nature, 2016. **537**(7621): p. 553-557.
290. Siklenka, K., et al., *Disruption of histone methylation in developing sperm impairs offspring health transgenerationally.* Science, 2015. **350**(6261): p. aab2006.
291. Stringer, J.M., et al., *Reduced PRC2 function alters male germline epigenetic programming and paternal inheritance.*, in *BMC Biol.* 2018, BioMed Central. p. 104.
292. Seisenberger, S., et al., *Reprogramming DNA methylation in the mammalian life cycle: building and breaking epigenetic barriers.*, in *Philos. Trans. R. Soc. Lond., B, Biol. Sci.* 2013. p. 20110330-20110330.
293. Puschendorf, M., et al., *PRC1 and Suv39h specify parental asymmetry at constitutive heterochromatin in early mouse embryos.*, in *Nature Genetics*. 2008, Nature Publishing Group. p. 411-420.
294. van de Werken, C., et al., *Paternal heterochromatin formation in human embryos is H3K9/HP1 directed and primed by sperm-derived histone modifications.* Nat Commun, 2014. **5**: p. 5868.
295. Quante, M., et al., *The LIFE child study: a life course approach to disease and health.*, in *BMC Public Health*. 2012, BioMed Central. p. 1021.
296. Poulain, T., et al., *The LIFE Child study: a population-based perinatal and pediatric cohort in Germany.*, in *Eur. J. Epidemiol.* 2017, Springer Netherlands. p. 145-158.
297. Goodrich, R., G. Johnson, and S.A. Krawetz, *The preparation of human spermatozoal RNA for clinical analysis.*, in *Archives of Andrology*. 2007. p. 161-167.
298. Neff, T., et al., *Polycomb repressive complex 2 is required for MLL-AF9 leukemia.*, in *Proc. Natl. Acad. Sci. U.S.A.* 2012, National Academy of Sciences. p. 5028-5033.
299. Rumbaugh, G. and C.A. Miller, *Epigenetic changes in the brain: measuring global histone modifications.*, in *Methods Mol. Biol.* 2011, Humana Press. p. 263-274.
300. Galarraga, M., et al., *Adiposoft: automated software for the analysis of white adipose tissue cellularity in histological sections*, in *J. Lipid Res.* 2012. p. 2791-2796.
301. Sass, S., et al., *Epigenetic germline inheritance of diet-induced obesity and insulin resistance*, in *Nature Genetics*. 2016, Nature Publishing Group. p. 1-4.
302. Torres-Padilla, M.E., et al., *Dynamic distribution of the replacement histone variant H3.3 in the mouse oocyte and preimplantation embryos.* Int J Dev Biol, 2006. **50**(5): p. 455-61.
303. Tarazona, S., et al., *Differential expression in RNA-seq: A matter of depth*, in *Genome Res.* 2011. p. 2213-2223.

304. Mammana, A. and H.-R. Chung, *Chromatin segmentation based on a probabilistic model for read counts explains a large portion of the epigenome.*, in *Genome Biol.* 2015, BioMed Central. p. 151.
305. Buenrostro, J.D., et al., *Transposition of native chromatin for fast and sensitive epigenomic profiling of open chromatin, DNA-binding proteins and nucleosome position.*, in *Nat Methods*. 2013, Nature Publishing Group. p. 1213-1218.
306. Kleiser, C., et al., *Potential determinants of obesity among children and adolescents in Germany: results from the cross-sectional KiGGS Study.*, in *BMC Public Health*. 2009, BioMed Central. p. 46.
307. Jääskeläinen, A., et al., *Intergenerational transmission of overweight among Finnish adolescents and their parents: a 16-year follow-up study.*, in *Int J Obes (Lond)*. 2011, Nature Publishing Group. p. 1289-1294.
308. Tschop, M. and M.L. Heiman, *Rodent obesity models: an overview.* Exp Clin Endocrinol Diabetes, 2001. **109**(6): p. 307-19.
309. Della Vedova, M.C., et al., *A Mouse Model of Diet-Induced Obesity Resembling Most Features of Human Metabolic Syndrome.*, in *Nutr Metab Insights*. 2016, SAGE PublicationsSage UK: London, England. p. 93-102.
310. Fan, Y., et al., *Diet-induced obesity in male C57BL/6 mice decreases fertility as a consequence of disrupted blood-testis barrier.* PLoS One, 2015. **10**(4): p. e0120775.
311. Stefan, N., H.-U. Häring, and M.B. Schulze, *Metabolically healthy obesity: the low-hanging fruit in obesity treatment?*, in *Lancet Diabetes Endocrinol*. 2018. p. 249-258.
312. Lee, Y.S., et al., *Inflammation is necessary for long-term but not short-term high-fat diet-induced insulin resistance.*, in *Diabetes*. 2011, American Diabetes Association. p. 2474-2483.
313. Honka, M.-J., et al., *Insulin-stimulated glucose uptake in skeletal muscle, adipose tissue and liver: a positron emission tomography study.*, in *Eur. J. Endocrinol.* 2018, Bioscientifica Ltd. p. 523-531.
314. Dearden, L., S.G. Bouret, and S.E. Ozanne, *Sex and gender differences in developmental programming of metabolism.* Mol Metab, 2018. **15**: p. 8-19.
315. Karp, N.A., et al., *Prevalence of sexual dimorphism in mammalian phenotypic traits.* Nat Commun, 2017. **8**: p. 15475.
316. Huypens, P., et al., *Epigenetic germline inheritance of diet-induced obesity and insulin resistance*, in *Nature Genetics*. 2016. p. 497-499.
317. Kanatsu-Shinohara, M., et al., *Dynamic changes in EPCAM expression during spermatogonial stem cell differentiation in the mouse testis.*, in *PLoS ONE*. 2011, Public Library of Science. p. e23663.
318. Hamatani, T., et al., *Dynamics of global gene expression changes during mouse preimplantation development.*, in *Developmental Cell*. 2004. p. 117-131.
319. Larsson, N.G., et al., *Mitochondrial transcription factor A is necessary for mtDNA maintenance and embryogenesis in mice.*, in *Nature Genetics*. 1998, Nature Publishing Group. p. 231-236.
320. van der Heijden, G.W., et al., *Sperm-derived histones contribute to zygotic chromatin in humans.*, in *BMC Dev. Biol.* 2008, BioMed Central. p. 34.

321. Margueron, R., et al., *Role of the polycomb protein EED in the propagation of repressive histone marks.*, in *Nature*. 2009, Nature Publishing Group. p. 762-767.
322. Johnsson, I.W., et al., *A high birth weight is associated with increased risk of type 2 diabetes and obesity.*, in *Pediatr Obes*. 2015, John Wiley & Sons, Ltd (10.1111). p. 77-83.
323. Skilton, M.R., et al., *High birth weight is associated with obesity and increased carotid wall thickness in young adults: the cardiovascular risk in young Finns study.*, in *Arteriosclerosis, Thrombosis, and Vascular Biology*. 2014, Lippincott Williams & Wilkins Hagerstown, MD. p. 1064-1068.
324. Ravelli, G.P., Z.A. Stein, and M.W. Susser, *Obesity in young men after famine exposure in utero and early infancy.*, in *N. Engl. J. Med.* 1976. p. 349-353.
325. Heijmans, B.T., et al., *Persistent epigenetic differences associated with prenatal exposure to famine in humans.*, in *Proc. Natl. Acad. Sci. U.S.A.* 2008. p. 17046-17049.
326. Collins, S., et al., *Genetic vulnerability to diet-induced obesity in the C57BL/6J mouse: physiological and molecular characteristics.*, in *Physiol. Behav.* 2004. p. 243-248.
327. Dalgaard, K., et al., *Trim28 Haploinsufficiency Triggers Bi-stable Epigenetic Obesity.* Cell, 2016. **164**(3): p. 353-64.
328. Clayton, J.A., *Sex influences in neurological disorders: case studies and perspectives.* Dialogues Clin Neurosci, 2016. **18**(4): p. 357-360.
329. Clayton, J.A., *Studying both sexes: a guiding principle for biomedicine.* FASEB J, 2016. **30**(2): p. 519-24.
330. Laprell, F., K. Finkl, and J. Müller, *Propagation of Polycomb-repressed chromatin requires sequence-specific recruitment to DNA.*, in *Science*. 2017, American Association for the Advancement of Science. p. 85-88.
331. Ciabrelli, F., et al., *Stable Polycomb-dependent transgenerational inheritance of chromatin states in Drosophila*, in *Nature Genetics*. 2017, Nature Publishing Group. p. 1-14.
332. Zenk, F., et al., *Germ line-inherited H3K27me3 restricts enhancer function during maternal-to-zygotic transition.*, in *Science*. 2017. p. 212-216.
333. Donohoe, D.R. and S.J. Bultman, *Metaboloepigenetics: interrelationships between energy metabolism and epigenetic control of gene expression.*, in *J. Cell. Physiol.* 2012, John Wiley & Sons, Ltd. p. 3169-3177.
334. Etchegaray, J.-P. and R. Mostoslavsky, *Interplay between Metabolism and Epigenetics: A Nuclear Adaptation to Environmental Changes.*, in *Molecular Cell*. 2016. p. 695-711.
335. Tzika, E., T. Dreker, and A. Imhof, *Epigenetics and Metabolism in Health and Disease.*, in *Front Genet*. 2018, Frontiers. p. 361.
336. Somer, R.A. and C.S. Thummel, *ScienceDirect Epigenetic inheritance of metabolic state*, in *Curr. Opin. Genet. Dev.* 2014, Elsevier Ltd. p. 43-47.
337. Hojfeldt, J.W., et al., *Accurate H3K27 methylation can be established de novo by SUZ12-directed PRC2.* Nat Struct Mol Biol, 2018. **25**(3): p. 225-232.

338. Ho, L., et al., *esBAF facilitates pluripotency by conditioning the genome for LIF/STAT3 signalling and by regulating polycomb function.* Nat Cell Biol, 2011. **13**(8): p. 903-13.
339. Sharma, U. and O.J. Rando, *Metabolic Inputs into the Epigenome*, in *Cell Metabolism*. 2017, Elsevier Inc. p. 544-558.
340. Mu, W., et al., *Repression of the soma-specific transcriptome by Polycomb-repressive complex 2 promotes male germ cell development.* Genes Dev, 2014. **28**(18): p. 2056-69.
341. Maezawa, S., et al., *Polycomb directs timely activation of germline genes in spermatogenesis.*, in *Genes Dev.* 2017. p. 1693-1703.
342. Maezawa, S., et al., *Polycomb protein SCML2 facilitates H3K27me3 to establish bivalent domains in the male germline.*, in *Proc. Natl. Acad. Sci. U.S.A.* 2018, National Academy of Sciences. p. 4957-4962.
343. Gou, L.-T., et al., *Ubiquitination-Deficient Mutations in Human Piwi Cause Male Infertility by Impairing Histone-to-Protamine Exchange during Spermiogenesis.*, in *Cell*. 2017. p. 1090-1104.e13.
344. Seisenberger, S., et al., *The dynamics of genome-wide DNA methylation reprogramming in mouse primordial germ cells.*, in *Molecular Cell*. 2012. p. 849-862.
345. Casa, V. and D. Gabellini, *A repetitive elements perspective in Polycomb epigenetics.*, in *Front Genet*. 2012, Frontiers. p. 199.
346. Chu, C., et al., *Epididymal small non-coding RNA studies: progress over the past decade.*, in *Andrology*. 2019. p. 1061.
347. Brockdorff, N., *Noncoding RNA and Polycomb recruitment.*, in *RNA*. 2013. p. 429-442.
348. Walter, M., et al., *An epigenetic switch ensures transposon repression upon dynamic loss of DNA methylation in embryonic stem cells.*, in *Elife*. 2016, eLife Sciences Publications Limited. p. R87.
349. Skinner, M.K., et al., *Ancestral dichlorodiphenyltrichloroethane (DDT) exposure promotes epigenetic transgenerational inheritance of obesity.*, in *BMC Med*. 2013, BioMed Central. p. 228.